



**UNIVERSITY OF
KWAZULU-NATAL**

**INYUVESI
YAKWAZULU-NATALI**

**DRYING AND PASTEURISATION OF VIP LATRINE FAECAL
SLUDGE USING A BENCH SCALE MEDIUM INFRARED
MACHINE**

By

Mirara Simon Waweru

BScEng. (Agricultural) Egerton University

This dissertation is submitted in Partial fulfilment of the requirements for the degree

MScEng. (CHEMICAL)

Faculty of Engineering

College of Agriculture, Engineering and Science

UNIVERSITY OF KWAZULU-NATAL

Supervisor:	Professor Chris Buckley
Co Supervisors	Dr. Santiago Septien
	Dr. Konstantina Velkushanova
	Mrs Anusha Singh

FEBRUARY 2017

Declaration 1 - Plagiarism

I,, declare that

1. The research reported in this dissertation, except where otherwise indicated, and is my original work.
2. This dissertation has not been submitted for examination or degree at any other university.
3. This dissertation does not contain other persons' data, pictures, graphs or other information unless specifically acknowledged as being sourced from other persons.
4. This thesis does not contain other persons' writing, unless specifically acknowledged as being sourced from other researchers. Where other written sources have been quoted, then:
 - a) Their words have been re-written but the general information attributed to them has been referenced
 - b) Where their exact words have been used, then their writing has been placed in italics and inside quotation marks and referenced.
- 5 This thesis does not contain text, graphics or tables copied and pasted from the internet, unless specifically acknowledged, and the source being detailed in the thesis and in the references sections.

Candidate Mirara Simon W.
Signature.....Date.....

This Dissertation is submitted for examination with our approval as the candidate's supervisors

Supervisor Prof. C.A. Buckley
Signature.....Date

Co- supervisors Dr. S. Septien
SignatureDate.....

Mrs Anusha Singh
Signature.....Date.....

Declaration 2 - Publications and Presentation

The following papers that have a link with this dissertation either have been written or are in process of being written

- 1) Mirara S.W., Velkushanova K., Anusha Singh, Septiens S., Buckley C.A. Drying of sludge from a belt, MIR dryer; The Latrine Dehydration and Pasteurisation (LaDePa) process (**paper in progress**)
- 2) Mirara S.W., Velkushanova K., Anusha Singh, Septiens S., Buckley C.A. Characteristics of raw VIP sludge and pellets dried by an MIR belt drier (**paper in progress**)
- 3) Septien S, Singh A., Mirara S.W., Makununika, B, Teba L., Velkushanova K., Buckley C.A., Overview of a Medium Wave Infrared Process, 'LaDePa', for Drying and pasteurisation of Faecal Sludge from VIP latrines, 4th YWP-ZA Biennial and 1st African YWP Conference. Pretoria, South Africa, November 16-18, 2015 (article available in proceeding).
- 4) Xiangmei M., Martijn S., Mirara S. & Wiebren D., Jong. 2014. Experimental Study of Drying Different Sludges Using a Belt-Mir LaDePa Dryer. *European Biomass Conference and Exhibition Delft*, Netherlands.

A poster of the work in this dissertation was presented at the third eThekweni-University Research Symposium in November 2014. This was facilitated by the Municipal Institute of Learning (MILE) and other universities.

The poster presented is attached as **Appendix F**.

Acknowledgements

I am especially grateful to God for giving me good health of body and mind for me to be able to carry out this work.

I wish also to thank my supervisor Pr. C.A. Buckley for all the guidance he gave throughout my work and for giving me the opportunity to do my masters with the Pollution Research Group. I also thank Dr. S. Septien, Dr. K. Velkushanova, Mrs A. Singh and Dr. J. Pocock for having been always available for consultation and for sharing their knowledge and leading me into successfully completing my work. In a special way, I thank Dr. S.Septien for his dedication, encouragement, advice and for his critics that helped me in my work.

Much thanks to members of the Pollution Research Group and in a special way Mrs Kerry Philip, administrator at Pollution Research Group for her continued support to ensure smooth running of the project. Mrs M. Reddy, Mr M. Sikhosana, Mr T. Zikalala, for their support while undertaking my laboratory work. I also thank Mr. K. Jack and his workshop team for their support in fixing the pilot LaDePa whenever there were problems.

Thanks to the Water Research Commission for funding this study. Without this support, I would not have been able to complete this work. I also appreciate the assistance given by the eThekweni Water and Sanitation together with the Particle Separation Systems (PSS), in particular Mr. Dave Wilson, Mr. John Harrison and Mr. Rein Buisman.

Many thanks to my family for their continued support, encouragement and prayers in the course of my study.

Abstract

The main challenge with Ventilated Improved Pit (VIP) latrines is that they eventually fill up. Solutions therefore have to be sought with the common practice being to cover up the hole and dig a new pit. This however is not sustainable especially in peri-urban areas due to lack of space for the new pits. The other option is to empty the pits and dispose of the sludge.

After the creation of the eThekweni municipality in 1999, over 60 000 ventilated improved pit (VIP) latrines were inherited from the incorporated local entities. In 2009, the municipality set out to empty over 35 000 VIP latrines, which were already full. One of the challenges from this operation was the disposal of the sludge in an environmentally safe way. The initial idea was to dispose of the sludge in wastewater treatment plants but this caused overloading of the treatment plants and so the municipality had to seek alternatives. This led to the concept of the *Latrine Dehydration and Pasteurization* (LaDePa) machine. This machine is used to process the emptied sludge into dry, pasteurized, pellets, which can be used in agricultural crop production, as a fertilizer or a soil conditioner. The resultant pellets could also be combusted as a fuel. The LaDePa machine uses a screw extruder to form “spaghetti-like” pellets, which are subsequently dried and pasteurised by means of medium infrared (MIR) radiation lamps. Air that flows over the pellets facilitates removal of moisture from the surface of pellets and away from the drying chamber.

Although this machine has been operational, there has been no scientific data on the phenomenological process and on how it affects the characteristics of raw sludge and resultant pellets. An important aspect in processing the pellets in the machine is their processing temperature. At an average drying temperature of 136.5 °C, it was found that core and surface temperature are only isothermal in the initial stages of drying. As drying progresses, the difference in temperature between the surface and the core increases. A low moisture content also causes lower heat transfer from the pellet’s surface to the core. An interesting finding from this study is that core temperature rises and remains constant at 80 °C for the emitter intensity that was used.

Among the parameters, investigated emitter intensity was found to be the most significant in drying and pasteurisation. At a drying temperature of approximately 214 °C, moisture is reduced by 41.5 % (wet basis) in only 8 min while all *Ascaris* eggs were destroyed. The highest drying temperature investigated was found to be the most efficient in terms of energy consumed. However, fast drying of pellets causes a high thermal gradient between the pellet core and surface, which leads to charring of the pellets. A decrease in height of emitters above the porous steel belt leads to a higher drying rate when emitter power supply and other parameters are kept constant. Reduced airflow leads to decreased drying rate. Small diameter pellets dry out faster and power consumption in their drying is the most efficient compared to larger pellets.

Biological analysis shows that the LaDePa process is very efficient at deactivating helminths. *Ascaris* eggs, which were the most persistent. They were deactivated either immediately or upon storage when processed at a residence time of more than 8 min and at a temperature about 87 °C or higher.

The concentration of P, K, Mg and Ca, in raw sludge and the resultant pellets was found to increase with drying. However, the actual content is not affected by drying. For dry pellets to supply P, K, Mg and Ca at the same level as organic fertilizer, the application rate should be 10 times more. The application rate of dry pellets should be, however, about 6 times more than most manure sources. The LaDePa process has a negative effect as it reduces the total soluble N content in sludge. This is as depicted by reduced ammonium, nitrates and nitrites in the resultant pellets. Physical analysis shows that the calorific value of dried pellets is above 10 MJ / kg wet solid at a moisture content below 35 % (wet basis). This is close to the range of most biomass materials but 2 to 3 times lower than that of fossil fuels. Thermal conductivity and heat capacity of dried pellets decreases with increased drying which makes pellets less suitable as a fuel at very low moisture content.

In summary, the LaDePa process was found to be a satisfactory process in drying and pasteurisation of faecal sludge of VIP origin. To ensure that the process is efficient the emitter intensity should be kept relatively high, there should be a high airflow around the pellets, height of emitter above the belt should be low and pellet diameter should be small.

Table of Contents

Declaration 1 - Plagiarism	ii
Declaration 2 - Publications and Presentation	iii
Acknowledgements	iv
Abstract	v
List of Tables	xi
List of Figures	xii
List of Abbreviations	xv
Nomenclature	xvi
1 Introduction	1
1.1 Aim of the project.....	2
1.2 Specific objectives.....	2
1.3 Scope of the project	3
1.4 Significance of the research.....	3
1.5 Expected outcome	3
2 Literature Review	4
2.1 VIP latrines.....	4
2.1.1 Content of VIP latrines	4
2.1.2 Physical-chemical characteristics of faecal sludge from VIP latrines	6
2.1.3 Management of sludge from VIP latrines.....	7
2.1.4 Use of excreta as a fertilizer	8
2.2 Pasteurisation.....	8
2.2.1 Types of pathogens.....	9
2.2.2 Pasteurisation kinetics	10
2.2.3 Indicator of pathogen content	13
2.3 Drying.....	13
2.3.1 Psychrometry	13
2.3.2 Types of moisture	15
2.3.3 Drying phenomenology	15

2.3.4	Drying kinetics	16
2.3.5	Factors affecting drying.....	17
2.3.6	Applications of drying in sludge processing	18
2.4	Infrared radiation heating	18
2.4.1	Production and transmission of infrared rays	19
2.4.2	Design and selection of infrared dryers.....	21
2.4.3	Applications of infrared drying	22
2.5	Summary.....	22
3	Materials and Methods	24
3.1	Feed material	24
3.2	Experimental facility	24
3.2.1	Laboratory scale LaDePa.....	24
3.2.2	Temperature measurement	27
3.2.3	Extrusion of pellets.....	28
3.3	Experimental procedure.....	28
3.3.1	LaDePa experiments.....	28
3.3.2	Temperature measurement procedure.....	30
3.3.3	Calibrations in the LaDePa.....	30
3.3.4	Energy consumption and drying rate calculations.....	31
3.3.5	Characterisation of the raw sludge and processed pellets	31
3.3.6	Data statistical analysis.....	34
3.4	Characteristic time and dimensionless analysis.....	35
3.4.1	Characteristic time calculations.....	36
3.4.2	Pellet properties in characteristic time calculations.....	39
4	Results and Discussion	40
4.1	Characteristic time analysis	40
4.2	Temperature of pellets during drying	42
4.2.1	Heating of 8 mm diameter pellets.....	42
4.2.2	Heating of 14 mm diameter pellets.....	44

4.2.3	Comparison of the heating of 8 and 14 mm diameter pellets	45
4.2.4	Summary on temperature evolution for different pellet diameter and residence times	46
4.3	Influence of the operating parameters on drying	47
4.3.1	MIR emitter intensity.....	47
4.3.2	Effect of distance between the emitters and the pellets	51
4.3.3	Effect of airflow around the pellets	53
4.3.4	Effect of pellet diameter	55
4.3.5	Effect of the feedstock.....	58
4.4	Pasteurisation efficiency.....	60
4.5	Nutrient analysis	61
4.5.1	Elemental Analysis	62
4.5.2	Soluble Nutrient ions	64
4.5.3	Comparison with literature	67
4.5.4	Summary of the nutrient analysis	69
4.6	Thermal analysis.....	72
4.6.1	Calorific value	72
4.6.2	Thermal conductivity.....	74
4.6.3	Heat capacity	75
4.6.4	Thermal diffusivity.....	77
4.6.5	Summary.....	78
5	Conclusion.....	79
6	Perspectives.....	81
	References	83
7	Appendix	I
7.1	Appendix A: Calibration tests	I
7.1.1	Drying temperature.....	I
7.1.2	Power input into emitters.....	II
7.1.3	Belt speed calibration	III
7.2	Appendix B: Rheological analysis of raw sludge.....	IV

7.2.1	Viscosity of sludge as function of the shear rate	IV
7.2.2	Storage modulus as a function of the angular frequency.....	V
7.2.3	Loss modulus as a function of the angular frequency	VI
7.2.4	Storage and complex modulus comparison	VI
7.3	Appendix C: Temperature profiles	VII
7.4	Appendix D: Psychometric charts for low, high and medium temperatures	VIII
7.5	Appendix E: Deliverables submitted to Water Research Commission	XI
7.6	Appendix F: Poster presented at MILE symposium 2014.....	XII

List of Tables

Table 3-1: Comparison between the laboratory and full scale LaDePa.....	25
Table 3-2: Summary of the experimental plan.....	29
Table 3-3: MIR intensity settings and corresponding temperatures.....	29
Table 3-4: Summary of the analyses done in the raw faecal sludge and processed pellets.....	34
Table 3-5: Dimensionless numbers related to drying.....	36
Table 3-6: Air physical properties at 293 K.....	39
Table 3-7: Pellets physical properties.....	39
Table 4-1: Dimensionless numbers and characteristic times for different suction air	41
Table 4-2: Characteristic times and their ratios for different pellet diameters.....	42
Table 4-3: Viable and dead parasite eggs at different operating conditions.....	61
Table 4-4: Nutrient content in sludge before and after processing and comparison with literature data (Lopez et al., 2002, Mnkeni and Austin, 2009).....	68
Table 4-5: Nutrient content in dried pellets and some manure types and inorganic fertilizers.....	70
Table 7-1 E: Deliverables submitted as part of WRC project K5/2137.....	XI

List of Figures

Figure 2-1: Theoretical layers in VIP latrines (Buckley et al., 2008).....	5
Figure 2-2: Modified layers theory in VIP latrine (Zuma et al., 2013).....	6
Figure 2-3: Transmission routes of pathogens (Franceys et al., 1992) cited by (Austin, 2001, Phasha, 2006)....	9
Figure 2-4: Effect of temperature on kinetics disinfection (Atkinson and Mavituna, 1983, Najafpour, 2007)...	11
Figure 2-5: Temperature - time relation for the disinfection of pathogens in night soil and faecal sludge (Feachem et al., 1983).....	12
Figure 2-6: Types of moisture found in wet materials (Mujumdar and Devahastin, 2000).....	15
Figure 2-7: Typical drying curve of a wet material (Moyers and Baldwin, 1997).....	17
Figure 2-8: Propagation of irradiation on an incident body.....	19
Figure 2-9: Illustration of the view factor (Hewitt et al., 1994).....	21
Figure 3-1: Photograph of the laboratory scale LaDePa machine.....	25
Figure 3-2 Drying chamber with the emitters off (left) and on (right).....	26
Figure 3-3: Scheme of the laboratory scale LaDePa (Harrison and Wilson, 2012).....	26
Figure 3-4: Control panel of the laboratory scale LaDePa.....	27
Figure 3-5: Photograph of the hand held capillary extruder and plates to vary extrusion size.....	28
Figure 3-6: Illustration of thermal couple position within the pellets.....	30
Figure 3-7: Thermocouple distance in the pellets.....	30
Figure 4-1: Temperature at core of the 8 mm pellets at different residence times as a function of length from the inlet of the drying chamber.....	43
Figure 4-2: Surface and core temperatures of the 8 mm pellets during processing in the laboratory scale LaDePa.....	43
Figure 4-3: Temperature at the top and side surfaces of the 14 mm pellets during processing in the laboratory scale LaDePa.....	44
Figure 4-4: Temperature of 14 mm pellets as a function of the length from the inlet of the drying chamber.....	45
Figure 4-5: Surface temperature of the 8 and 14 mm pellets as a function of length from inlet of the drying chamber.....	45
Figure 4-6: Core temperature for 8 and 14 mm diameter pellets as a function of length from the inlet of the drying chamber.....	46
Figure 4-7: Drying curves at different MIR intensities.....	48
Figure 4-8: Drying rate as a function of residence time at varying emitter intensity.....	49
Figure 4-9: Volatile solids content at different MIR intensities at varying residence time.....	50

Figure 4-10: Ash content at different MIR intensities.....	50
Figure 4-11: Energy consumption as a function of moisture removal at different MIR intensities.....	51
Figure 4-12: Drying curve at different emitter heights above the belt.....	52
Figure 4-13: Moisture removal as a function energy consumption at different emitter height above the belt...	52
Figure 4-14: Drying curves for different airflow rates.....	53
Figure 4-15: Drying rate at different airflow rate around pellets.....	54
Figure 4-16: Energy consumption as a function of residence time at varying airflow around pellets.....	54
Figure 4-17: Drying curves for different pellet diameters.....	55
Figure 4-18: Drying rate for the different pellet diameters.....	56
Figure 4-19: Volatile solids content for the different pellet diameters.....	57
Figure 4-20: Ash content for the different pellet diameters.....	57
Figure 4-21: Energy consumed in drying pellets of varying diameters.....	58
Figure 4-22: Drying curves of the different feedstock.....	59
Figure 4-23: Volatile solids for different sludge processed at varying residence time.....	59
Figure 4-24: Ash content for different sludge processed at varying residence time.....	60
Figure 4-25: P and K content (dry basis) of pellets processed at different MIR intensities.....	62
Figure 4-26: Mg and Ca content (dry basis) of pellets processed at different MIR intensities.....	63
Figure 4-27: P and K content (wet basis) of pellets processed at different MIR intensities.....	63
Figure 4-28: Mg and Ca content (wet basis) of pellets processed at different MIR intensities.....	64
Figure 4-29: NH_4^+ content as a function of residence time for pellets processed at different emitter intensities...	65
Figure 4-30: NO_3^- content as a function of residence time for pellets processed at varying emitter intensity...	65
Figure 4-31: NO_2^- content as a function of residence time for pellets processed at varying emitter intensity...	66
Figure 4-32: PO_4^{3-} content of the pellets processed at different MIR intensities.....	67
Figure 4-33: Calorific value in dry basis of the pellets processed at different MIR intensities, as a function of moisture content.....	73
Figure 4-34: Calorific value in dry basis for pellets of different diameters as a function of the moisture content.	73
Figure 4-35: Thermal conductivity of pellets processed at different MIR intensities, as a function of residence time.....	74
Figure 4-36: Thermal conductivity of pellets processed at different MIR intensities, as a function of moisture content.....	75
Figure 4-37: Heat capacity of the pellets processed at different MIR intensities, as a function of residence time.....	76

Figure 4-38: Heat capacity of the processed pellets at different MIR intensities, as a function of moisture content.....	76
Figure 4-39: Thermal diffusivity of processed pellets at different MIR intensities, as a function of residence time.....	77
Figure 4-40: Thermal diffusivity of pellets processed at different emitter intensities as a function of moisture content.....	77
Figure 7-1 A: Temperature of the MIR emitter 1 at different intensities and height above the belt.....	I
Figure 7-2 A: Temperature of the MIR emitter 2 at different intensities and height above the belt.....	II
Figure 7-3 A: Corresponding power input for different MIR intensities.....	III
Figure 7-4 A: Residence time as a function of dial readings of the porous steel belt.....	IV
Figure 7-5 B: Viscosity of faecal sludge with and without sawdust as a function of shear rate.....	V
Figure 7-6 B: Storage modulus of faecal sludge with and without sawdust, as a function of the angular frequency.....	V
Figure 7-7 B: Loss modulus of faecal sludge with and without sawdust, as a function of the angular frequency.....	VI
Figure 7-8 B: Storage and complex modulus as a function of angular frequency.....	VII
Figure 7-9 C: Temperature of the 8 mm diameter pellets at the surface and at the core.....	VII
Figure 7-10 E: Psychometric chart for low temperatures.....	VIII
Figure 7-11 E: Psychometric chart for medium temperatures.....	IX
Figure 7-12 D: Psychometric chart for high temperatures.....	X

List of Abbreviations

CAB	Community Ablution Blocks
DWAF	Department of Water Affairs and Forestry
FIR	Far-infrared
ICP	Inductively Coupled Plasma
LaDePa	Latrine Dehydration and Pasteurisation
MIR	Medium-infrared
NIR	Near-infrared
PRG	Pollution Research Group
RH	Relative humidity
TKN	Total Kjeldahl Nitrogen
UD	Urine Diversion
UKZN	University of KwaZulu-Natal
VIP	Ventilated Improved Pit
WRC	Water Research Commission
WWTW	Wastewater treatment works

Nomenclature

A_i	Area of surface i	[m ²]
A_j	Area of surface j	[m ²]
A	Area	[m ²]
D	Decimal reduction time	[min]
E	Activation energy	[kJ/ mol]
F_{ij}	Shape or view factor between surfaces i and j	[-]
H	Absolute humidity	[kg/m ³]
H_s	Air saturation humidity	[kg/m ³]
h_m	Mass exchange coefficient	[m/s]
h_t	Heat exchange coefficient	[W/m ² /K]
i	Sample number	[-]
k_o	Factor of frequency	[min ⁻¹]
k_d	Thermal death rate	[min ⁻¹]
MC	Moisture content	[g water / g dry solid]
M_w	Molecular mass of water	[g/mol]
M_a	Molecular mass of air	[g/mol]
N_o	Initial microbial population	[no/gm]
N_t	Microbial population at t	[no/gm]
n	Number of samples	[-]
p_s	Saturation partial pressure	[atm]
P_{tot}	Total pressure	[atm]
p_w	Partial pressure of vapour	[atm]
R	Universal gas constant	[J/ (K.mol)]
Q_r	Heat exchanged between two bodies	[W]
q	Energy emission rate	[W]
T	Temperature	[K]
T_i	Temperature of surface i	[K]
T_j	Temperature of surface j	[K]
t	Time	[min]
t_c	Characteristic time	[s]

TS	Total solids	[g]
VS	Volatile solids	[g volatile/ g ash]
w_f	Final weight of sample	[g]
w_{f1}	Mass after oven drying	[g]
w_{f2}	Mass after furnace combustion	[g]
w_i	Initial weight of sample	[g]
x	Individual value of data	[-]
\bar{x}	Mean value	[-]
α	Absorptivity	[-]
ε_i	Emissivity of surface i	[-]
ε_j	Emissivity of surface j	[-]
ρ	Reflectivity	[-]
ρ_i	Reflectivity of surface i	[-]
ρ_j	Reflectivity of surface j	[-]
σ	Stefan-Boltzmann constant	[W/m ² .K ⁴]
σ_n	Standard deviation	[-]
σ^2	Variance	[-]
τ	Transmissivity	[-]

1 Introduction

When the first South African government was democratically elected in 1994, many of its citizens did not have access to proper sanitation. Out of a population of over 40 million, about half did not have access to basic sanitation (DWAF et al., 2012). Therefore, access to water and basic sanitation became a priority for the newly elected government. Over the years, the government has formulated a framework of registration, policies and guidelines to attain this goal (Still and Foxon, 2012b). One of the policies was that the national government covers the initial costs of the sanitation services while the users should cover the rest, i.e. maintenance and operation. However, this was not the case due to poverty and the high costs associated with operation, especially concerning water supply schemes (DWAF et al., 2012).

The various sanitation systems may be categorised as those that flush and discharge, and those that drop and store. Flush and discharge systems have been highly regarded for urban areas where population is high and there is adequate supply of water. This therefore necessitates the construction of a wastewater treatment plant or septic tanks to handle the resultant waste. However, in most African countries, water supply is a major problem and so the system of drop and store is common, especially in the rural and peri-urban areas. The drop and store, also called dry onsite system, include the urine diversion (UD) toilets and pit latrines, which may be of the improved or un-improved type (Esrey et al., 1998). A convectional pit latrine is described by as one that is made up of a pit and the super structure. Excreta and the anal cleansing material are deposited and stored in the pit. The pit may be lined to prevent it from collapsing and provide support to the superstructure (Tilley et al., 2008). Ventilated improved pit (VIP) is similar to a convectional pit latrine by includes a ventilation pipe which carries odour away from the latrine. The pipe is fitted with a screen at the top to prevent flies from getting out or into the pit (Still et al., 2009). The simple nature of the VIPs could be the reason which makes the South African government consider ventilated improved pit (VIP) latrines as the basic acceptable system to provide decent sanitation (Buckley et al., 2008). These systems are usually of low-cost as most of the structure can be constructed from local inexpensive materials.

The main challenge with VIP latrines is that they fill up after continuous use. Solutions have to be then found in order to have a permanent functional sanitation system. Usually, the common practice is to cover up the hole and dig a new pit, but this is not a sustainable solution in densely populated areas due to lack of space to relocate the pit. In this case, the main option is to empty the pits and dispose of the sludge (Still and Foxon, 2012b).

After the creation of the eThekweni municipality in 1999, over 60 000 ventilated improved pit (VIP) latrines were inherited from the incorporated local entities (Brouckaert et al., 2013). In 2009, the municipality set out to empty over 35 000 VIP latrines which were already full (Still and Foxon, 2012b). One of the challenges from this operation was the disposal of the sludge in an environmentally safe way. The initial idea was to dispose of the sludge in wastewater treatment plants but this caused overloading and subsequent failure of the system and so the municipality had to seek an alternative. This led to the concept and design of the *Latrine Dehydration and Pasteurization* (LaDePa). This is based on a machine that aims at processing the emptied faecal sludge into dry and pasteurized pellets, which could be used as a soil conditioner or fertilizer or which could be combusted as a fuel. During operation, a screw extruder leads to the formation of “spaghetti-like” pellets, which are subsequently dried and pasteurised by means of medium infrared (MIR) radiation lamps (Harrison and Wilson, 2012). Drying is defined as the removal of moisture or any other liquid from a solid while pasteurisation is the reduction in pathogen content of a substance. A combination of these two processes could make handling of faecal matter easier and safe. However there is need to establish the level of drying and pasteurisation that is achieved with a combination of parameters such as drying time and drying temperature among other parameters.

1.1 Aim of the project

The phenomenological processes occurring in the full-scale LaDePa machine are not well understood, and so the level of drying and pasteurisation have not been mastered. In addition, the machine utilizes considerable energy for its operation. It was therefore necessary to carry out a scientific study in order to understand and optimize the process. This study was performed in a laboratory-scale prototype at the Pollution Research Group (PRG) at the University of Kwa-Zulu Natal, which is a replica of the full scale LaDePa. This research project was funded by the Water Research Commission (WRC). The deliverables from this project are presented in Appendix F.

This study therefore focused not only in understanding the processes occurring in the LaDePa but also in evaluation of the resultant pellets for reuse in agriculture or as a biofuel.

1.2 Specific objectives

In order to achieve to the aim of this study, the following objectives were formulated:

- a) To investigate the influence of the actual parameter that affect drying and pasteurisation in the laboratory-scale LaDePa; These parameters include:
 - i) Emitter intensity; which is the level of energy generated by the emitters. It affects the drying temperature
 - ii) The residence time; this is the time in which samples are subjected to the experimental conditions
 - iii) Distance between the emitters and the pellets.
 - iv) Rate of airflow around the pellets; this is the speed at which air moves around the pellets to remove evaporated moisture

- v) Diameter of the pellets; this is on the size of the pellets that affect the rate of heat transfer from the surface of pellets to the core and consequently affect the drying rate of pellets.
- b) To characterise the raw sludge and pellets for nutrient content and thermal properties.

1.3 Scope of the project

In this study, the material used is faecal sludge obtained from VIP latrines within the eThekweni municipality. Parameters investigated are the effect of varying the MIR intensity, height of MIR above the pellets, airflow rate and size of the pellets. Resultant pellets were then analysed for nutrient content, pathogen content and for fuel properties.

1.4 Significance of the research

This study will help come up with important information that helps compare the LaDePa process with other existing methods of disposing off sludge from onsite sanitation facilities. As the first scientific study on the LaDePa process, it also maps out its significance in solving the problem of sanitation in low-income countries.

1.5 Expected outcome

The data obtained in this research will contribute to the improvement of the design and operation of the LaDePa machine, to ensure that the process uses minimum energy and produces valuable dried and pasteurised pellets. These pellets could be used either for energy generation or in agriculture as a fertilizer or soil conditioner.

2 Literature Review

To understand LaDePa process, it is important to review the type of sludge found in VIP latrines and the drying and pasteurisation processes. In this literature review, the VIP latrines and the management of the generated sludge will be first discussed. Then, the different types of pathogens likely to be found in VIP sludge and the means to deactivate them will be reviewed. Lastly, the process of drying and infrared radiation heating will be described.

2.1 VIP latrines

The South African Department of Water Affairs and Forestry (DWAF) defines a sanitation system as the process by which waste is managed from the generation point to the disposal or recycle point. This is achieved by the use of a sanitation facility, which is infrastructure that enables handling, storage, removal and treatment of human excreta (DWAF, 2003, Still et al., 2009).

Esrey et al. (1998) broadly categorises the sanitation systems as those that flush and discharge, and those that drop and store. Flush and discharge systems have been highly regarded for urban areas where population is high and there is adequate supply of water. This therefore necessitates the construction of a wastewater treatment plant or septic tanks to handle the resultant waste. However, in most African countries, water is a major problem and so the system of drop and store is common, especially in the rural and peri-urban areas. The drop and store, also called dry onsite system, include the urine diversion (UD) toilets and pit latrines, which may be of the improved or un-improved type (Esrey et al., 1998). A ventilated improved pit latrine (VIP) is fitted with a vent pipe which facilitates airflow within the pit and thus removal of bad odour. The pipe is installed with a fly screen at the top, which stops flies from leaving or entering the pit latrine (Mara, 1984).

2.1.1 Content of VIP latrines

There are variations in the content of VIP latrines depending on demographic, geophysical and biological factors. Pit latrines are sometimes used to dump household waste and therefore it is common to find materials such as plastic bags, newspapers, magazines bottles, rags, glass and polythene among others (Bakare et al., 2012).

According to Buckley et al. (2008), the content of the pit varies depending on user feeding habits and anal cleansing material used. There are also differences in the properties of the sludge as a function of the pit depth. Buckley further proposed four theoretical sludge layers in the pit, as shown in **Figure 2-1**. The first layer is located at the top, just below the pit hole. In this layer, the main process is aerobic degradation by microorganisms acting on freshly deposited faeces. The second layer is at the top of the pit but not directly below the pit hole. In this layer, the remaining organic material from the fresh faeces is aerobically degraded. In the third layer, the material is assumed to undergo anaerobic degradation where the remaining organic material is converted to soluble products, carbon dioxide and methane. The fourth layer is at the bottommost part of the pit and is composed of stable non-biodegradable material (Buckley et al., 2008).

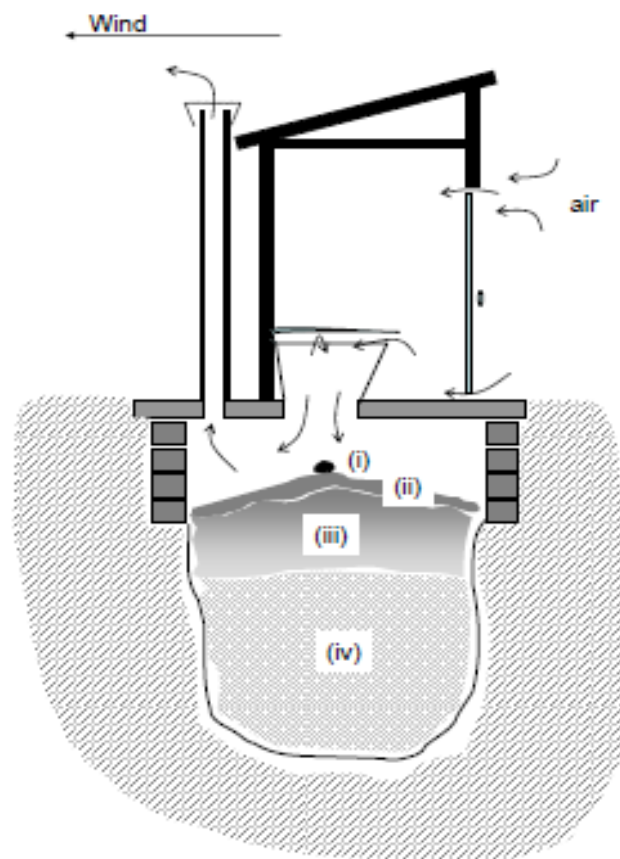


Figure 2-1: Theoretical layers in VIP latrines (Buckley et al., 2008)

Zuma et al. (2013) further proposed a division of the pit layers into front and back section on the theoretical layers proposed by Buckley et al (2008). The pit may therefore be subdivided into eight layers as shown in **Figure 2-2**.

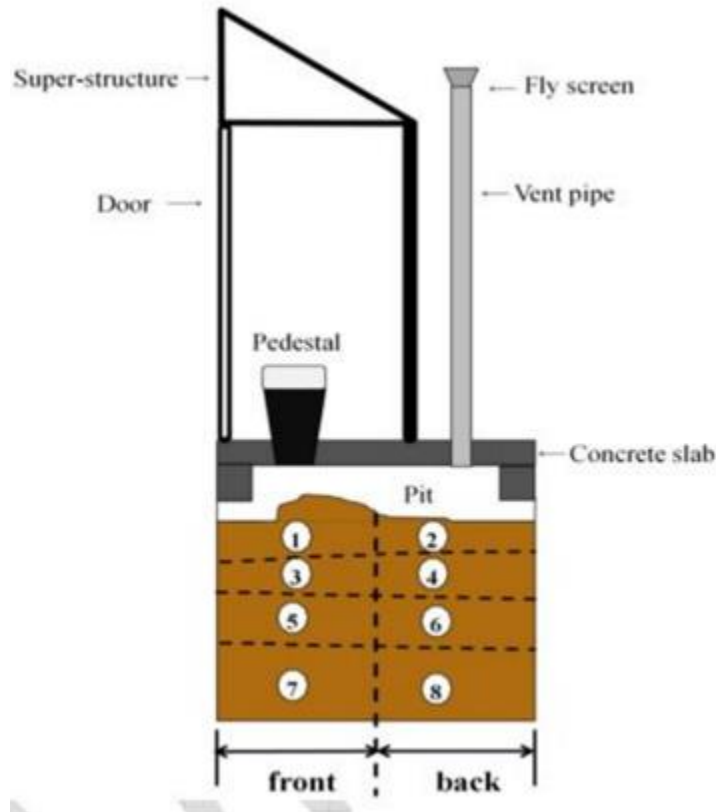


Figure 2-2: Modified layers theory in VIP latrine (Zuma et al., 2013)

2.1.2 Physical-chemical characteristics of faecal sludge from VIP latrines

Zuma et al. (2013) studied the chemical and thermal properties of faecal sludge from VIP latrines within the eThekweni Municipality, Durban, South Africa. Some of the properties analysed were moisture content, ammonia content, TKN content, orthophosphate content, thermal conductivity and calorific value.

Moisture content was found to be in the range of 60 to 70% at the bottom of the pit and 80 to 90% at the top (on wet basis). This result is similar to that found in literature, such as the results of (Bakare et al., 2012) with a moisture content of 67% at the bottom layer of the pit versus 77% at the top layer (in wet basis). This therefore indicates that the characteristics of the material at the top and bottom of the pit are different.

There was no variation in the composition of P and N along the depth of the pit, as indicated by the total potassium, Kjeldahl nitrogen (TKN) and ammonia content. The thermal conductivity and calorific value did not also show any variation as a function of the pit depth.

Over 90% of the analysed sludge had a total Kjeldahl nitrogen (TKN) between 4 and 14 mg/g of wet sludge. The maximum ammonia recorded was 5.87 mg/g of wet sludge and the lowest value in the range of 0 to 1 mg/g of wet sludge. Ortho-phosphate was found to be lower than 0.06 mg/g of wet sludge. Thermal conductivity was in the range of 0.51 and 0.59 W/m.K. Calorific value varied widely from a minimum of 0.0029 to maximum of 0.0238 MJ/g of dry sludge (Zuma et al., 2013).

2.1.3 Management of sludge from VIP latrines

While in use, VIP latrines eventually fill up and thus they either could be covered up and new pits dug, or emptied and the removed sludge disposed onsite or transported for disposal.

Alternatives given by Dave Still (2012) for dealing with faecal sludge include burial in an onsite pit, anaerobic digestion to produce biogas, treatment in waste water treatment works (WWTW), use of black soldier flies, deep row entrenchment and composting (Still and Foxon, 2012a). Energy can be recovered from sludge treatment through thermochemical process such as pyrolysis, combustion or gasification (Williams, 2013). Hydrothermal process such as hydrothermal carbonization and supercritical oxidation (Sevilla and Fuertes, 2009) is also used. These methods have been mostly used for sewage sludge, which has similarities with VIP sludge.

Anaerobic digestion to produce methane has been proposed as a method of treating faecal sludge while recovering energy in the form of biogas. This method necessitates the addition of water to the sludge, which is counterproductive as it is easier to handle, transport and dispose of dry materials.

Pit sludge could be disposed of in sewers or WWTW. This method is however not viable, as it causes shock loading to the plant. Sludge from pit latrines is 10 to 100 times more concentrated than sewage sludge. It is estimated that 1.5 m³ of faecal sludge has a load equivalent to 1000 m³ of sewage sludge. Moreover, non - biodegradable material in pit sludge is another challenge on the disposal in WWTW as it interferes with the decomposition process (Still and Foxon, 2012a).

Black soldier flies could be used to consume faecal sludge. The larvae, which they would subsequently produce, could be processed into a biofuel or compost or used as high protein animal feed (Newton et al., 2005, Strande et al., 2014). This method has however not been fully explored with human waste.

Deep row entrenchment is a method that involves burying sludge in a ditch of 200 000 mm long, 600 mm wide and 1 200 to 1 500 mm deep. This method could improve soil fertility where sludge acts as a slow release fertilizer. It can thus benefit the agroforestry sector as it increases the growth rate of trees and helps in recovering waste land such as mine spoils (Still and Foxon, 2012b).

Sludge can also be disposed by incineration to reduce the volume and burying the resultant ash in a landfill site. An alternative to incineration is pyrolysis and gasification. Pyrolysis is a thermal degradation of organic waste in the absence of oxygen to produce a carbonaceous charcoal, tar and combustible gases. Gasification differs from pyrolysis in that organic material is degraded in limited supply of oxygen, or in the presence of steam or carbon dioxide, so as to produce a gaseous fuel product mainly composed of carbon monoxide and hydrogen, tar and ash (Williams, 2013). Hydrothermal carbonization is the process in which organic material is decomposed in water at temperatures between 150 to 350°C to form a product with high carbon content (Sevilla and Fuertes, 2009). Supercritical water oxidation is another option for sludge utilization. It utilizes water at temperatures and pressures above 374°C and 221 bar respectively, to decompose organic compounds. This process enables energy recovery while an inorganic stable material is produced (Veriansyah and Jae-Duck, 2007, Gidner et al., 2001).

2.1.4 Use of excreta as a fertilizer

Human excreta can be recycled and used as a soil conditioner or a fertilizer. A person is able to produce approximately 1.8 L of excreta per day. This consists of approximately 30 g of carbon, 10 g of nitrogen, 2 g of phosphorous and 3 g of potassium (Cofie et al., 2005). The excreta a person produces in a year is equivalent to the amount of fertiliser required to produce 250 kg of cereal, which is the amount a person could consume in one year (Wolgast, 1993). Therefore, the use of human excreta in agriculture reduces the need of chemical fertilizers, thus increasing the sustainability of agricultural production (Austin, 2001).

Apart from providing essential plant nutrients, excreta can also act as a soil conditioner, unlike chemical fertilizers. A soil conditioner improves the soil structure, increases water-holding capacity, reduces pests and diseases, and neutralizes soil toxins and heavy metals. It can be particularly useful in tropical soils which are in dire need of conditioning (Nikiema et al., 2012).

Cofie et al. (2005) reports the wide use of human waste in agriculture in the northern part of Ghana. This study determined the driving factors, constraints and potential of this practice. The report gives the specific methods used by farmers in handling faecal sludge (from latrines, public toilets and septic tanks) for crop production. This involves long exposure time of the sludge to the relative high temperatures and low air moisture contents from the savannah, which is able to deactivate most of the microorganisms. This method had its demerits in that some farmers still complained of itching feet and foot rot, after working with faecal sludge without wearing protective foot covering. Apart from the filthy smell, problem in transportation and public mockery were constraints in the usage of human excreta (Cofie et al., 2005).

2.2 Pasteurisation

Pasteurisation is defined as the treatment that kills heat sensitive pathogens present in a substance, in order to produce a biologically safe product (Boucher, 1980). The widely known application domain of pasteurisation is in food processing. The oldest and most known form of pasteurisation has been applied for milk processing (Juffs and Deeth, 2007). Although sludge is a different substrate from food products, the general principles of pasteurisation are the same.

In a given pasteurisation process, the first step is to identify the microorganisms to deactivate and define their characteristics. After this, the treatment process to apply, such as heating, addition of chemical reactants, irradiation, use of high electric field pulses, light pulses and oscillating magnetic fields, will be selected (Butz and Tauscher, 2002).

In thermal disinfection, it is important to determine the heating rate to which the material is exposed and the kinetics of disinfection. This will assist to define the time and temperature for process design (Romdhana et al., 2009). For example, for sewage sludge pasteurization, it is suggested heating to a minimum temperature of 71°C for 30 min (Luker et al., 2000).

2.2.1 Types of pathogens

Human excreta contain pathogens, which are organisms that cause diseases. Most of the pathogens are found in faeces while urine is mostly sterile and poses risk only in special cases.

In faeces, microorganisms of concern to humans may be classified into four main groups: bacteria, viruses, protozoa and helminths. Once defecated, bacteria and viruses are instantly infectious. Protozoa and helminths are defecated as cysts. This enables them survive outside the human body for a given period. If the excreted pathogens subsist, they can contaminate the environment and infect new hosts in various ways. These could be from contact with contaminated hands, flies, water, or food (Esrey et al., 1998). The various transmission paths are shown in **Figure 2-3**.

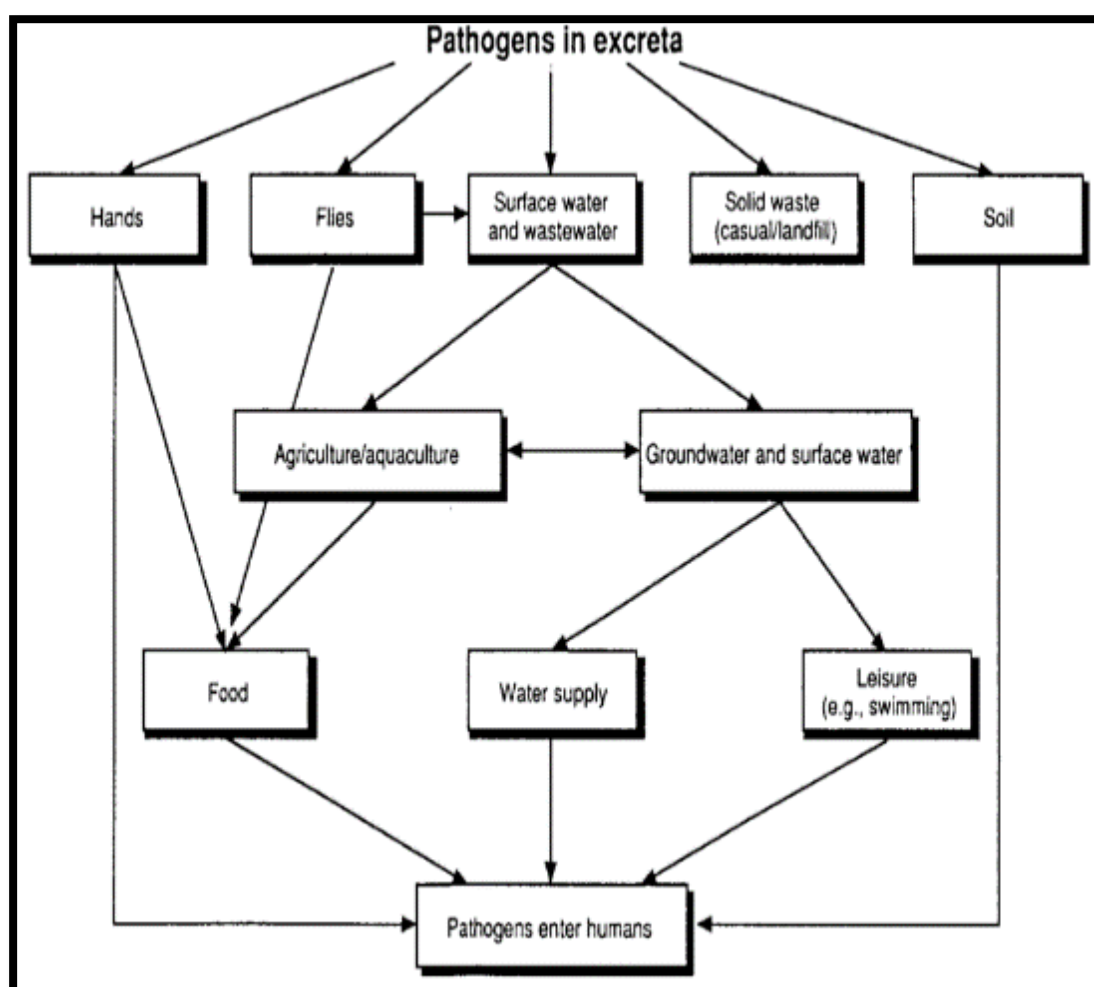


Figure 2-3: Transmission routes of pathogens (Franceys et al., 1992) cited by (Austin, 2001, Phasha, 2006)

Bacteria found in excreta include *Salmonella*, *Campylobacter*, *Enterhaemorrhagic*, and *Leptospira Interrogans*, among others. The mode of transmission for bacterial pathogens is mostly by ingestion, inhalation or via the eyes. The main indicator of presence of bacteria in a sample is through the identification of faecal coliform, *E. Coli*, in laboratory tests.

Protozoa parasites are able to encyst and thus resist chemicals added to water for disinfection. This enables them to survive for long periods. The two best-known protozoa parasites are the *Cryptosporidium Parvum* and *Giardia Lamblia/ Intestinalis*, which are highly infectious to humans. Diseases caused by protozoa include diarrhoea and dysentery. The concentration of protozoa microorganisms may be determined either by direct measurements or by inference. The inference method is applied by determining the concentration in the raw material and the removal efficiency of the treatment process (Teunis and Havelaar, 2002).

Viruses in general are passed through faeces since they mostly affect the intestinal tract. Then, they can infect new hosts after ingestion or inhalation. Some of the viruses in human excreta include rotaviruses, adenoviruses, hepatitis A, reoviruses, enteric viruses and diarrhoea-causing viruses. The common identification method is spiking of samples with high concentrations of viruses and then following their survival, transport and eventual fate at a given set of conditions (Sobsey and Meschke, 2003).

Helminths (parasite worms) do not proliferate within their hosts, unlike the other pathogens. Helminths grow, moult, mature and then produce eggs, which are voided from the host to infect new hosts. Their infections are of great concern in developing countries. They cause serious illnesses by displaying only a few symptoms. When excreta is to be used in agriculture, helminths should be a major concern as they resist most of the commonly used sludge treatment processes. *Ascaris Lumbricoides* are one of the most common helminth types and are highly infectious, affecting to about a quarter of the world population (Phasha, 2006).

2.2.2 Pasteurisation kinetics

Atkinson and Mavituna (1983), and Najafpour (2007) gave a general model describing microbial population decrease from the first order of Chick's law. This model, used to predict the survivor population N , is shown in equation (1). Equation (2) gives the analytical solution of equation (1).

$$\frac{dN}{dt} = -k_d N \quad (1)$$

$$N(t) = N_o e^{-k_d t} \quad (2)$$

N_t microbial population at t [no/gm],

t sterilization time [min],

N_o initial microbial population [no/gm],

k_d thermal death rate [min^{-1}],

After re-arranging equation (2), a linear equation as a function of time, (3), can be obtained.

$$\ln \frac{N(t)}{N_0} = -k_d t \quad (3)$$

Equation (3) can be graphically represented as a straight line with a negative slope of value $-k_d$.

The thermal death rate is a temperature dependent function, which follows Arrhenius law, as shown in Equation (4).

$$k_d = k_0 \cdot e^{-\frac{E}{RT}} \quad (4)$$

k_0 factor of frequency [min^{-1}]

E activation energy [kJ/mol]

R universal gas constant [$\text{kJ}/(\text{K}\cdot\text{mol})$]

T disinfection temperature [K]

The activation energy lies between 251 to 293 kJ / mol for microorganisms, 418 to 628 kJ / mol for spores and 125 to 167 kJ / mol for media with vitamins and protein solution.

An example of disinfection kinetics is shown in **Figure 2-4**. In this case, as temperature increases from 105 to 121°C, the slope of equation (3) increases thus increasing the death rate. This implies that the number of viable cells at a fixed time of sterilisation decreases exponentially with a temperature increase of 16°C.

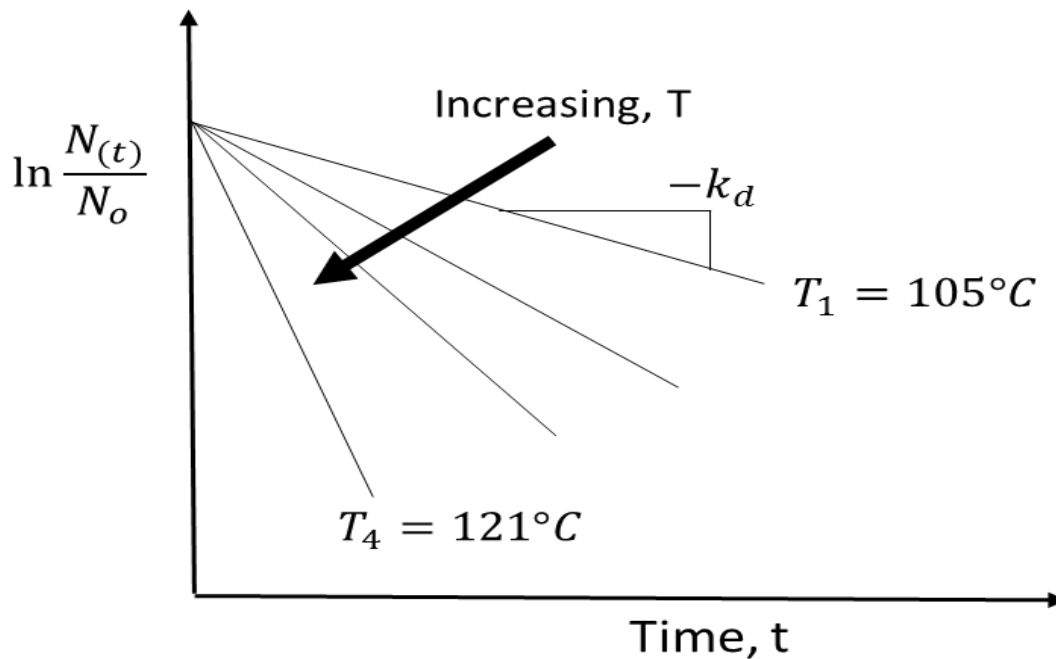


Figure 2-4: Effect of temperature on kinetics disinfection (Atkinson and Mavituna, 1983, Najafpour, 2007)

A commonly used term is the decimal reduction time D , defined as the time to reduce the number of viable organisms by one decade, i.e. a reduction of 90%. (Atkinson and Mavituna, 1983, Najafpour, 2007). This parameter is determined using equation (5)

$$D \text{ (min)} = \frac{2.303}{k_d} \tag{5}$$

k_d is the thermal death rate [min⁻¹]

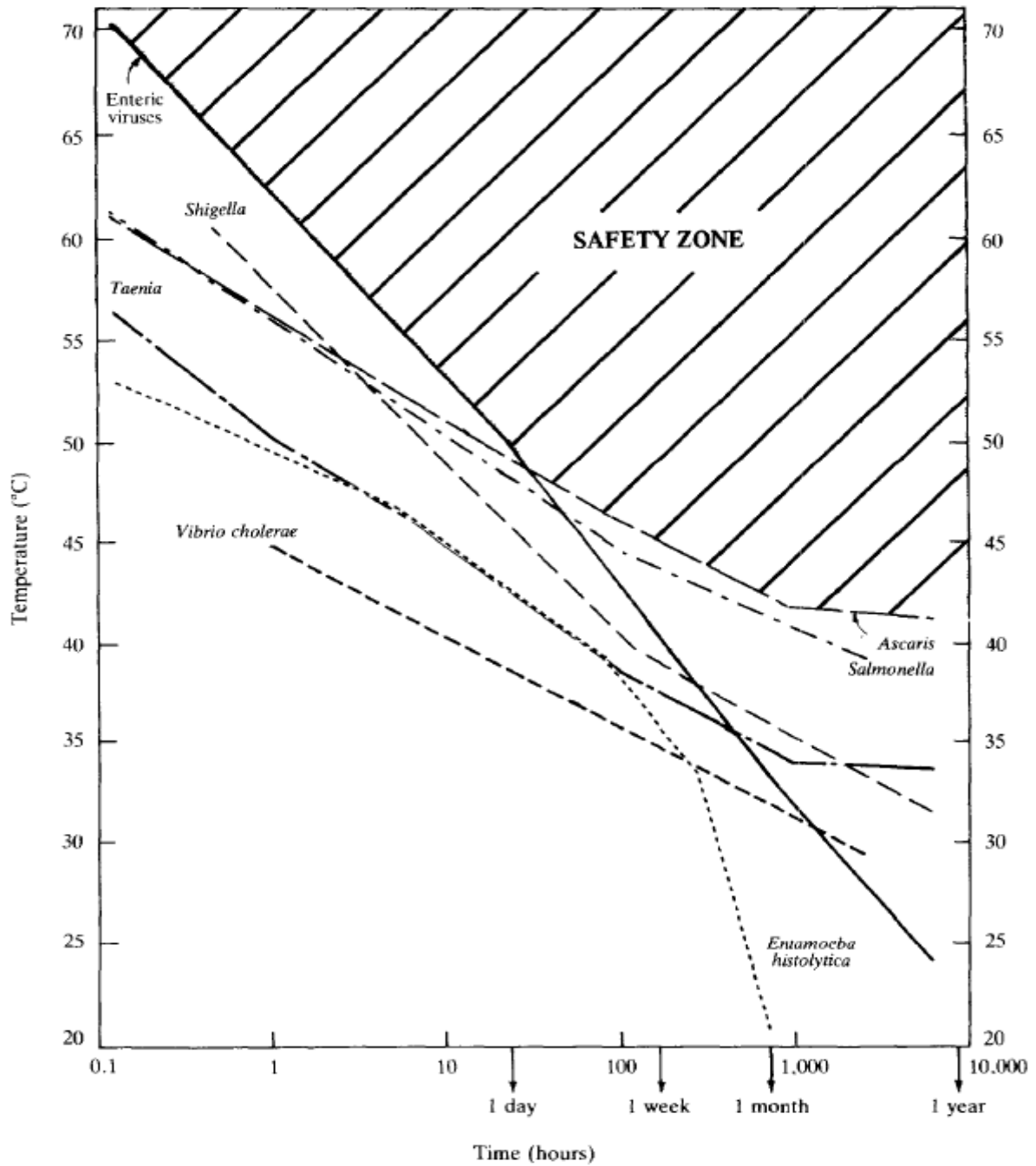


Figure 2-5: Temperature - time relation for the disinfection of pathogens in night soil and faecal sludge (Feachem et al., 1983)

Error! Reference source not found. gives the temperature-time combination required for the inactivation of pathogens. A treatment process with time-temperature on the safety zone should be lethal to all pathogens. The disinfection time needed to be in the safety zone is about one week at a temperature of about 46°C, one day at 50°C, one hour at 62°C and few minutes at temperatures above 70°C.

2.2.3 Indicator of pathogen content

Ascaris eggs are usually chosen as the indicator of pathogens because they are resistant and able to survive in the environment for long periods. They can also be found in great concentrations in the faecal matter. A study was carried out on the survival of microorganisms under various treatment conditions. It was found that after pasteurisation at 90 °C and a pH increase of 3.4, *Ascaris* and *Trichuris* eggs count reduced from 5.9 and 0.8 / g total solids to 2.8 and 0.3 / g total solids respectively, while all *Taenia* eggs were destroyed (Phasha, 2006).

Maya (2012) studied the viability of different helminth eggs under various conditions. At the non-larval stage, *Ascaris* eggs were the most resistant to temperature followed by *Toxocara*, then *Taenia* while *Trichuris* eggs were the most sensitive to temperature. At the larval stage, *Ascaris* eggs were the most resistant followed by *Trichuris*, then *Toxocara* eggs (Maya et al., 2012).

2.3 Drying

Drying is defined as the excessive removal of water or any other liquid from a solid. This process is an essential unit operation with diverse applications in chemical, agricultural, biotechnology, food, polymer, ceramics, pharmaceutical, pulp and paper, mineral and wood processing industries (Mujumdar, 2006).

When a material is exposed to air at a particular temperature and humidity, the material will either gain or lose water until an equilibrium condition is achieved (Coulson et al., 2005). The moisture content of a solid material in thermodynamic equilibrium is referred as the equilibrium moisture content. This varies with both temperature and ambient humidity (Lewis, 1921). There are many forms of drying but thermal drying is the widely used method.

2.3.1 Psychrometry

Psychrometry may be described as the science concerned with the determination of physical and thermodynamic properties of gas - vapour mixtures, most commonly air - water vapour mixtures (Moyers and Baldwin, 1997). An important tool used is the psychrometric chart, which is the graph of the thermodynamic properties of moist air at constant pressure, often equated to that at sea level. These thermodynamic properties include: dry bulb, wet bulb and dew point temperatures, relative humidity, humidity ratio, specific enthalpy and specific volume (McCormick, 2000). Typical psychrometric charts for low, medium and high temperatures are found in Appendix D.

Mujumdar and Devahastin (2000) give various definitions relevant to psychrometry:

- **Absolute humidity** is defined as mass of water vapour carried per mass of dry air. If ideal-gas behaviour is assumed, it can be written as equation (6).

$$H = \frac{M_w p_w}{[M_a(P_{tot} - p_w)]} \quad (6)$$

H	absolute humidity [g/m ³]
M_w	molecular mass of water [g/mol]
M_a	molecular mass of air [g/mol]
p_w	partial pressure of vapour [atm]
P_{tot}	total pressure [atm]

When the partial pressure of the water vapour in the air at a given temperature equals to the vapour pressure of liquid water at the same temperature, the air is said to be saturated and the absolute humidity is designated as the saturation humidity.

- **Percentage absolute humidity**; which gives the percentage of saturation, is the ratio of absolute humidity to saturation humidity at a defined temperature, and is given by equation (7).

$$100 \frac{H}{H_s} = \frac{100 P_w (P_{tot} - P_s)}{P_s (P_{tot} - P_w)} \quad (7)$$

H_s	air saturation humidity [kg/m ³]
p	absolute pressure [atm]
p_s	saturation partial pressure [atm]

- **Percentage relative humidity (RH)** is defined as the partial pressure of water vapour in air divided by the vapour pressure of water at a given temperature: $RH = 100 \frac{p_w}{p_s}$, expressed as a percentage.
- **Dew point, or saturation temperature**, is the temperature at which a given air – water mixture is saturated in vapour ($RH = 100\%$). The unit of measurement is °C.
- **Specific heat** is the heat required to raise the temperature of a unit mass of dry air and its related vapour by one degree. (kJ/kg dry air).
- **Specific volume** is the volume of the dry air and water vapour per unit mass. Saturated volume is the humid volume when the air is saturated. (m³/kg dry air).

- **Wet-bulb temperature** is the temperature reading from a thermometer maintained wet. It refers to the temperature attained by vapour evaporating into an unsaturated gas - vapour mixture. Saturation of the mixture decreases the temperature ($^{\circ}\text{C}$).
- **Dry bulb temperature** is the actual temperature of the gas-vapour mixture (Mujumdar and Devahastin, 2000) ($^{\circ}\text{C}$).

2.3.2 Types of moisture

As described by Robert (1981), there are two different types of moisture found in a material, which give different drying rates. Bound moisture refers to the liquid that is bound to the solid matrix and exerts a vapour pressure less than that of the pure liquid at the same temperature. Unbound moisture is that which exerts a vapour pressure equal to that of the pure liquid at the same temperature. It is not bonded to the solid.

Free moisture is the total liquid content that can be removed at a specific temperature and humidity. It is equal to the average moisture content minus the equilibrium moisture content for the specific drying conditions (Robert, 1981, Mujumdar and Devahastin, 2000).

The various types of moisture found in a material are illustrated in **Figure 2-6**.

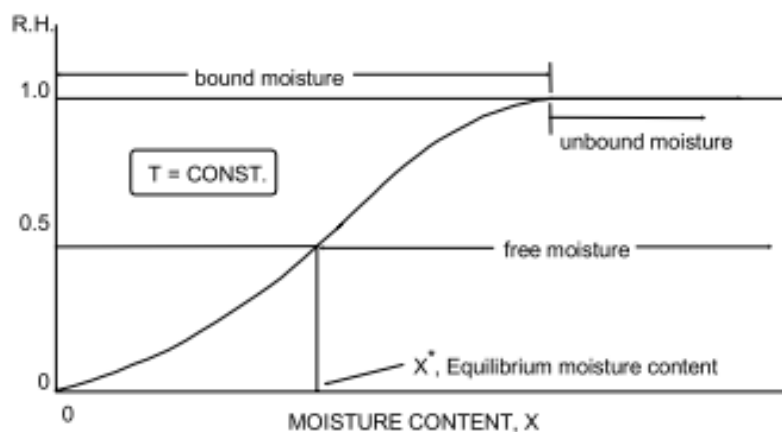


Figure 2-6: Types of moisture found in wet materials (Mujumdar and Devahastin, 2000)

2.3.3 Drying phenomenology

Thermal drying occurs when energy is provided as heat to the solid for the evaporation of its moisture.

The main processes occurring in drying are heat and mass transfer. Heat provided to the material increases its temperature and supplies the required latent heat of vaporisation for both the water within the solid and at the surface (Cserta, 2012). The modes of heat transfer include conduction, convection and radiation. In most cases, they occur simultaneously but distinctions can be made by considering the dominant mode. Heat is transferred from the source to the material by convection or radiation while internal heating occurs mainly by conduction (Welty et al., 2007).

The processes of heat and mass transfer occur at the same time. When heat is supplied to the material, internal moisture migrates to the surface then to the surrounding air through convection or molecular gas diffusion. The driving force for this process is the difference in moisture concentration between the core and the surface (Mujumdar, 2006). The movement of moisture within a solid is influenced by the temperature gradient resulting from the heating phase. The transport of moisture within the material may occur as capillary movement or through diffusion. In capillary movement, evaporation of water from the surface of the material exerts capillary forces, pulling the unbounded moisture through the pores due to the superficial tension created between the water and the material. (Cavusoglu, 2008). Diffusion may be classified as liquid, vapour or surface diffusion. Liquid diffusion occurs if the wet solid is at a temperature that is below the boiling point of the liquid (Mujumdar and Devahastin, 2000). Vapour diffusion occurs when the liquid has been evaporated within the material.

2.3.4 Drying kinetics

In an ideal case the moisture content decrease during drying and can be expressed as a curve from which the rate of the process can be studied. Typically, the drying curve can be divided into three distinct sections: the constant rate period, the first falling rate period and the second falling rate period (Coulson et al., 2005). This may however vary in real cases with some parts of the curves missing entirely from the curve.

Figure 2-7 shows the moisture content curve while drying a wet material according to Moyers and Baldwin (1997). Preceded by section AB the section BC represents the constant rate period. In this stage, internal moisture diffusion occurs rapidly, leading to saturated conditions at the surface of the material. The drying rate is then controlled by external conditions as discussed in the next section. At point C, corresponding to the critical moisture content, the drying rate starts to decrease. The portion CD is known as the falling rate period, which is divided into two parts. In the first falling rate period, the surface cannot maintained saturated by moisture diffusion from the core of the material. During this stage, evaporation is dependent on factors affecting internal and external mass transfer. In some cases, this part of the curve may be absent or constitute the entire falling rate period.

In the second falling rate period, drying is only controlled by moisture diffusion within the solid to the surface and the influence of external factors significantly diminishes. Therefore, this stage is influenced by factors influencing moisture diffusion (Moyers and Baldwin, 1997).

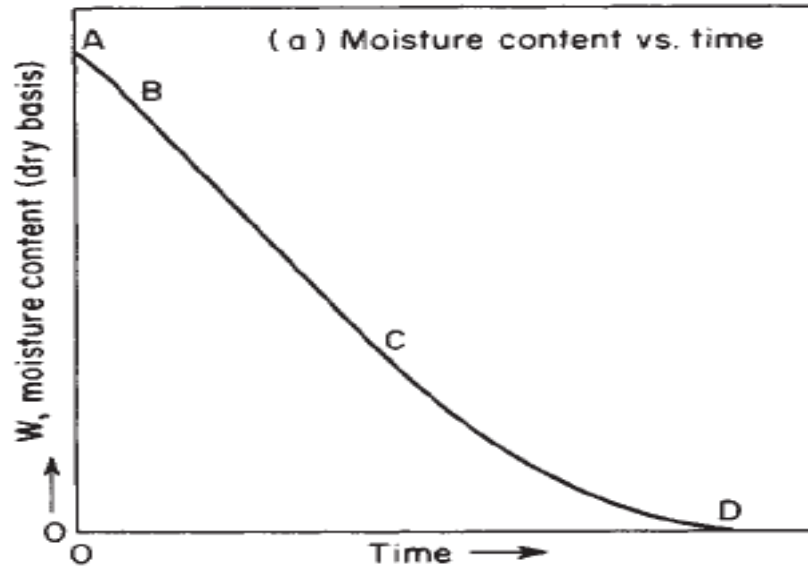


Figure 2-7: Typical drying curve of a wet material (Moyers and Baldwin, 1997)

In certain cases, considerable shrinkage occurs due to excessive surface evaporation after the initial moisture has been removed, thus setting up high moisture gradients between the surface and interior of the material (Mujumdar, 2006).

2.3.5 Factors affecting drying

Factors that affect drying rate may be either internal or external. External factors include air properties, such as temperature, humidity, airflow rate and flow direction. Other external factors include the geometry and size of the solid, the movement of the material and its support in the drying chamber. External factors affect the removal of moisture from the surface of the material and influence drying kinetics mostly during the constant rate period. They also affect the heating rate of the material. (Mujumdar, 2006).

Moisture movement within the material is affected by internal conditions such as material temperature, morphological characteristics and moisture concentration. Material temperature is influenced by internal heating of the solid, which depends on the external heating rate and thermal properties of the material. These factors are the most significant on kinetics during the falling rate period. (Mujumdar, 2006).

2.3.6 Applications of drying in sludge processing

There are few documented applications of drying in the treatment of sludge from pit latrines. Use of drying beds is one of the methods used to dewater sludge. It is used in the treatment of sludge from onsite sanitation facilities (septic tanks, pit latrines, aqua privies and un-sewered community ablution blocks). Drying beds could be planted or unplanted. Drying beds are composed of a sand and gravel layer with an under drain at the bottom to collect leachate. They normally act as a primary treatment method. This is due to ineffective pathogen removal in both leachate and dried sludge and lack of nutrient recovery in the dried sludge. They also require a large area, which is a problem in densely populated areas (Strande et al., 2014).

Drying has, however, been widely applied in the treatment of sludge from wastewater treatment plant. Sewage sludge has some similarities with pit latrine sludge. Raw sewage sludge is seen as unattractive substance due to its high water content of up to 99% (wet basis). This sludge, therefore, has to be prepared for handling by moisture removal. Indeed, drying diminishes volume of sewage sludge per unit of mass and makes it hygienic. This makes it easier to handle. The dried sludge could then be used as a fertilizer or as a soil conditioner, which has a less negative impact to the environment compared to artificial fertilizers (Flaga, 2005). The calorific value of sludge also increases with drying making it suitable to be used as a fuel.

Drying of sewage sludge uses various types of dryers, which may be classified based on the method of heat supply. These dryers include convective dryers, contact dryers and mixed convective-contact dryers. In the convective dryers, hot air comes into direct contact with the material to be dried. The dryers used in this category include pneumatic dryers, drum dryers and fluidized beds. In contact or indirect dryers, heat is provided by contact with a hot surface. They include paddle dryers, hollow flight dryers, disc dryers, and multi-shelf dryers. These have the advantage of reduced odours emission and dust explosion risk. Their disadvantage is that drying takes a longer time, making them less economically attractive.

2.4 Infrared radiation heating

Infrared radiation is considered as thermal radiation because it generates heat, which makes it applicable in thermal drying. The wavelength of thermal radiation ranges between 0.1 and 100 μm in the electromagnetic spectrum (Ratti and Mujumdar, 1995). Based on the wavelength, thermal radiation may be classified into three arbitrary classes:

- near infrared (NIR) with a wavelength range of 0.75 to 3.00 μm ,
- medium infrared (MIR) with a wavelength range of 3.00 to 25 μm and
- far infrared (FIR) with a range of 25 to 100 μm (Mongpraneet et al., 2004).

2.4.1 Production and transmission of infrared rays

Infrared radiation can be produced by heating a body, for example by passing an electric current through an element of high electrical resistance. The hot element radiates thermal energy as infrared radiation, which behaves in a similar way to light radiation. Elements operating at temperatures above 2,000°C have the highest conversion of electrical energy into infrared radiation. Emitters that achieve temperatures lower than 800°C only convert about half of the energy supply into radiation. The remaining energy is dissipated to the surroundings. There are five types of emitters used to generate infrared radiation: short wave heat lamps, short wave quartz tubes, medium wave quartz tubes, long wave metal-sheathed elements and long wave ceramic emitters (Hewitt et al., 1994).

When thermal radiation is incident on a body, it may be absorbed and then converted into heat, and/or reflected from the surface and/or transmitted through the material. The propagation of infrared radiation on an incident body is illustrated in **Figure 2-8**. It can be mathematically expressed by equation (8). The fraction of incident radiation reflected is called reflectivity, fraction transmitted, transmissivity and fraction absorbed is called absorptivity.

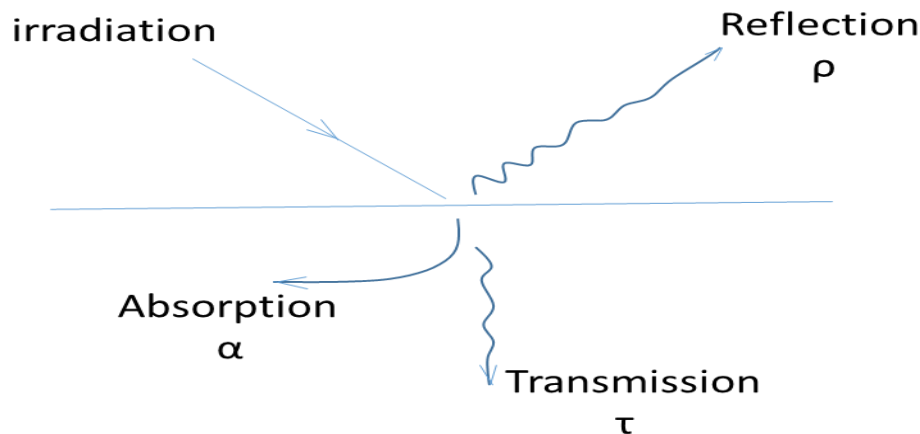


Figure 2-8: Propagation of irradiation on an incident body

$$\rho + \alpha + \tau = 1 \tag{8}$$

ρ reflectivity [-]

α absorptivity [-]

τ transmissivity [-]

In order to accomplish an efficient infrared drying process, it is important to understand the key properties of radiation, which are emissivity, absorptivity, reflectivity and transmissivity. Particularly, emissivity and absorptivity are the controlling factors of heat exchange by radiation. The emissivity of a body is the ratio of its total emissive power to that of a black body at the same temperature. The total emissive power is defined as the total rate of thermal energy emitted via radiation from a surface in all directions and at all wavelengths per unit surface area (Welty et al., 2007). The amount of energy emitted by a body depends on temperature and its characteristics (Ratti and Mujumdar, 1995). A black body is defined as an ideal body absorbing all the incident energy without reflecting or transmitting it. A black body emits maximum radiation per unit area, which is expressed using Stefan Boltzmann equation. It only depends on the fourth power of temperature and is expressed as equation (9).

$$\frac{q}{A} = \sigma T^4 \quad (9)$$

- q energy emission rate [W]
 A area of the emitting surface [m²]
 σ Stefan-Boltzmann constant [W/m².K⁴]
 T temperature [K]

Most bodies do not behave as black bodies but rather as grey bodies. These are defined as bodies with the same emissivity over the entire wavelength spectrum. They also have emissivity of less than one. The net radiation exchange between two grey bodies is given by equation (10).

$$Q_r = \frac{\sigma(T_i^4 + T_j^4)}{\left(\frac{\rho_i}{\varepsilon_i A_i} + \frac{1}{A_i F_{ij}} + \frac{\rho_j}{\varepsilon_j A_j}\right)} \quad (10)$$

- Q_r heat exchange between two bodies [W]
 T_i temperature of surface i [K]
 T_j temperature of surface j [K]
 ρ_j reflectivity of surface j [-]
 ρ_i reflectivity of surface i [-]
 F_{ij} shape or view factor between surfaces i and j [-]
 ε_i emissivity of surface i [-]
 ε_j emissivity of surface j [-]
 A_i area of surface i [m²]
 A_j area of surface j [m²]

The view factor is described by Hewitt et al.(1994) as the geometrical relationship between surfaces exchanging radiation, as illustrated in **Figure 2-9**. In other words, it refers to the fraction of the radiation emitted from A_1 that is intercepted by A_2 . The view factor is expressed as shown in equation (11).

$$F_{12} = \frac{\text{energy leaving } A_1 \text{ that is intercepted by } A_2}{\text{energy leaving } A_1 \text{ in all directions in the forward hemisphere}} \quad (11)$$

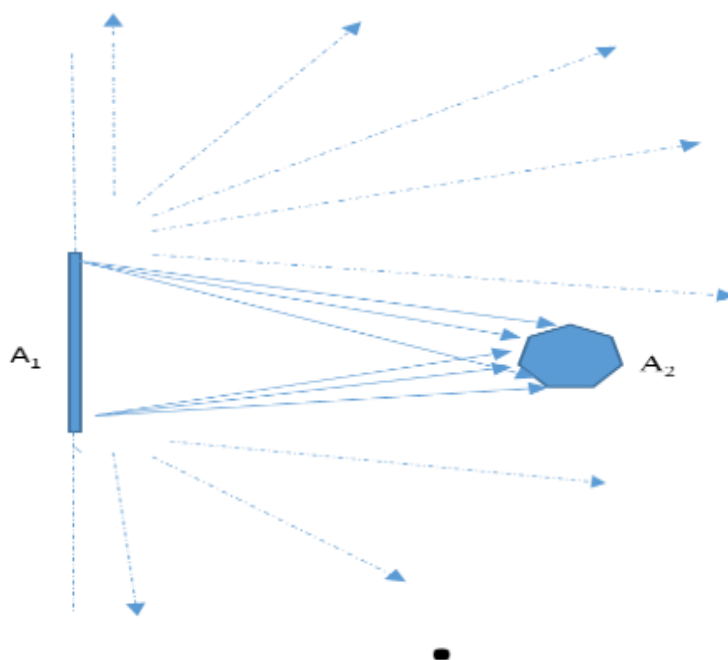


Figure 2-9: Illustration of the view factor (Hewitt et al., 1994)

2.4.2 Design and selection of infrared dryers

Infrared driers can be categorised as either batch or continuous. Ideally, the operation of the dryer must be tested in a laboratory scale prototype as initial phase. This unit will be then scaled up based on experimental data. Relevant parameters include the intensity of radiation, the distance between the material and the emitters, and the residence time. Airflow is required in the heating zone to cool and protect the dryer, as well as to remove the evaporated moisture. The selection between natural or forced convection is based on the level of heating in a given application (Ratti and Mujumdar, 1995).

An important aspect in electrically heated emitters is the peak radiation wavelength. This is inversely proportional to the temperature of the emitter. Emitters at the same temperature will then have the same peak wavelength, which means that they will have similar characteristics. The choice of an emitter for a particular application is based on the type of material to be dried, the area of the material exposed to radiation, the type of control that the process requires and the fraction of convective to radiative heat (Ratti and Mujumdar, 1995).

The type of material is important as it affects the absorptivity of thermal radiation. The properties of importance include colour, roughness and chemical structure. Heat is most commonly applied on flat surfaces compared to surfaces with irregularities, as these take more time to be heated due to shadowed areas that globally decrease the surface of the material available for radiation. Thickness of the material is considered in selection of class of infrared to be used. At short wavelength it is transmitted through water but absorbed at the surface at long wavelength (Sakai and Hanzawa, 1994). It is therefore more appropriate to dry thin materials using FIR infrared and thick materials using NIR radiation (Nowak and Lewicki, 2004).

Another important factor in design of infrared dryers are the conditions under which the plant operates. This leads to design or selection of driers that caters for mechanical shocks, corrosion and thermal shock (Hewitt et al., 1994).

2.4.3 Applications of infrared drying

The literature review conducted did not find any studies on infrared drying of faecal sludge. However, infrared drying has been widely studied on the drying of food products. Some studies compare hot air drying and a combination of infrared and hot air drying (Hebbar et al., 2004, Toğrul, 2006, Nowak and Lewicki, 2004). It was reported that the use of infrared heating increased the drying rate. In a study to model infrared drying of olive husks, it was concluded that when temperature was increased from 80°C to 140°C, the drying time was reduced from 105 to 35 min (Ruiz Celma et al., 2008). Nowak and Lewicki (2004) investigated drying of apple slices using NIR at a peak wavelength of 1 200 nm. The conclusion of the study was that the drying rate was inversely proportional to the distance between the emitters and the irradiated surfaces, and the velocity of the airflow (Nowak and Lewicki, 2004).

2.5 Summary

Conventional latrines and VIP latrines are common sanitation facilities in developing countries, which will probably be a sanitation option for long time. The problem with latrines is that they eventually fill up and thus alternatives have to be searched to continue providing the service. A sustainable option is to empty the full pits and reuse the sludge from the pits. One of the possible reuse of the sludge is as fertilizer, a practice used in countries such as Ghana (Cofie et al., 2005) and Uganda (Schroeder, 2011). This sludge could also be used as a biofuel (Muspratt et al., 2014).

The major problem faced during sludge recycling is the potential high pathogen content of faecal material, which needs to be then deactivated before its use in agriculture. Sludge can also be difficult and expensive to handle, especially if it is wet. Drying could solve both problems. The heat input necessary for the removal of moisture can deactivate the pathogens, and the dried product can be handled more easily and moved with less effort.

Drying can be performed by the use of infrared heating, which has been widely applied with success in various applications. Compared to the conventional convective drying, IR radiation offers the advantage that it penetrates within the material, it is a more efficient mode than convection and that IR dryers are smaller due to their high efficiency. The first application of IR drying in treatment of faecal sludge has been done by the eThekweni municipality, using the LaDePa machine. An investigation was conducted in order to characterise the process and determine the quality of the products for their reuse.

3 Materials and Methods

The purpose of this chapter is to describe the facilities used in the study and to present the experimental procedure. In the first section, the feed material and its preparation are described. The next section describes the laboratory-scale LaDePa plant and its instrumentation. The last section shows the experiments carried out in the LaDePa prototype and the characterization of the sludge before and after processing at different conditions.

3.1 Feed material

Faecal sludge from ventilated improve pit (VIP) latrines was used as the feed material. The sample was collected during pit emptying campaigns in informal settlements within the eThekweni municipality. The sample was a mixture of the sludge from different layers of a single pit. In the laboratory, the sampled faecal sludge was passed through a 5.6 mm sieve. This was done to remove trash material, such as polythene bags, plastics, clothes, metal cans and other kinds of domestic waste, which could interrupt the process. Sawdust was added to the sample in order to improve pellets formation (as explained by section 7.2 in the appendix). The fraction of sawdust represents 4% of the total mass. The faecal sludge was stored in a cold room at 4°C, while not in use. Some of the sludge with sawdust was partially dried and then mixed with freshly collected VIP sludge to obtain a sample with lower starting moisture.

3.2 Experimental facility

A laboratory scale LaDePa was installed in the laboratory of the Pollution Research Group, at the University of KwaZulu-Natal. This machine enables to investigate drying and pasteurisation of faecal sludge from VIP latrines in a controlled environment and at lower operation cost.

3.2.1 Laboratory scale LaDePa

The laboratory scale LaDePa machine is presented in **Figure 3-1**. It is a replica of the pilot plant situated at Tongaat with a size reduction of approximately 10:1. This full-scale plant has slight differences from the pilot scale LaDePa at the Pollution Research Group. It in has a pre-drying zone just after the extruder which utilizes waste heat from exhaust of a diesel engine. The other difference is that the full scale LaDePa is powered by the diesel generator while the pilot LaDePa at the Pollution Research Group is powered by the mains electricity supply. Comparison in terms of size for the laboratory and full-scale LaDePa machine is given in **Table 3-1**. The data generated using the small scale LaDePa is important in the operation of the full-scale plant.



Figure 3-1: Photograph of the laboratory scale LaDePa machine

Table 3-1: Comparison between the laboratory and full scale LaDePa

Feature	Full scale LaDePa	Laboratory scale LaDePa
Belt width (mm)	950	250
Belt aperture opening (μm)	300	200
Heated width (mm)	1 350	220
Heated length (mm)	11 000	880
Number of MIR emitters	3	2
MIR power (kW)	48	3.7
Blower power (kW)	5.5	0.75

The LaDePa machine is composed of three parts: an extruder, the MIR dryer and the control panel. The extruder is composed of a hopper, a screw shaft and a motor. This part was not used in the study due to operation problems, as described in section 3.3.1.

The drying section is composed of a porous steel belt, two medium infrared (MIR) emitters, vacuum chutes and a discharge hopper. **Figure 3-2** shows the inner section of the drying chamber when the MIR emitters are off and on.



Figure 3-2 Drying chamber with the emitters off (left) and on (right)

The steel belt is driven by rollers while its tracking is regulated using compressed air. During operation, pellets produced by the extruder are deposited on the belt and then conveyed into the heating zone where they are exposed to thermal radiation emitted by the two successive MIR emitters. The processed pellets are then discharged at the chute for collection. A vacuum under the belt, created by a blower, induces an airflow in the heating zone in order to remove the evaporated moisture and thus enhance the drying process. A damper valve is placed in the pipe connecting the vacuum chamber and the blower to regulate the airflow through the machine. A schematic diagram of the laboratory LaDePa prototype is shown in **Figure 3-3**.

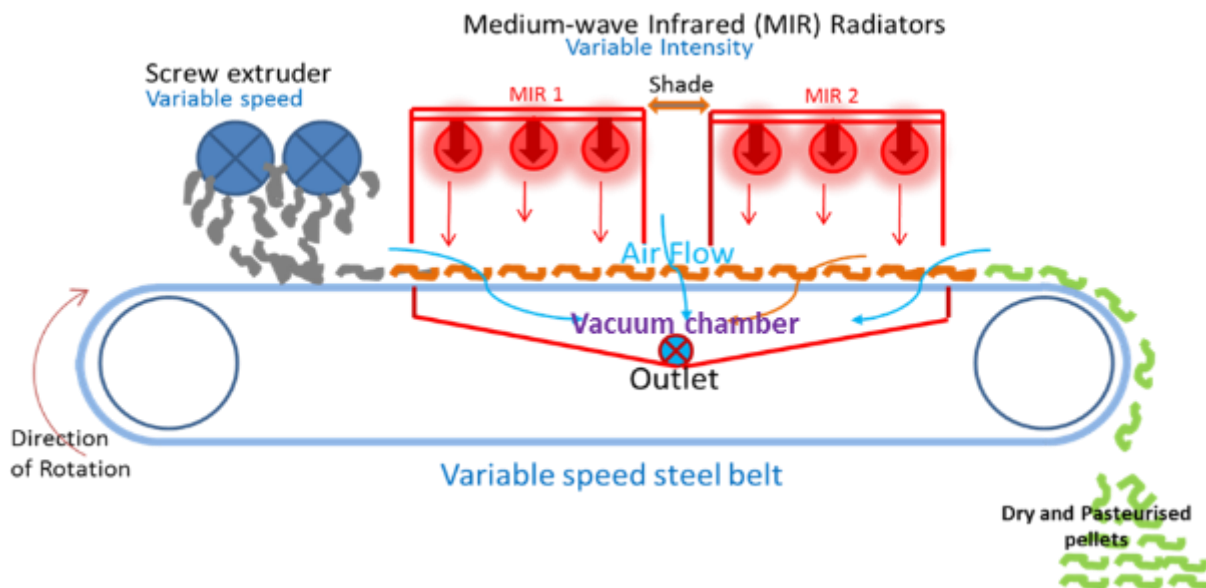


Figure 3-3: Scheme of the laboratory scale LaDePa (Harrison and Wilson, 2012)

The control panel (**Figure 3-4**) is composed of: knobs to regulate the speed of the belt, and the power supply to MIR 1 and MIR 2; the shutdown switch; switches to turn on and off the MIRs, the belt, the screws motor and the blowers; the emergency switch.



Figure 3-4: Control panel of the laboratory scale LaDePa

3.2.2 Temperature measurement

The temperature measurements were performed using k-type thermocouples, which are made from chromel - alumel. This kind of thermocouple has a high accuracy of $\pm 1.1^{\circ}\text{C}$, and is able to measure temperatures up to $1\ 260^{\circ}\text{C}$. These characteristics make it suitable to measure temperatures in LaDePa experiments. The temperature readings as a function of time were recorded in an Easy – log E1 - USB data logger from where the data can be transferred to computer. The drying chamber temperature was monitored by two thermocouples that were placed below the centre of each MIR emitter, 20 mm from the edge and 10 mm above the porous steel belt.

Optical sensors installed on the machine also displayed temperature readings. The readings displayed were however verified to be wrong. This is because these optical sensors are placed in the wrong place. Their position is such that they measure temperature of the belt after cooling by suction air.

3.2.3 Extrusion of pellets

The screw extruder from the LaDePa prototype faced several operation problems as the faecal sludge output rate had high fluctuations and eventually stopped due to clogging. This caused uneven loading on the belt thus leading to inconsistent results. Therefore, pellets were produced using a hand held capillary extruder, shown in **Figure 3-5**.

This device is composed of a polyvinyl chloride water pipe with a diameter of 64 mm, with connectors on either end. Caps are fitted to both sides using the connectors. One of the caps has an air inlet through a valve. The other has a hole with a diameter of 14 mm for the extrusion of the material. Plates of 8, 10 and 12 mm diameter could be inserted on the inner parts of the cap to vary the diameter of the extrusion hole.



Figure 3-5: Photograph of the hand held capillary extruder and plates to vary extrusion size

Prior to operation, the capillary extruder was filled with sludge and connected to the compressed air line. To extrude, pressure was set between 5 and 10 kPa, and then the valve was opened so that the compressed air forced the faecal sludge to go out through the extrusion hole.

3.3 Experimental procedure

This section describes the experiments carried out in the laboratory LaDePa prototype, as well as the chemical, physical and biological analysis performed on the raw sludge and on the resultant pellets.

3.3.1 LaDePa experiments

Experiments in the laboratory scale LaDePa were conducted by varying the residence time, airflow rate around the pellets, emitter's intensity and their distance with respect to the porous steel belt. Both emitter's intensity and distance above the belt have an influence on temperature.

The belt speed can be varied from 0.03 to 1.5 m/min, which corresponds to a residence time interval of 40 to 1 min. Power supply to the MIR emitter was varied using a potential meter, whose operational range is 0 to 100%. At the maximum, power supply is 3.7 kW to each of the emitters. The corresponding power for the different dial positions is given in section 7.1.2 in the appendix. The distance between the belt and the MIR emitters was varied between 50 and 115 mm. Airflow rate was varied by changing the opening angle of the damper valve.

To determine the effect of solid size on drying, the pellet diameter was varied from 8 to 14 mm.

A summary of the different tests carried out is presented in **Table 3-2**. To study the influence of each parameter, the other variables were kept constant.

Table 3-3 presents the different temperatures achieved with different MIR intensities. It shows that different settings had to be used for the MIR emitters to achieve a given drying temperature. The temperature given is the drying chamber temperature as measured by use of K-type thermocouples.

Table 3-2: Summary of the experimental plan

Parameter/variable	Range of operation	Settings used
1) MIR intensity (%)	0 to 100	30, 50 and 80
2) MIR height (mm)	50 to 115	50, 80 and 115
3) Belt speed (%)	0 to 100	55, 35, 30, 27.5, 26, 25
Belt speed (min)	0 to 40	4, 8, 12, 17, 25, 40
4) Pellet diameter (mm)	8 to 14	8, 10, 12 and 14
5) Air flow rate (m/s)	8.2 to 18.3	8.2, 11.1 and 18.3

Table 3-3: MIR intensity settings and corresponding temperatures

MIR 1 Intensity		MIR 2 Intensity		Temperature range	Average Temperature
[%]	[kW]	[%]	[kW]	[°C]	[°C]
25	1.5	30	1.5	84 to 91	87
43	2.4	50	2.3	133 to 140	136
70	3.2	80	3.3	209 to 220	214

3.3.2 Temperature measurement procedure

To understand the heating behaviour of the solid during LaDePa process, temperature was measured on the surface and at the core of the pellets. During these experiments, pellets were placed on the belt and a thermocouple was placed on the top or side surface, or the centre of random pellets, as presented in **Figure 3-6**. This figure demonstrates the position of the pellets below the drying chamber and the different position in which the thermocouple was placed on the pellets. **Figure 3-7** shows the white thermocouple placed inside the dark pellet. A ruler is placed beside it to show the distance of the thermocouple tip from the pellets edge.

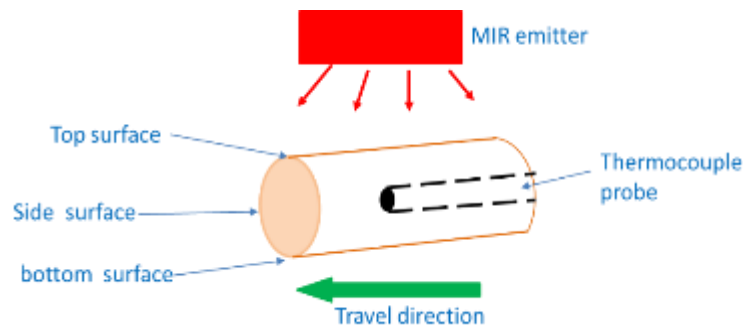


Figure 3-6: Illustration of thermal couple position within the pellets



Figure 3-7: Thermocouple distance in the pellets

All experiments on temperature evolution were carried out at a constant airflow of 18.3 m/s and an average chamber temperature of 136° C, for 8 and 14 mm diameter pellets.

3.3.3 Calibrations in the LaDePa

Calibrations were performed in the laboratory scale LaDePa. The parameters calibrated include the temperature in the drying zone, the power of the MIR emitters and the conveyer belt speed. Temperature calibration involved determining the drying chamber temperature at different dial settings. MIR emitters settings helped determined the power consumed at different MIR setting. Conveyer belt speed helped in determining the actual residence time at different belt speed settings. The calibrations are presented with more detail in **Appendix A**.

The suction airflow rate was determined by measuring the air velocity at the outlet from the blower when the damper valve was fully open, half closed and fully closed: airflow rates were 18.3, 11.1 and 8.2 m / s respectively.

3.3.4 Energy consumption and drying rate calculations

The energy consumed by the emitters was calculated by summing up the product of the power to the emitters and the corresponding residence time. This data was useful in obtaining the trend of energy consumed against the moisture evaporated from pellets by drying.

Drying rate were obtained by first determining the trend line equation for the drying curves. This equation was then used to determine the moisture content for varying residence time. Moisture removed was then calculated by determining the difference in moisture content from the initial and the moisture content for a particular residence time. Drying rate is then the moisture removed per corresponding residence time.

3.3.5 Characterisation of the raw sludge and processed pellets

The pellets processed in the laboratory scale LaDePa were recovered during the experiments and thereafter stored in a cold room at 4°C for further analysis. Moisture content, total solids, volatile solids and ash content were firstly analysed, followed by pathogen, nutrient and thermal analysis. Visual inspections was also done to detect charring or burning of the material.

Rheological analysis was conducted to determine the flow behaviour of the faecal sludge. This study is presented in section 7.2 Appendix B.

3.3.5.1 Moisture content, total solid, volatile solids and ash content analysis

Moisture and total solid content were determined according to the standard operating procedures used at the Pollution Research Group. For this analysis, the sample was placed in an oven at a temperature of approximately 105°C for 24 hours. Total solid is the mass fraction that remains after drying. Moisture and total solids contents are related by equation (12).

$$TS = w_f \quad (12)$$

TS total solids [g]

MC moisture content [g/ g dry solid]

The moisture content is determined by equation (13).

$$MC = \frac{w_i - w_f}{w_f} \quad (13)$$

MC moisture content on wet basis [g water/ g dry solid]
 w_f final weight of sample after oven drying [g]
 w_i initial weight of sample [g]

Ash content is the amount of material that remains after combustion in the oven at 550°C for 2 h. It is calculated by equation (14).

$$\text{Ash content} = \frac{w_{f1}}{w_f} \quad (14)$$

w_{f1} mass after combustion [g]

3.3.5.2 Pathogen content

The concentration of the viable and deactivated parasite *Ascaris*, *Trichuris* and *Taenia* eggs were measured in the raw and processed samples. *Ascaris* eggs are highly resistant to sterilization and pasteurisation treatment processes. Therefore, they are usually used as an indicator of the level of pasteurisation and sterilization. Indeed, it is assumed that all pathogens should be inactivated if *Ascaris* eggs were fully destroyed (Strande et al., 2014). In the method to determine the parasite eggs content, washing, filtration, centrifugation and flotation processes are performed in the sample in order to isolate the eggs from the waste medium. A liquid and solid deposit are then obtained. The deposit is analysed in the microscope to determine the number of viable, potentially viable and dead eggs. Viable eggs are ones, which could infect new hosts if ingested. Potentially viable eggs are ones, which are partially dead. Deactivated eggs are ones, which would not affect new hosts even if ingested. This analysis was done by an external laboratory (parasitology department at Westville campus UKZN).

Laboratory testing for helminths involve incubation of samples, washing, filtration, centrifugation and flotation of the eggs to remove them from the various waste mediums. Ammonium bicarbonate is used both as wash solution and to dissociate the eggs from the soil particles. After this filtration, using 100µm and/or 20µm sieves is done to separate larger and smaller particles from the eggs both after washing and after flotation. The next step is centrifugation. The first step in centrifugation is sedimentation of the deposit after which water is removed before flotation. Finally, sedimentation is done on the final sieved and washed eggs retrieved during flotation. In the flotation process, a solution of zinc sulphate at a specific gravity of 1.3 is used to float eggs with a relative density of less than 1.3 out of the matter retained after using a 20µm sieve. After this, the sample obtained is placed on a microscope. The microscope is then used to examine and count the viable and dead helminth eggs.

3.3.5.3 Nutrient analysis

Chemical analyses were done to determine the content of the samples on chemical compounds valuable in agriculture.

Elemental analysis was performed in a Microwave Plasma - Atomic Emission spectrometer (Agilent 4100 MP - AES). It utilizes nitrogen gas to produce plasma discharge. Samples are first atomised prior to passing through the plasma where electrons are excited. These electrons produce light whose spectrum and intensity is measured by a detector calibrated for each element. The analysed elements included phosphorous, potassium, calcium and magnesium, which are all macronutrients. Prior to the analysis, 0.1 g of the sample was mixed with 10 ml of nitric acid and the overall was placed in a microwave digester, model Ethos 1-Milistone, where it was heated up to 130°C for 1 h for the dissolution of the solid.

Ammonium, nitrates, nitrites and phosphates were determined in a SQ 118 photometer using standard operating procedures developed by the Pollution Research Group. The photometer test involves first converting the sample into a coloured compound by the use of reagents. Buffer solutions are also added to set the pH to a given value. The chemicals added to the sample are available as a commercial test kit. The colour intensity of the solution, which is measured using the photometers as absorbance, corresponds to the concentration of the ion of interest.

Total ammonia was determined by diluting the solid in a strong alkaline to form monochloramine, which turned into a blue indophenol derivative after adding a thymol solution. Total phosphates were determined by reacting orthophosphate ions with molybdate in a sulphuric solution to form molybdophosphoric acid, which was then reduced by ascorbic acid to form blue phosphomolybdenum. Total nitrate was determined by reacting the solid with 2,6-dimethylphenol in a phosphoric solution, reaction through which the nitrate ions are converted into 4-nitro-2,5-dimethylpheno, which is white in colour. Total nitrite was determined through the formation of a reddish purple azo dye at a pH between 2.0 and 2.5, by coupling diazotized sulphanilamide with 1-Naphthyl-ethylenediamine dihydrochloride.

3.3.5.4 Thermal analysis

Thermal analysis was conducted to evaluate the use of processed pellets as biofuel. The properties to analyse include calorific value, heat capacity, thermal conductivity and thermal diffusivity. The calorific value was determined in a Parr 6200 oxygen bomb calorimetric where the sample was combusted in a high-pressure oxygen atmosphere. The heat released by combustion was measured and lead to the determination of the gross calorific value.

Heat capacity, thermal conductivity and thermal diffusivity were determined using the C-Them TCi. A volume sample of 2.5 ml is placed in a test cell sensor. The TCi then produces a current that results in a temperature rise between the interface of the sample and sensor. This induces a voltage drop on the heater element, which is then translated into effusivity values. Conductivity and thermal diffusivity are then calculated. Heat capacity is then deduced by density, previously measured.

3.3.5.5 Summary

Table 3-4 lists the properties investigated, the equipment and method used for the analysis, and the reasons for carrying out the test.

Table 3-4: Summary of the analyses done in the raw faecal sludge and processed pellets

Property	Equipment /method of analysis	Interest of the analysis
Moisture content (MC)	Oven drying at 105°C for 24 hr.	Indicator of the level of drying
Ash content	Incineration in muffle furnace at 550°C for 2 hr.	Indicator of eventual thermal degradation of the solid
Ascaris, Trichuris, Taenia egg concentration	Egg count by use of a microscope	Indicator of pasteurisation
Nitrates , nitrites, ammonia and phosphates contents	SQ118 Spectrophotometer	Indicator of the agricultural value of the processed sludge
Potassium, phosphorous, calcium and magnesium contents	MP-AES	Indicator of the agricultural value of the processed sludge
Thermal conductivity, heat capacity and thermal diffusivity	TCi machine	Parameters related to the drying and combustion characteristics of the material
Calorific value	Bomb calorimeter	Indicator of the value of the material as a biofuel

3.3.6 Data statistical analysis

For each set of conditions during the experiments in the laboratory scale LaDePa, three runs were performed and three pellets were collected per run. From the data obtained at given conditions, the mean value were calculated using equation (15).

$$\bar{x} = \frac{\sum_{i=1}^n x_i}{n} \quad (15)$$

\bar{x} mean value

n number of samples

x_i individual value of the sample

Standard deviation refers to the average deviation with respect to the mean value. It is calculated by equation (16).

$$\sigma_n = \sqrt{\frac{1}{n} \sum_{i=1}^n (x_i - \bar{x})^2} \quad (16)$$

σ_n standard deviation [-]

The actual values (x) lies between the uncertainty bar and is calculate using equation (17)

$$x = x \text{ average} \pm s \quad (17)$$

x actual values

s uncertainty

The uncertainty bar was determined through t-Student distribution using a confidence interval of 95%, using equation (18).

$$s = \frac{\sigma}{\sqrt{n}} \quad (18)$$

3.4 Characteristic time and dimensionless analysis

Characteristic time is the theoretical time required for a given process to occur when it is controlled by a particular phenomenon. The characteristic time analysis is used to evaluate the phenomenon that has the greatest influence on a process by comparing their time scales (Septien, 2011). Dimensionless numbers can be determined from the ratio of characteristic times.

Characteristic time analysis could be employed in order to characterize the physical phenomena in the LaDePa process. No literature was found about characteristic time application in the drying process. It has however been used in the pyrolysis, combustion and gasification processes (Septien, 2011, Dupont et al., 2007), in which heat and mass transfer has some similarities to drying.

During drying pellets in the LaDePa machine, the phenomena considered are the internal conduction, external convection and radiation. Indeed, pellets are heated by radiation and at the same time cooled by suction airflow at ambient temperature. Internal heat transfer is assumed to occur by conduction. A Characteristic time analysis may be done by direct comparison of various phenomena characteristic times or by intermediary of dimensionless number. It is said that the later procedure is more practical in determining the limiting phenomenon in a process but it does not reveal the time scale. The two methods are therefore used together as they complement each other (Septien, 2011).

3.4.1 Characteristic time calculations

Some of the ratios of characteristic times that could be relevant to the LaDePa process are presented in **Table 3-5**. The ratio of radiation to convection compares the amount of heat pellets absorbs from the emitters to that of cooling by suction air. The ratio of radiation to conduction compares external heating to internal heat transfer and thus help determine whether the pellet is isothermal during processing. The LaDePa pellets are cylindrical in shape thus the equations used are those of geometry shape.

Table 3-5: Dimensionless numbers related to drying

Ratio between external radiation and convection	t_{rad} / t_{conv}
Ratio between external radiation and internal conduction	t_{rad} / t_{cond}

t_{cond}	characteristic time of internal heat conduction [s]
t_{conv}	characteristic time of external heat convection [s]
t_{rad}	characteristic time of external radiation [s]

The expression of external convective heat is presented in equation (19).

$$t_{conv} = \frac{\rho_p \times C_{p_p} \times d_p}{4 \times h_t} \quad (19)$$

ρ_p	particle density	[kg/m ³]
C_{p_p}	particle heat capacity	[J/kg/K]
d_p	particle diameter	[m]
h_t	heat exchange coefficient	[W/m ² /K]

The heat and mass exchange coefficients are calculated from Nusselt and Sherwood numbers in equation (25) and equation (26) respectively. They can be expressed as a function of Pr and Sc respectively, and Re in both cases.

The Reynolds number (Re) is an important parameter in fluid mechanics as it characterizes the flow regime as laminar and turbulent. It compares the inertial to the viscous forces in a flow. It is calculated using equation (20).

$$Re = \frac{\rho v d_p}{\mu} \quad (20)$$

Re	Reynolds number [-]
ρ	density of the fluid [kg/m ³]
v	velocity of the fluid [m/s]
μ	fluid dynamic viscosity [Pa.s]

At values lower than 2000, the flow is considered laminar. At values higher than 4000, the flow regime is turbulent. A transition zone lies between the two regimes. At large Reynolds numbers, the inertial forces are more dominant than the viscous ones, and the thickness of boundary layer of the fluid is small. At small Reynolds numbers, viscous forces dominate and the boundary layer is thicker.

The Prandtl (Pr) number gives the ratio of momentum diffusivity to thermal diffusivity. It is determined using equation (21). It compares the thickness of the velocity and thermal boundary layers. At $Pr = 1$ the boundary layers are equal.

$$Pr = \frac{\nu}{\alpha} = \frac{c_p \mu}{\lambda} \quad (21)$$

Pr	Prandtl number [-]
ν	momentum diffusivity [m ² /s]
α	thermal diffusivity [m ² /s]
C_p	specific heat of the fluid [MJ/ (kg.K)]
λ	thermal conductivity of the fluid [W/m.K]

Typical values of Pr numbers are as low as 0.004 to 0.03 for liquid metals and as high as 50 to 100 000 for oils. Gases have intermediate values, which range from 0.7 to 1.0.

The Nusselt number (Nu) is the ratio of convective to conductive heat transfer across the boundary layer. It gives an indication of the convective heat transfer at the surface and is calculated using equation (22).

$$Nu = \frac{h_t L}{\lambda} = f(Re, Pr) \quad (22)$$

h_t coefficient of convective heat transfer [W/m².K]

L characteristic length [m]

At values close to zero, heat transfer at the solid surface is mainly by conduction, while at high values heat transfer by convection is dominant.

The Nu and Sh numbers can be expressed by equations (25) and (26) respectively. These equations are valid for certain conditions: in this case, for cylindrical geometry (as LaDePa pellets could be considered) and for Pr and $Sc \geq 0.2$.

$$Nu = 0.3 + \frac{0.62Re^{1/2}Pr^{1/3}}{[1+(0.4/Pr)^{2/3}]^{1/4}} \times \left[1 + \left(\frac{Re}{282,000} \right)^{5/8} \right]^{4/5} \quad (25)$$

$$Sh = 0.3 + \frac{0.62Re^{1/2}Sc^{1/3}}{[1+(0.4/Sc)^{2/3}]^{1/4}} \times \left[1 + \left(\frac{Re}{282,000} \right)^{5/8} \right]^{4/5} \quad (26)$$

Characteristic time of internal heat conduction is expressed by equation (27).

$$t_{cond} = \frac{\rho_p \times Cp_p \times d_p^2}{16 \times \lambda_p} \quad (27)$$

λ_p particle thermal conductivity [W/m.K]

Characteristic time for external radiative heat transfer is calculated from equation (28).

$$t_{rad} = \frac{\rho_p \times Cp_p \times d_p}{4 \times \omega_p \times \sigma \times (T_g + T_p) \times (T_g^2 + T_p^2)} \quad (28)$$

t_{rad} characteristic time of external radioactive heat transfer [s]

ω_p particle emissivity [-]

σ Boltzmann constant [W/m².K⁴]

T_p initial particle temperature [K]

T_g temperature of the emitters [K]

Temperature at the surface of the emitter was calculated from equation (29).

$$E_b = \sigma T_g^4 \quad (29)$$

E_b emissive power (w/m²)

The properties of air at ambient temperature (293 K) used for the characteristic time calculations are presented in Table 3-6.

Table 3-6: Air physical properties at 293 K

Density (kg/m ³)	Specific heat (MJ/(kg·K))	Thermal conductivity (W/m. K)	Kinematic viscosity (×10 ⁻⁵ m ² /s)	Coefficient of water diffusion in air (×10 ⁻⁵ m ² /s)
1.67	0.001	0.03	1.60	3.00

3.4.2 Pellet properties in characteristic time calculations

The properties of processed pellets used in the characteristic time calculations are presented in Figure 4-4. Pellets have a dark brown colour, therefore the emissivity value was assumed as 0.9. Heat capacity and thermal conductivity were the values measured for pellets with a moisture content below 0.3 g / g dry solid. These results are presented in section 4.5.2 and 4.5.3. The constant of ideal gas and Boltzmann constant were 8.315 J / mol.K and $5.67 \times 10^{-8} W / m^2 \cdot K^4$ respectively.

Table 3-7: Pellets physical properties

Diameter (m)	Density (Kg/m ³)	Initial temperature (K)	Heat capacity (J/kg.K)	Thermal conductivity (W/m.K)	Emissivity (-)
0.008	800	293	440	0.06	0.9

4 Results and Discussion

This chapter presents and discusses the results from the experimental work conducted in the laboratory scale LaDePa. The first section is about the measurement of temperature at the surface and interior of the processed pellets during the process. The second section focuses on the study of the influence of several parameters on drying performance of LaDePa. The third section deals with the pasteurisation performance while the last sections are dedicated to the nutrient and thermal analysis.

4.1 Characteristic time analysis

Dimensionless numbers and characteristic times at different airflow rates are presented in **Table 4-1**. These results were obtained with a 4mm diameter pellet processed with the emitter at a height of 115 mm from the belt surface.

These values show that airflow through the drying chamber was laminar for all the experiments conducted, as Re was lower than 2 100. The Pr and Sc number are within the common range for gases, between 0.6 and 0.7. The Nu and Sh numbers are comprised between 1 and 10. This shows that the contribution of convection to external transfers is quite moderate.

The characteristic time of convective heat transfer increases with the decrease of airflow around the pellets. This is an expected result because a reduction of the airflow reduces air velocity, leading to the subsequent decrease of the heat transfer rate.

At the airflow rate investigated, the characteristic times ratio of radiation to convection resulted in values significantly lower than one. This suggests that the heating of the particles by radiation from the MIR emitters was considerably more important than the convective cooling effect from the suction air. The characteristic time of radiation and internal conduction are in the same order of magnitude with a ratio close to one. This implies that the heating of pellets is not isothermal.

Table 4-1: Dimensionless numbers and characteristic times for different suction air flowrates

Parameter	Air flow rate (m ³ /s)		
	18.3	11.1	8.2
<i>Re</i> (-)	273	166	122
<i>Pr</i> (-)	0.7	0.7	0.7
<i>Nu</i> (-)	9.4	6.6	5.7
<i>Sh</i> (-)	7.5	5.9	5.1
<i>h_t</i> (W.m ⁻² .K ⁻¹)	3.0	2.1	1.8
<i>h_m</i> (m.s ⁻¹)	1 990	1 563	1 353
<i>t_{conv}</i> (s)	235	335	388
<i>t_{rad}</i> (s)	13	13	13
<i>t_{cond}</i> (s)	23	23	23
<i>t_{rad}/t_{conv}</i> (-)	0.06	0.04	0.03
<i>t_{rad}/t_{cond}</i> (-)	0.6	0.6	0.6

The characteristic times as a function of pellet diameter at an airflow rate of 18.3 m³ / s are given in **Table 4-2**. The values show that the characteristic time of convection, radiation and internal heat conduction increase with the increase of pellet diameter. This is expected as larger pellets take more time to heat.

The characteristic time ratio of radiation to convection remains the same with the increase of pellet diameter. This suggests that increasing pellet diameter does not influence the heating mechanisms of the pellets (heating by radiation much more important than cooling by convection).

The ratio of radiation to conduction decreased did not vary significantly. This implies that the rate of heating for the 14 mm diameter pellets is also not isothermal.

Table 4-2: Characteristic times and their ratios for different pellet diameters

Parameter (-)	Pellet diameter (mm)	
	8	14
t_{conv} (s)	235	410
t_{rad} (s)	13	23
t_{cond} (s)	23	72
t_{rad}/t_{conv} (-)	0.06	0.06
t_{rad}/t_{cond} (-)	0.55	0.31

4.2 Temperature of pellets during drying

. In the investigation on the evolution of pellet temperature during drying, the data obtained at the surface and core of the 8 and 14 mm diameter pellets is presented in Figure 4-1, 4-2, 4-3, 4-4, 4-5 and Figure 4-6. Temperature change for the 8 and 14 mm diameter pellets is the same. It increases as pellets pass under the first MIR emitter, then decreases in the transition zone. It increases again under the second MIR emitter and finally decreases as pellets exit the machine.

4.2.1 Heating of 8 mm diameter pellets

Two aspects of temperature evolution for the 8 mm diameter pellets were investigated. The first investigated temperature variation with change of residence time. The second case investigated the difference in temperature at core and surface for the same residence time.

The core temperatures of the 8 mm pellets at different residence times, as a function of distance from the inlet of the drying chamber, is presented in **Figure 4-1**. The curves followed a similar trend under the first emitter while in the second emitter the curve obtained at 30 minutes residence time had a sharp increase. At a residence time of 30 min, pellets were exposed to prolonged heating compared to lower residence time. The residence time of 30 min may have facilitated complete drying of the surface of the pellets leading to the sharp increase in core temperature.

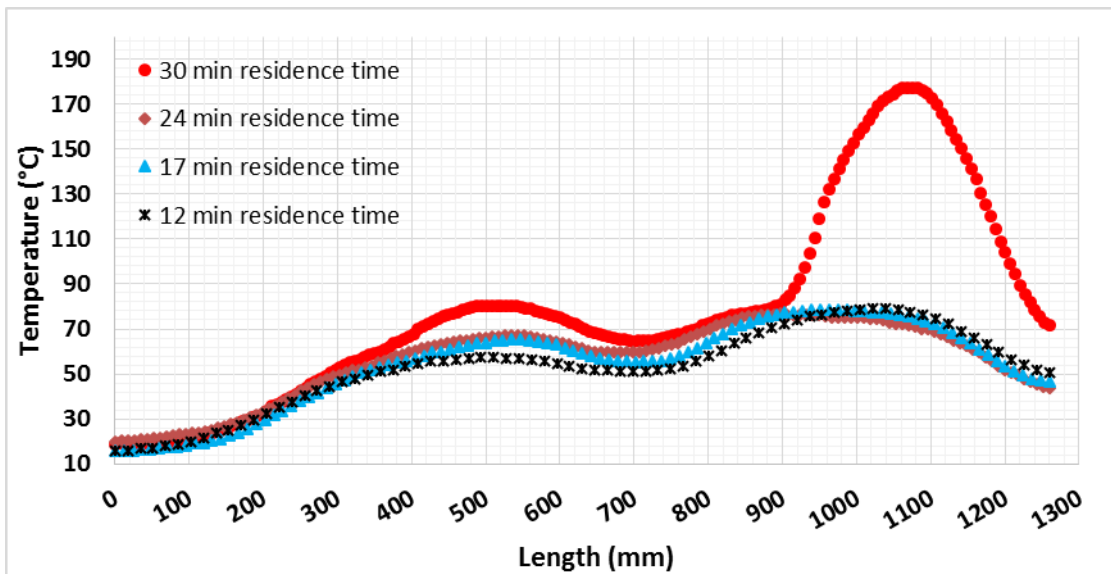


Figure 4-1: Temperature at core of the 8 mm pellets at different residence times as a function of length from the inlet of the drying chamber

The surface and core temperature of the 8 mm pellets is shown in Figure 4-2.

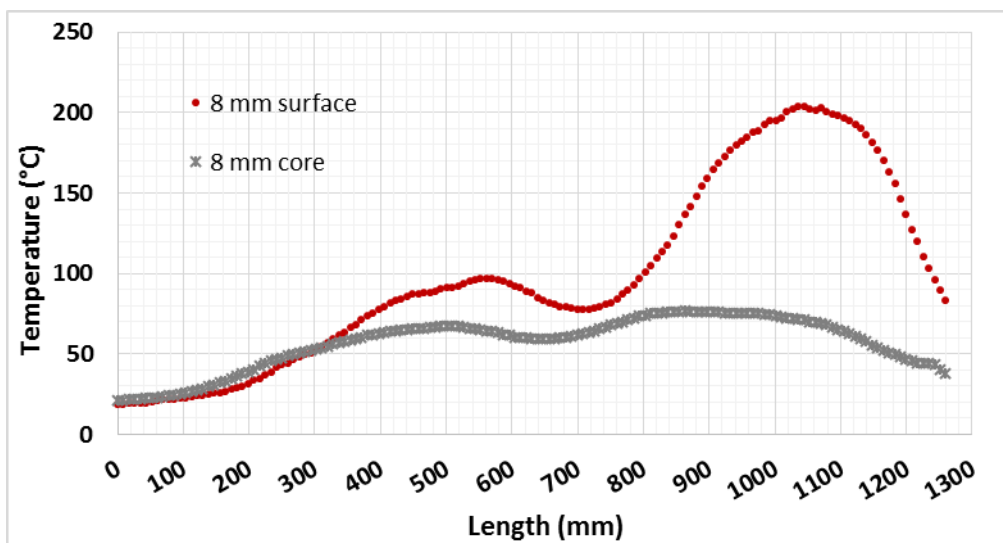


Figure 4-2: Surface and core temperatures of the 8 mm pellets during processing in the laboratory scale LaDePa

At the initial stage of drying, heat was transferred quite evenly within the pellets, and thus surface and core temperature were almost the same. As drying progressed, temperature became higher at the surface than at the core of the pellets. Core temperature did not rise above the boiling point of water (100°C) and attained a maximum of 80°C while at the surface it increased up to 200°C. This could be explained by moisture evaporation at the core, which kept it cool. It is further supported by data from section 4.3.1.2 where it was found at the conditions used drying is controlled by external factors. On the contrary, the surface was considerably dried and hence its temperature increased. The temperature difference between the surface and core of the pellet shows that drying of pellets was not isothermal during the process (Cserta, 2012). Therefore drying is more likely to be controlled by external factors since it mostly occurs in the constant rate period.

4.2.2 Heating of 14 mm diameter pellets

The evolution of temperature for the 14 mm diameter pellets, as a function of length in the drying chamber, is presented in **Figure 4-3** (temperature measured from the side and top surface of the pellet with respect to the emitter). The results show that higher temperatures were measured at the top of the pellets compared to the side. Indeed, the pellets were more exposed to the IR at the top compared to the side.

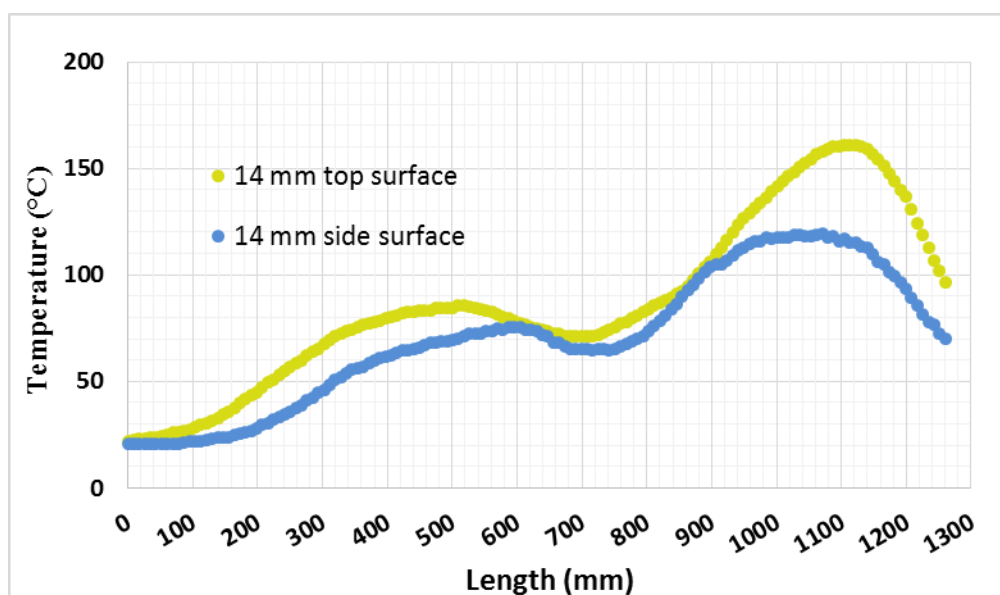


Figure 4-3: Temperature at the top and side surfaces of the 14 mm pellets during processing in the laboratory scale LaDePa

The evolution of temperature at the core and the surface of the 14 mm pellets is shown in **Figure 4-4**. These results are similar to those of 8 mm pellets where the surface temperature became higher than that of the core as drying progressed.

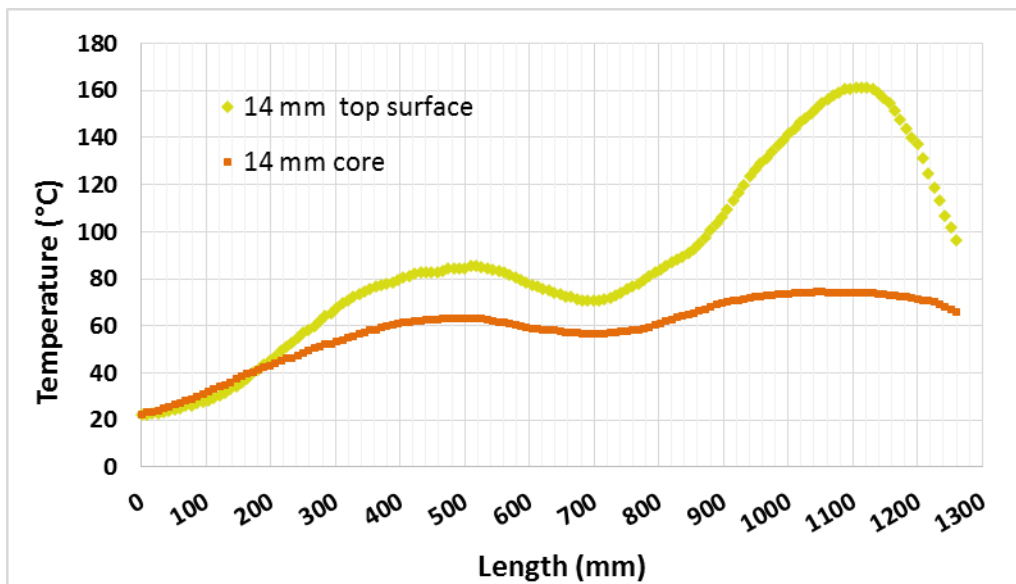


Figure 4-4: Temperature of 14 mm pellets as a function of the length from the inlet of the drying chamber

4.2.3 Comparison of the heating of 8 and 14 mm diameter pellets

Figure 4-5 presents the temperature evolution at the surface of the 8 mm and 14 mm pellets. The surface temperature of the 8 and 14 mm diameter pellets differed slightly as pellets passed through the first emitter. Under the second emitter, temperature of the 8 mm pellets increased considerably faster than the 14 mm diameter. This could be due to longer heat transfer for the 14 mm pellets compared to 8 mm pellets, leading to lower temperature for the 14 mm pellets.

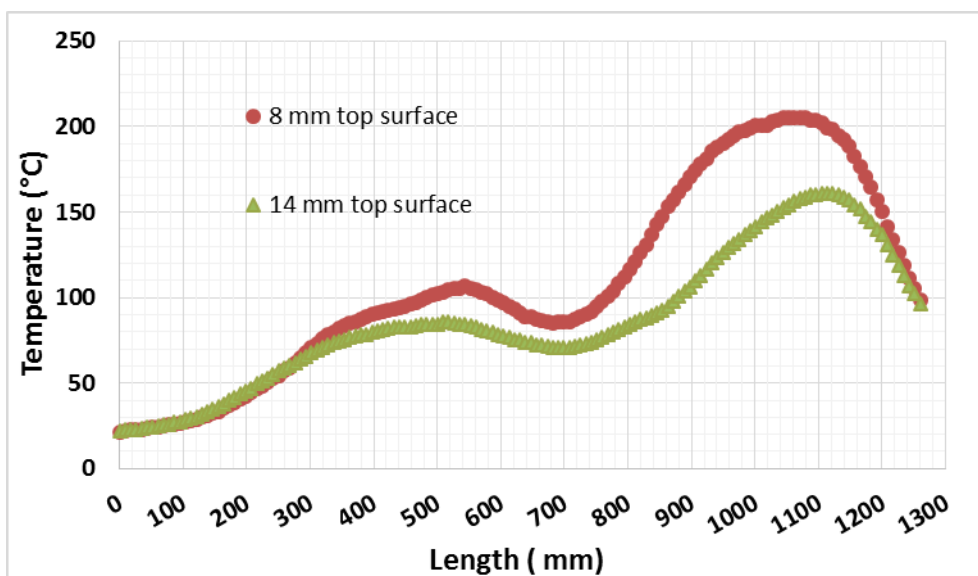


Figure 4-5: Surface temperature of the 8 and 14 mm pellets as a function of length from inlet of the drying chamber

The comparison between the core temperature of the 8 mm and 14 mm diameter pellets during the experiments is presented in **Figure 4-6**. Temperature at centre of the pellets was similar between the two pellet diameters. The only difference is that the 14 mm diameter pellets take a longer time to heat and cool as indicated by the temperature profile under the second MIR emitter. The reason for the prolonged time for cooling and heating is due to the larger size, which increase the time for heat transfer compared to the 8 mm pellets.

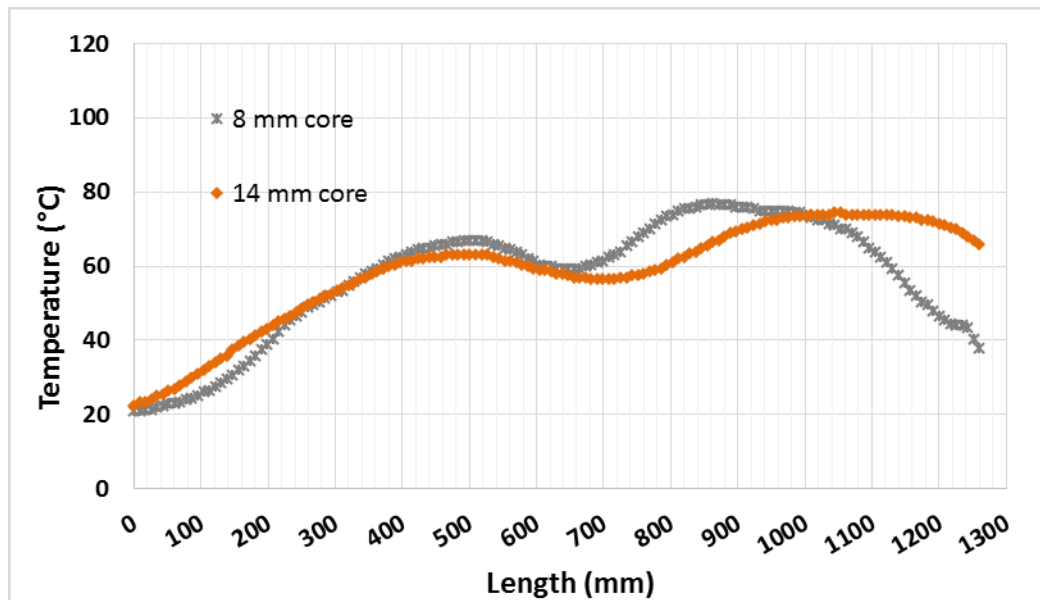


Figure 4-6: Core temperature for 8 and 14 mm diameter pellets as a function of length from the inlet of the drying chamber

4.2.4 Summary on temperature evolution for different pellet diameter and residence times

The temperature profile obtained at different residence time, pellet diameter, at the surface and core of pellet show that generally temperature increases with drying and as pellets are exposed to radiation from the emitters. There was no documented literature found on sludge drying investigating the temperature evolution. However, a study by Cserta on infrared wood drying gave similar results. The study found that the core and surface temperature increased with increase in irradiation time. However, the core temperature had a lag and remained constant at 90°C, which is below the boiling point of water. At an irradiation, time of 450 min the core temperature started to increase and finally surpassed the surface temperature. The stagnation in core temperature is caused by rapid evaporation occurring at the surface leading to lower heat transfer to the core (Cserta, 2012). These results conform to the ones found in this study and explains the reason for the rapid increase in core temperature at a residence time of 30 min shown in Figure 4-1. At prolonged drying time, all the core moisture has diffused to the surface and thus the latent heat of vaporisation has stopped causing an increase in core temperature.

4.3 Influence of the operating parameters on drying

The parameters that affect drying are presented in this section. Parameters investigated are the MIR emitter intensity, emitter height above the conveyer belt, airflow in the heating zone, pellet diameter and type of sludge. In studying each of the parameters drying curves, drying rates, volatile solid and ash content and lastly energy consumption during drying were studied.

Drying curves present the moisture lost in the sample after processing in the LaDePa at different residence time.

Drying rate curve were obtained by first calculating the amount of moisture lost during drying and dividing by the residence time used to process the pellets. These values are then plotted against the residence time. The limitation in this method of obtaining drying rate is that it depends on the accuracy of the drying curve values.

Volatile solids indicates the amount of combustible matter while the remaining material (ash content) indicate the inert material. The combustible content indicates the amount of material available for energetic purposes while the inert content indicate amount of waste that would be generated.

For the determination of energy consumption, the power input into the emitters presented in section 7.1.2, was multiplied by the residence time. The values obtained were then plotted versus the amount of moisture removed during pellets drying. In this case, values of residence time and moisture removed were obtained from the drying curve. For example 1.01 g water / g solid was removed in 9 min at an MIR intensity of 25%, which corresponds to a power rating of 1.5 W for each of the emitters. Therefore, the total energy consumed is 0.45 kWh

4.3.1 MIR emitter intensity

This section presents the study on the effect of varying MIR intensity and consequently the drying temperature. Three sets of MIR intensity were investigated and their influence on drying rate, volatile solids/ash content and on energy consumption determined. Intensities used were 30% (84°C), 50% (134°C) and 80% (121°C). This corresponds to power input of 1.5, 2.4 and 3.3 kW respectively. The intensities indicated correspond to the second MIR while the temperature is for both first and second emitter as presented in section 3.3.1.

4.3.1.1 Drying curves

The drying curves obtained after variation of the power input into the emitters are presented in **Figure 4-7**. The experiments were carried out at a constant airflow rate of 18.3 m³/s, height of emitters above the belt of 115 mm and pellet diameter of 8 mm.

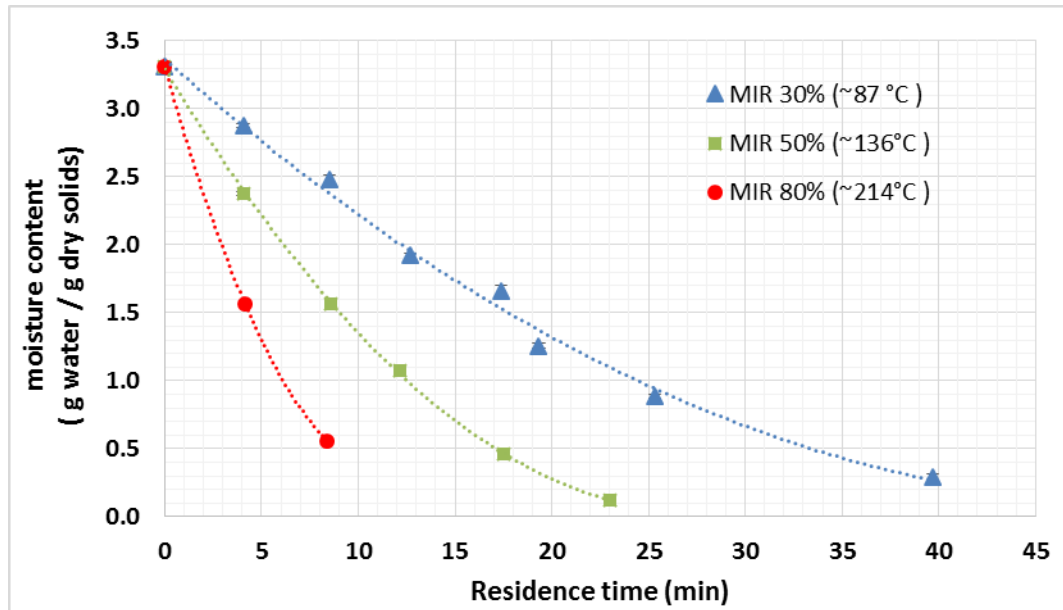


Figure 4-7: Drying curves at different MIR intensities

The drying curves show that as the infrared intensity and so the drying temperature was increased, the drying time reduced. The shape of the drying curves were similar to those from other studies, mostly from food drying (Cserta, 2012, Habib et al., 2014, Hebbar et al., 2004, Mongpraneet et al., 2004). An increase in power level (increasing emitter intensity) from 40 W to 100 W reduced the time required to dry onions from a moisture content of 11.5% to about 2% (dry basis) by about 100 min (Mongpraneet et al., 2004). The time required to reduce the moisture content of onion slices to 0.06 g water/dry matter at emitter intensities of 300, 400 and 500 W was 9, 7 and 4 min (Sharma et al., 2005).

At a residence time of 8 min and a temperature of about 214°C, pellets start to undergo charring. At a residence time of 12 min, pellets were completely burnt, so moisture content at higher residence time and intensities could not be measured. Charring of synthetic sludge at emitter intensities of 80% and residence time of 20 min was observed in earlier experiments using the laboratory scale, belt, MIR emitter, LaDePa dryer (Xiangmei et al., 2014).

A study on wood drying states that high emitter intensities lead to the fast drying of the solid surface, which can cause formation of a crust. This is opposed to the movement of moisture from the core to the surface, thus reducing surface cooling by moisture evaporation. It then leads to the accumulation of heat at the surface, eventually resulting to charring (Cserta, 2012).

4.3.1.2 Drying rate

The drying rate behaviour at different emitter intensities as a function of residence time is presented in **Figure 4-8**. Globally, the drying rate increased with increase in emitter intensity and consequently with increase in drying temperature. As residence time was increased drying rate remained relatively constant for the MIR 30% (87°C) which show that drying occurs at the constant rate period. Drying rate for MIR 50% (136°C) and MIR 80% (214°C) decreased with increase in residence time. This means that drying occurs in the falling rate period. These results on drying rate indicate that at higher intensities drying is controlled by diffusion while at lower intensities drying is more likely to be controlled by external factors since it mostly occurs in the constant rate period.

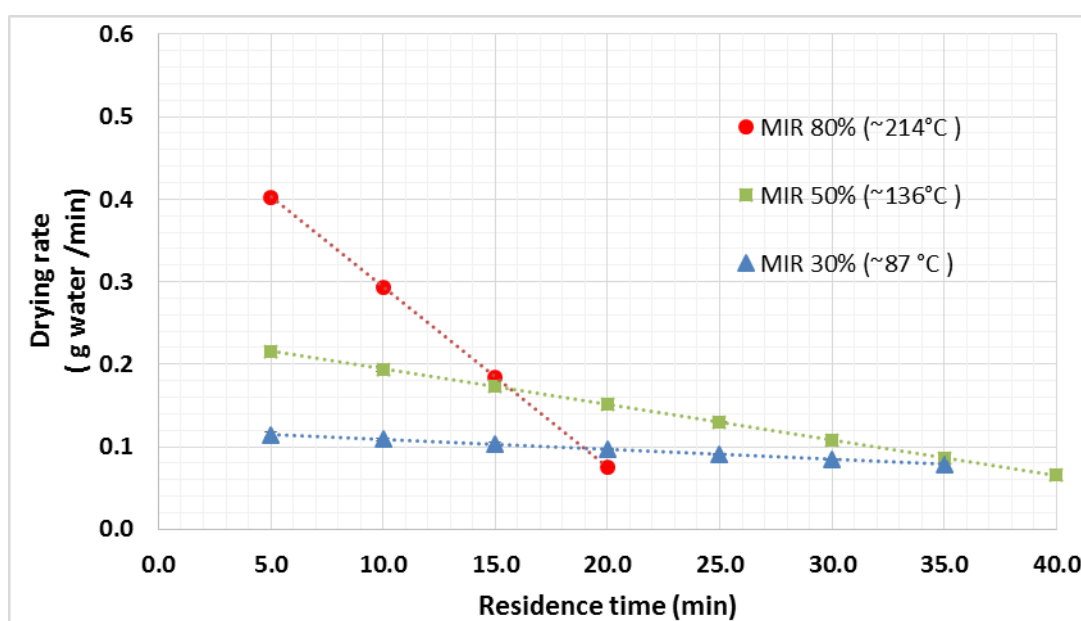


Figure 4-8: Drying rate as a function of residence time at varying emitter intensity

4.3.1.3 Volatile solids and ash content

The volatile solids and ash contents of pellets, as a function of the residence time for different MIR intensities, is presented in **Figure 4-9** and **Figure 4-10** respectively. Volatile solids and ash content did not vary in a particular trend with increase in residence time. Most of the samples had a volatile solid content of between 69 and 70 % total solid while the ash content ranged between 29 and 31%. The exception was the sample processed at 214°C, after 8 min of residence time where pellets had slightly lower volatile solids of 67% and higher ash of about 33% content. This could be due to thermal degradation of pellets, leading to the loss of volatile matter and the subsequent increase of ash content. This could have been the reason why smoke was observed during the experiment with the pellets obtained being seemingly darker and charred on the surface.

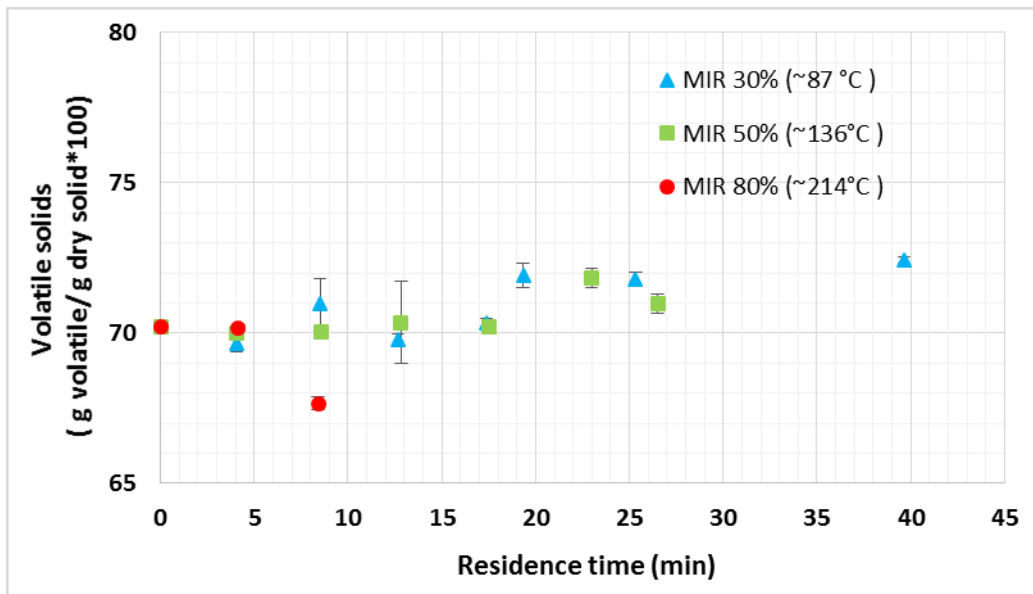


Figure 4-9: Volatile solids content at different MIR intensities at varying residence time

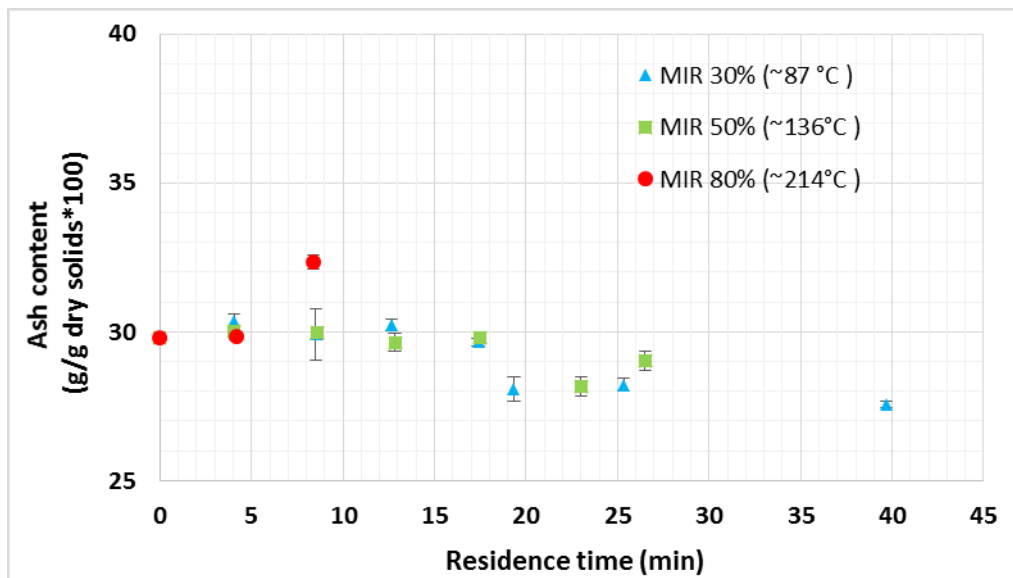


Figure 4-10: Ash content at different MIR intensities

4.3.1.4 Energy consumption

Figure 4-11 presents the power consumed by the two emitters as a function of moisture content removed from processed pellets at different MIR intensities. The energy required to remove a given amount of moisture decreased by increasing the MIR intensity. For example to remove 2.35 g water / g solid (27% wet weight) the energy consumed is 1.2, 1.02 and 0.65 kWh at 30, 50 and 80% intensity respectively. This implies that it would be a more affordable option to use higher intensities for drying since the process will require less energy.

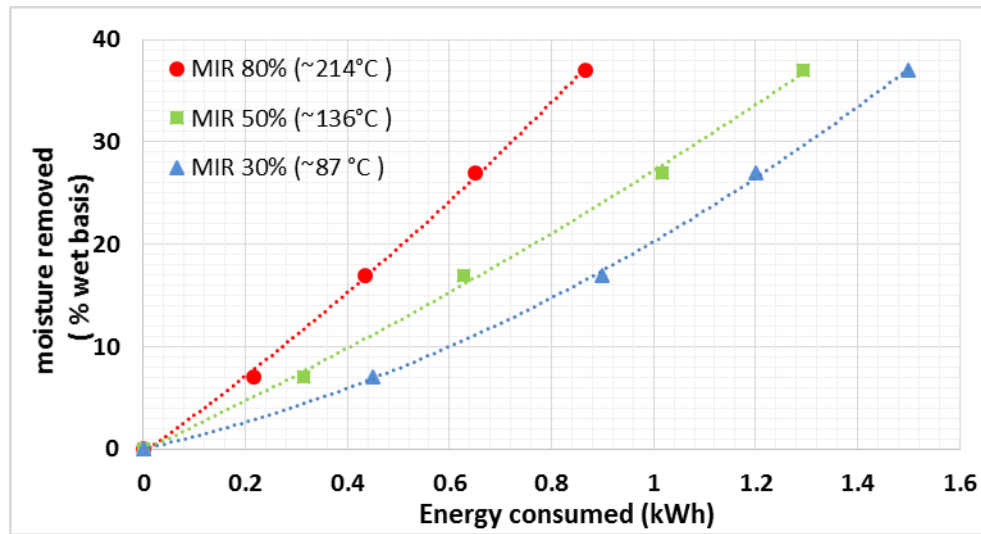


Figure 4-11: Energy consumption as a function of moisture removal at different MIR intensities

4.3.2 Effect of distance between the emitters and the pellets

To determine the effect of the distance between the emitters and the pellets, the height of the emitters above the porous belt was varied. Temperature was maintained constant at an average of 136°C by varying the power supply to the emitters. This was achieved after calibration of the emitter power as described in section 7.1.2 in the appendix section. To maintain a constant drying temperature, the power supply to the emitters was decreased while the height of emitters above the belt was reduced and vice versa. Airflow was kept at 18.3 m³ / s and the pellet diameter was 8 mm.

In this section, only the drying curves and energy consumption at varying emitter height were studied.

4.3.2.1 Drying curves

Drying curves obtained after varying the height of the emitter above the belt are presented in **Figure 4-12**. It shows that height of the MIR above the belt does not influence drying curve. This implies that similar drying behaviour can be obtained at different emitter's height so long as the drying temperature is kept constant.

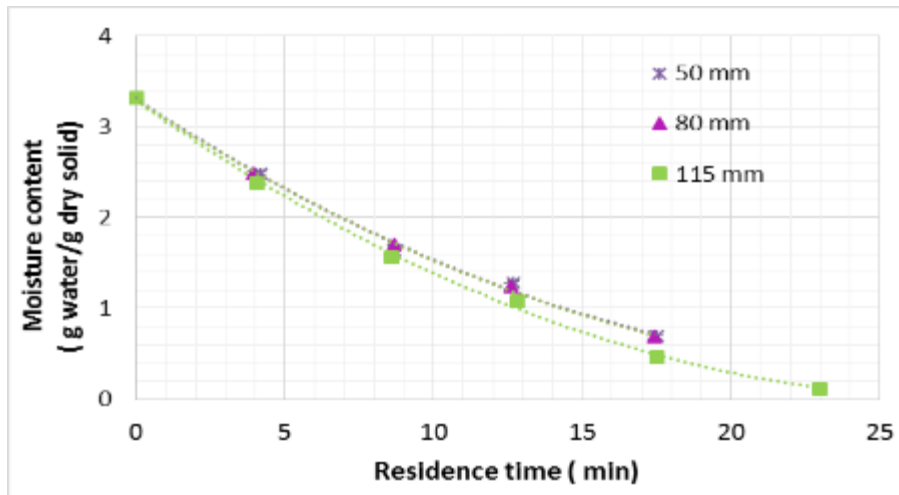


Figure 4-12: Drying curve at different emitter heights above the belt

4.3.2.2 Energy consumption

Figure 4-13 shows the moisture removed versus the energy consumed at different emitter heights above the belt. It can be seen that at height of 115 mm above the belt, more energy is used compared to heights of 50 mm and 80 mm. In the LaDePa process, not all energy is incident on the pellets some of it is lost to the conveyor belt and sidewalls. As the height of the emitters above the belt is increased, part of radiation incident on the pellets decreases. This leads to decrease in energy utilized in processing of pellets.

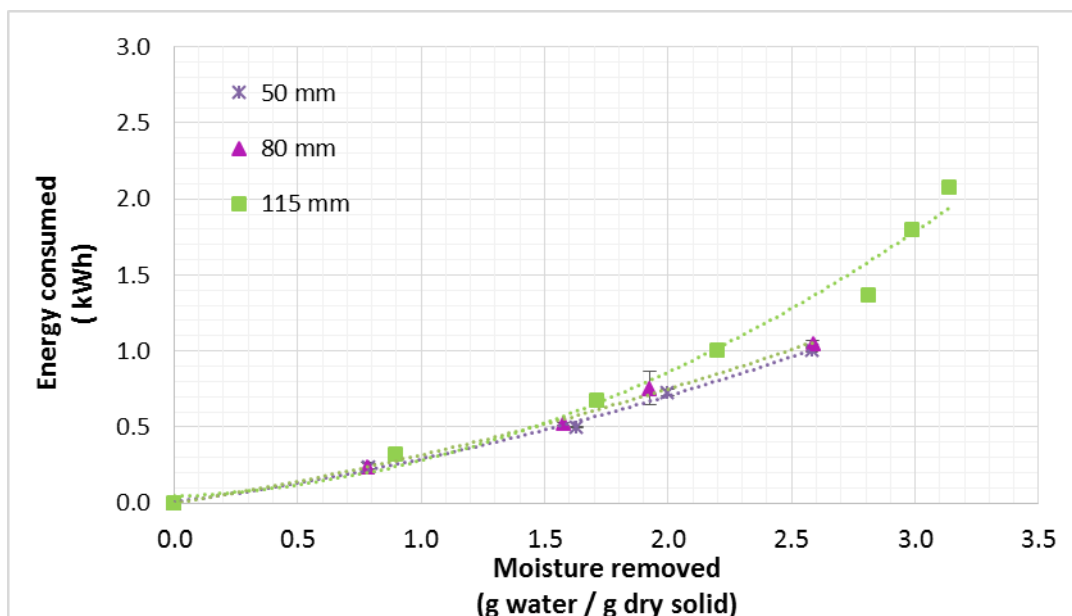


Figure 4-13: Moisture removal as a function energy consumption at different emitter height above the belt

4.3.3 Effect of airflow around the pellets

The effect of airflow around the pellets on drying was investigated in two cases. In the first case, emitter intensity was maintained constant while the position of the draught damper valve was changed. This caused drying temperature to vary as the ambient air drawn into the drying chamber caused cooling.

In the second case, emitter intensity and damper valve position were changed such that drying temperature remained constant. When the airflow rate was decreased, the emitters' intensity was decreased to maintain a constant drying temperature, as the cooling effect of the airflow in the drying chamber was lower. For these experiments, the pellet diameter was maintained at 8 mm, and the height of the emitters above 115 mm.

4.3.3.1 Drying curves

The drying curves obtained with different airflow rate are presented in **Figure 4-14**. At constant intensity, the drying curves were similar for the two airflow rates. This result could be explained as the lower mass transfer rate caused by lower airflow rate was counterbalanced by lower cooling effect.

At a constant temperature, achieved by adjusting emitter intensity, decrease in airflow leads to less mass transfer rate by air flowing over the pellets thus increasing drying time. This implies that reduction in cooling effect by reduction in airflow rate into the drier does not have a positive influence to the drying process.

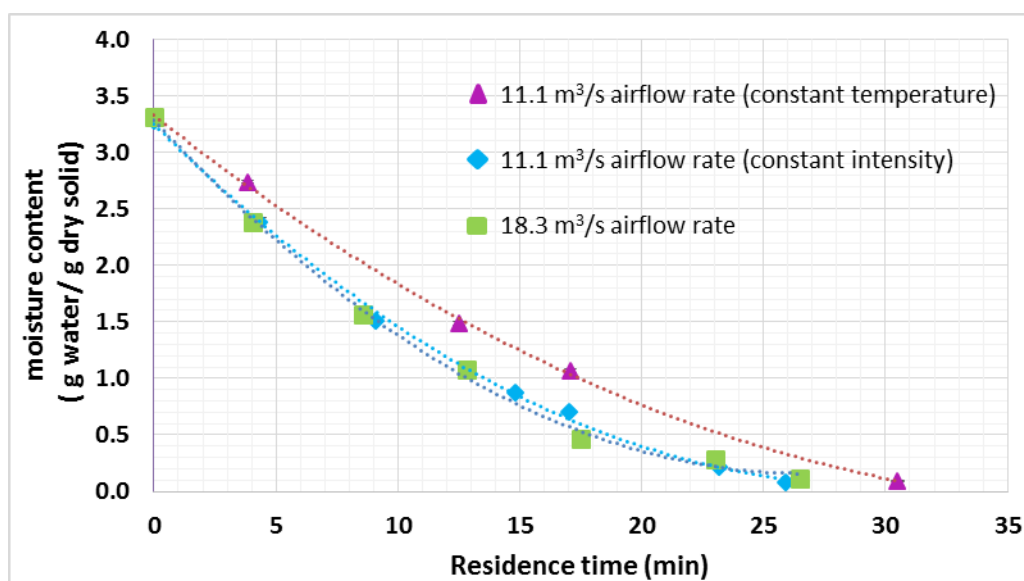


Figure 4-14: Drying curves for different airflow rates

4.3.3.2 Drying rate

Drying rates at different airflow rates around the pellets at varying moisture content are depicted in **Figure 4-15**. The curves obtained show that decreasing airflow rate decreases drying rate. Reduction in emitter intensity to achieve a constant temperature decreased the drying rate the most. This implies that drying is enhanced by higher airflow. This is despite the fact that air flowing over the pellets causes their cooling.

The curves also show that drying occurs in the falling rate period. This implies that drying is controlled by diffusion of moisture from the interior of the pellets.

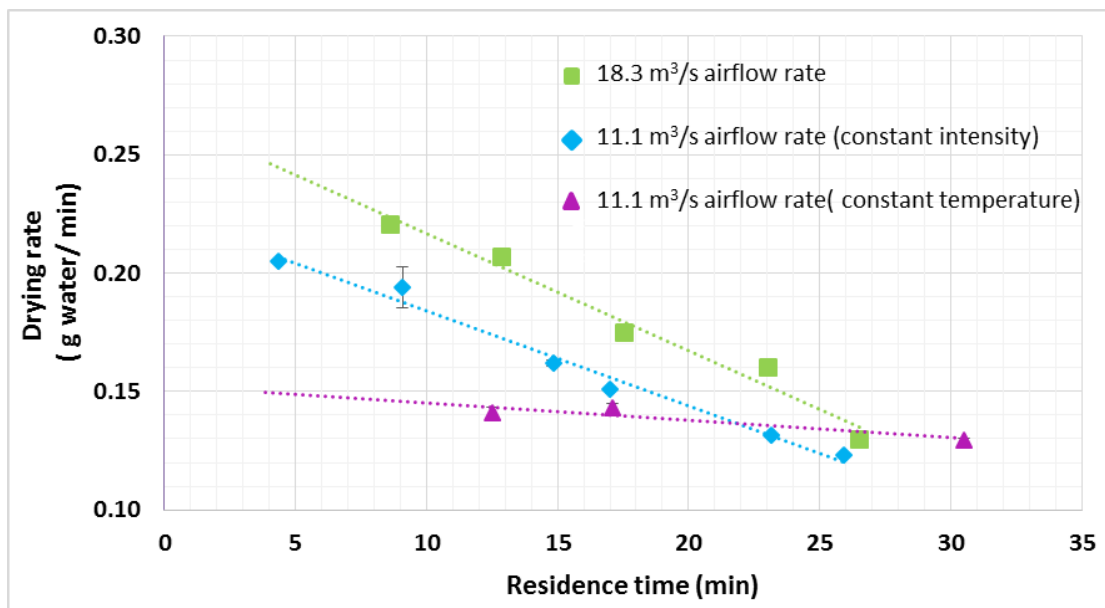


Figure 4-15: Drying rate at different airflow rate around pellets

4.3.3.3 Energy consumption

Energy consumption as a function of moisture removal at varying airflow rate is shown in **Figure 4-16**. Under the conditions investigated, energy consumption did not vary with change in the rate of airflow around the pellets. This implies that airflow rate has an insignificant effect on energy consumption in the laboratory scale LaDePa

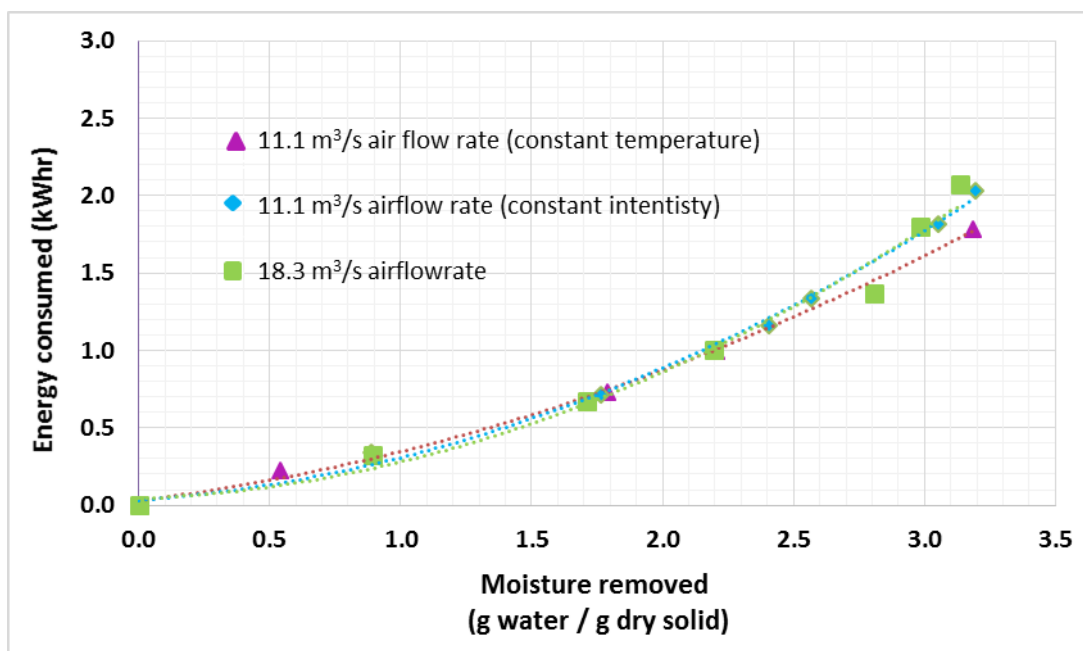


Figure 4-16: Energy consumption as a function of residence time at varying airflow around pellets

4.3.4 Effect of pellet diameter

The influence of four different pellet diameters on in processing was investigated. For this, the pellets were processed at a constant average temperature of 136°C, airflow of 18.3 m³ / s and an emitter height above the belt of 115 mm.

4.3.4.1 Drying curves

Results on drying curves for different pellet diameters are presented in **Figure 4-17**. Pellets with a larger diameter had longer drying time compared to those with lower size, as it could be expected.

The 14 mm pellets had the longest drying time followed by the 12, 10 and finally 8 mm pellets. At a residence time of 25 min, pellets with a diameter of 8 mm were dried to a moisture content below 0.5 g water / g dry solid while the pellets with a diameter of 14 mm had a moisture content of 1.2 g water / g dry solid. The results obtained are consistent with previous studies in literature where drying time increases with the increase of sample thickness (Praveen et al., 2005, Swasdisevi et al., 2007, Swasdisevi et al., 2009, Liu et al., 2014). This is due to the decrease in the effect of infrared penetration, heat transfer rate and mass transfer with increase in sample size (Krishnamurthy et al., 2008). The higher mass tranfer in smaller diameter pellets could also be due to higher surface area to volume ratio compared to larger diameter pellets.

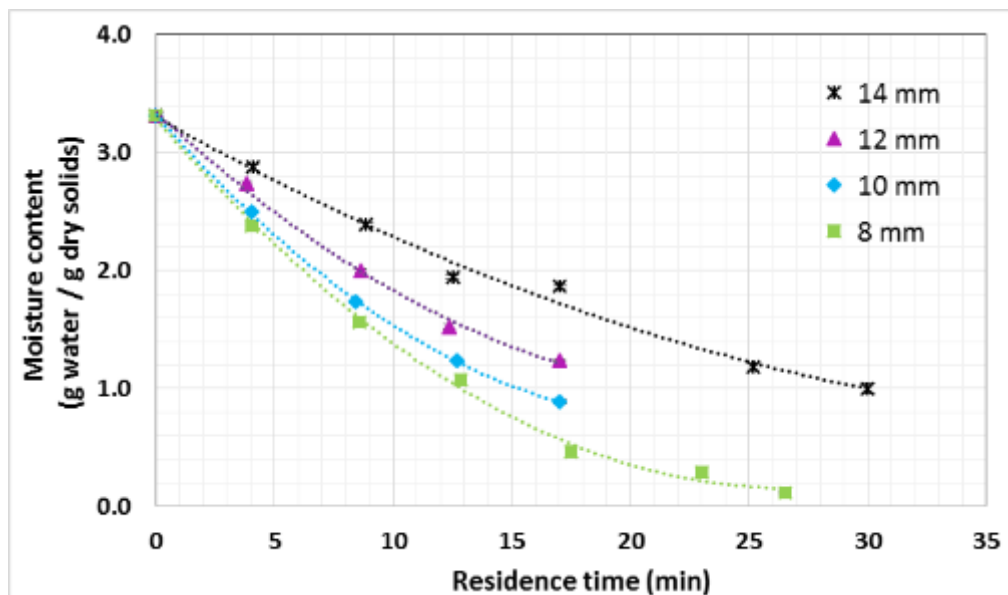


Figure 4-17: Drying curves for different pellet diameters

4.3.4.2 Drying rate

Figure 4-18 displays the drying rate curves for different pellet diameters. The curves show that the drying rate decreases with increase in pellet diameter and almost remains constant for the small diameters as shown by the 14mm pellet drying rate curve. These results are similar to findings from other studies on food drying (Sharma et al., 2005). This is because heat transfer to the core of the pellets is faster for pellets of small diameter and so is the moisture movement from the core to the surface of pellets.

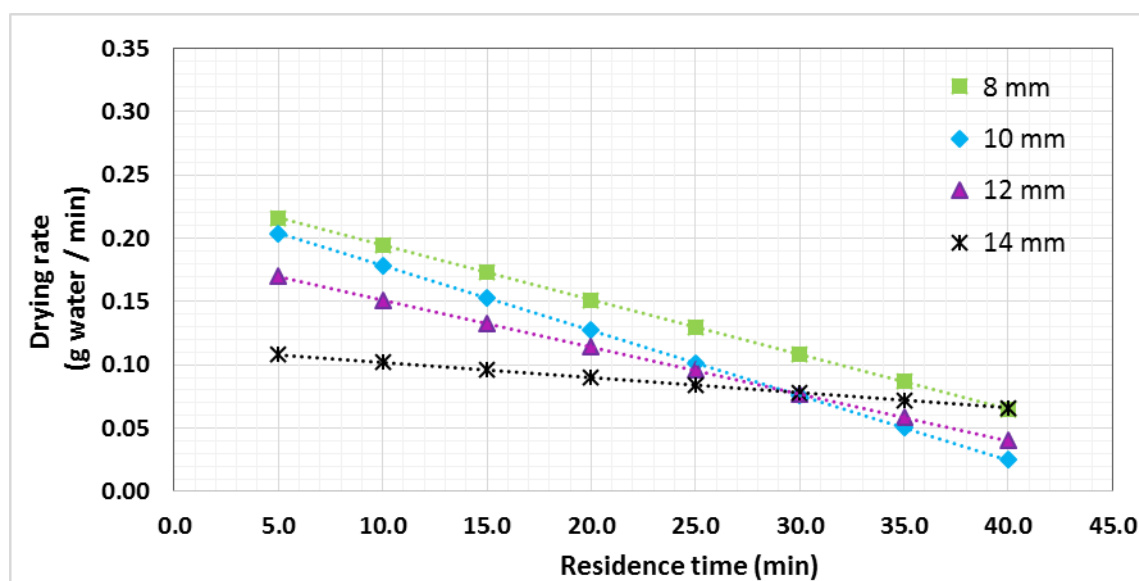


Figure 4-18: Drying rate for the different pellet diameters

4.3.4.3 Volatile solids and ash content

The volatile solids and ash contents of different pellet diameters processed in the laboratory scale LaDePa are presented in **Figure 4-19** and **Figure 4-20** respectively. The amount of volatile solids and ash content remained constant for the different pellet diameters. This implies that there is no thermal degradation in the LaDePa process.

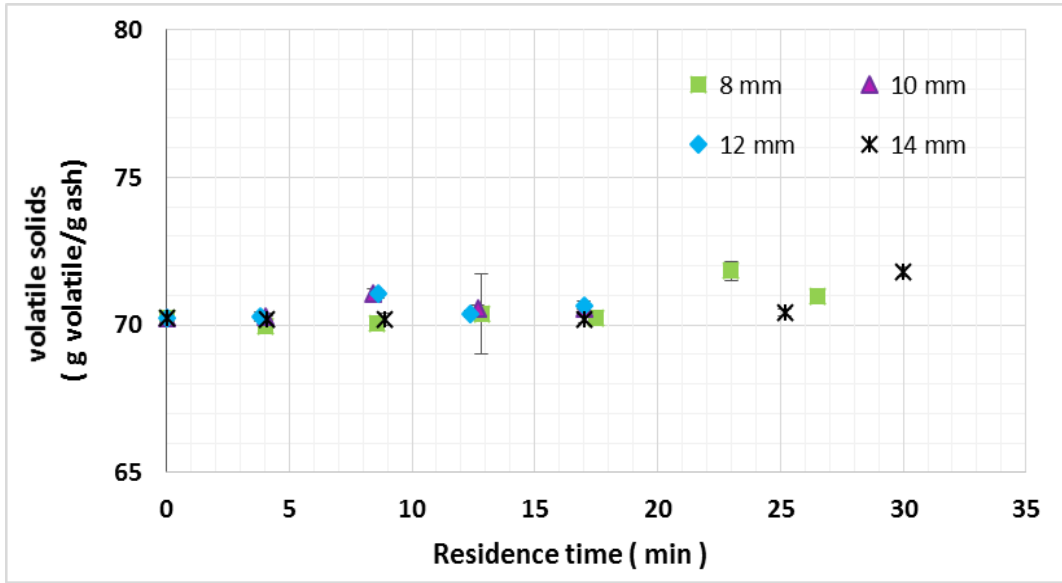


Figure 4-19: Volatile solids content for the different pellet diameters

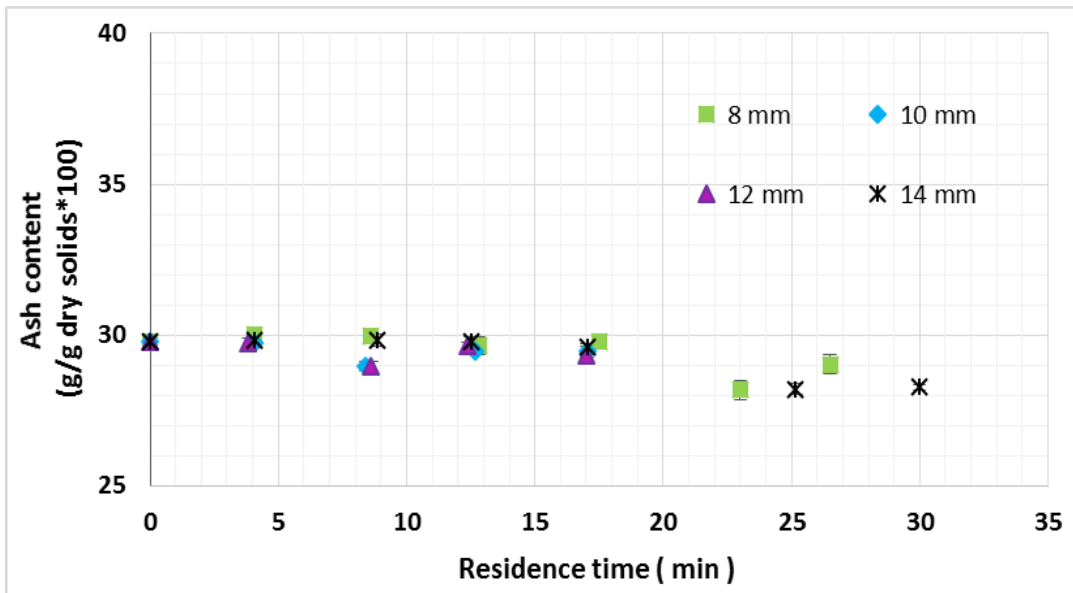


Figure 4-20: Ash content for the different pellet diameters

4.3.4.4 Energy consumption

Figure 4-21 presents the energy consumption as a function of moisture removal during the drying of pellets of different diameters. It shows that more energy was required to remove moisture of larger pellet sizes. As possible explanation to this, more energy would be required to enable mass transfer of moisture from the core to the surface of the sample.

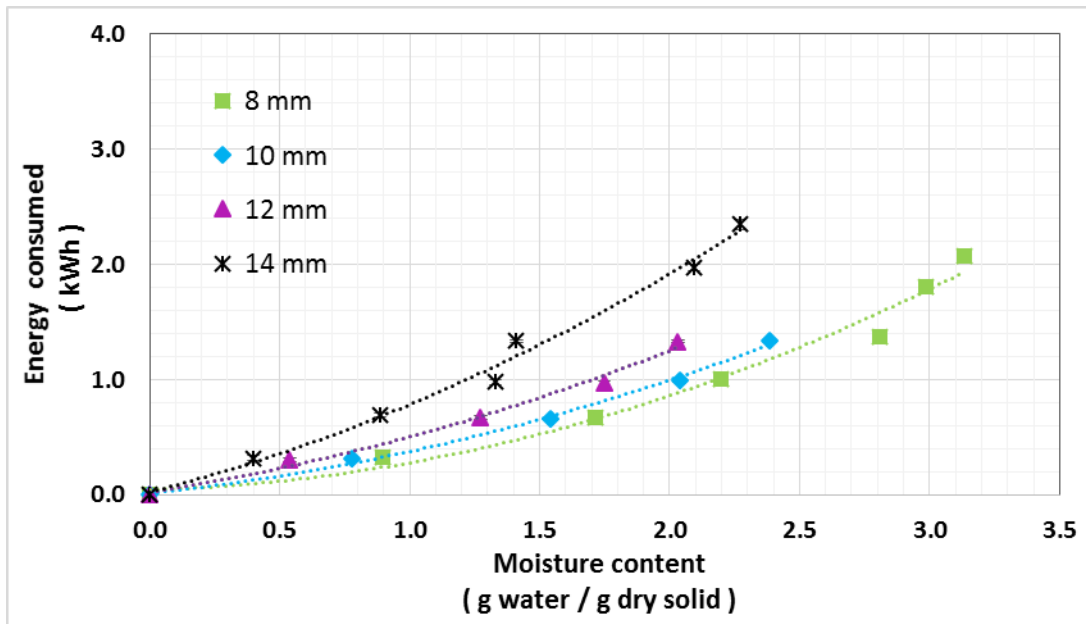


Figure 4-21: Energy consumed in drying pellets of varying diameters

4.3.5 Effect of the feedstock

The drying behaviour of sludge with a lower starting moisture content and sample without the addition of sawdust was compared to the feedstock used for the previous experiments (sludge mixed with sawdust). In this set of experiments, the height of the two emitters above the belt was 115 mm, the drying temperature was about 136°C, the pellet diameter was 8 mm, and the airflow rate was set at 18.3 m³ / s.

4.3.5.1 Drying curves

The drying curves obtained with the different feedstock are presented in **Figure 4-22**. It can be seen that there is a similar trend for the sludge with and without sawdust. The addition of sawdust did not affect the drying behaviour of sludge. However, it had an influence on the rheological characteristics of the sludge, as presented in section 1.2 Appendix B. Pre-drying of sludge seemed not to have any influence on the drying time for equilibrium moisture content to be reached.

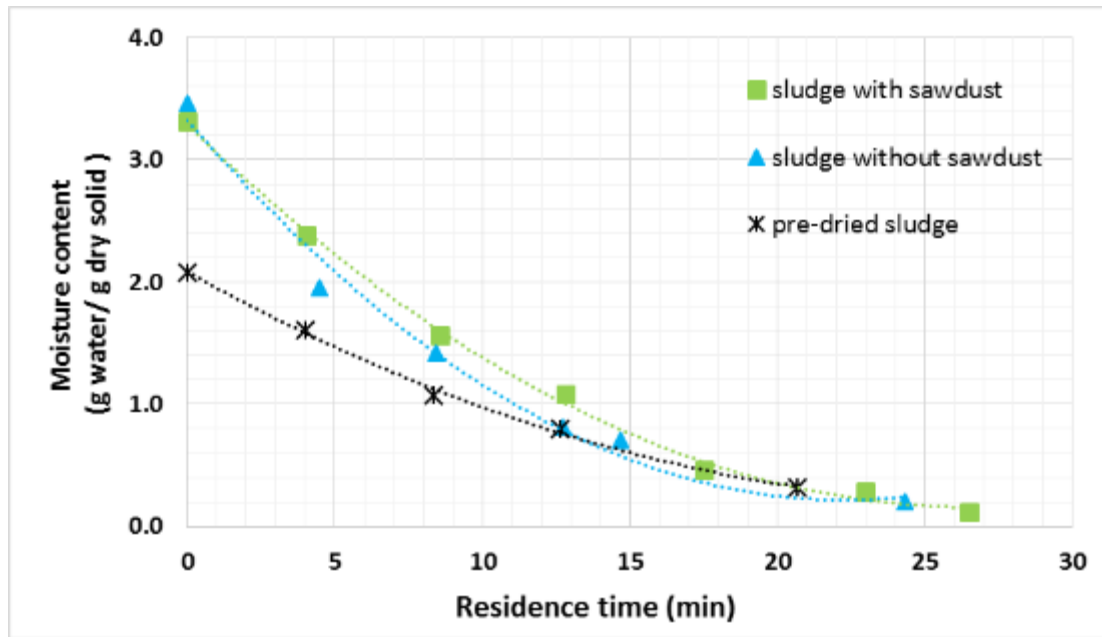


Figure 4-22: Drying curves of the different feedstock

4.3.5.2 Volatile solids and ash content

Figure 4-23 and Figure 4-24 shows the volatile solids and ash contents as a function of residence time for different feedstock. It can be observed that the volatile solids and ash content remained constant for the different samples during the process. Pre-drying the sludge does not influence ash and volatile solids contents. The addition of sawdust increased the volatile solids and lowered the ash content. This suggests that addition of sawdust could be beneficial if sludge were to be used for energy generation by combustion.

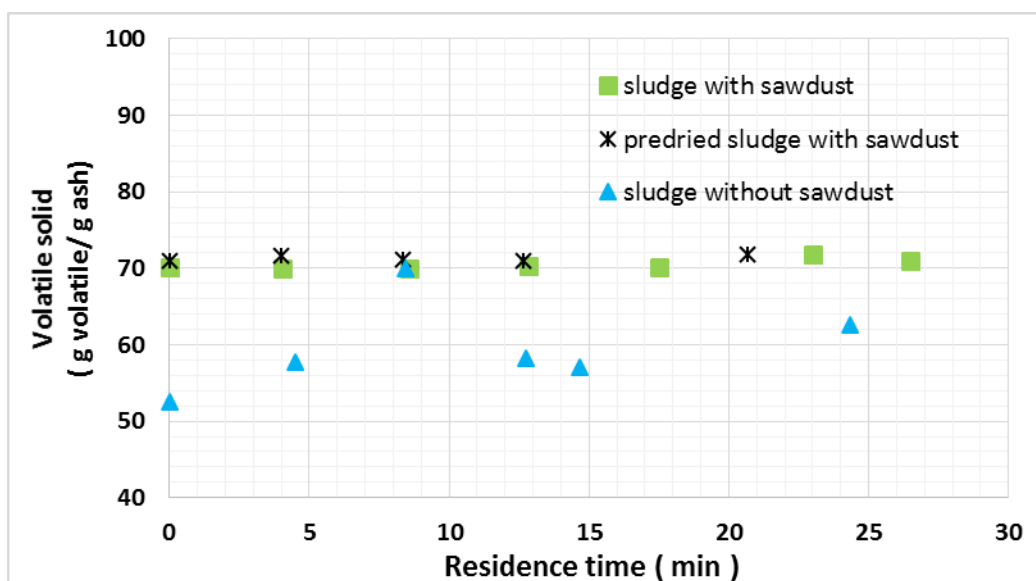


Figure 4-23: Volatile solids for different sludge processed at varying residence time

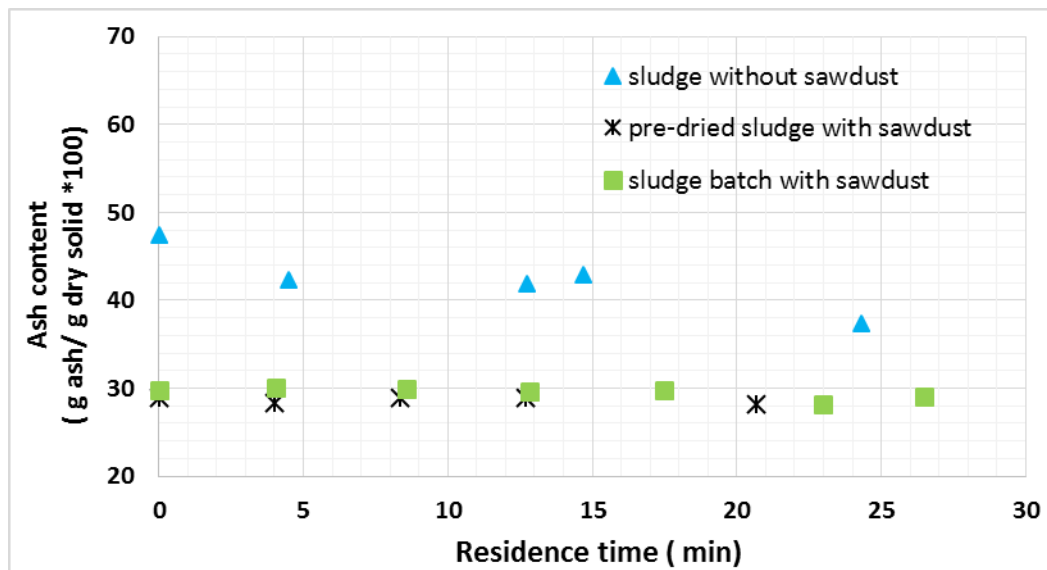


Figure 4-24: Ash content for different sludge processed at varying residence time

4.4 Pasteurisation efficiency

The level of pasteurisation was determined by measuring the number of viable and dead *Ascaris*, in raw sludge and in the resultant pellets. *Trichuris* and *Taenia* eggs in raw sludge was also investigated. Pellets of different diameters, processed at various MIR intensities and residence times, were analysed. The results obtained are displayed in **Table 4-3**.

In the raw faecal sludge, no *Taenia* eggs and only a few dead *Trichuris* eggs were detected while *Ascaris* eggs were found in considerable amounts. Therefore, effectiveness of the inactivation of *Taenia* and *Trichuris* could not be determined. The results obtained are consistent with findings reported by different authors that *Ascaris* eggs are found at the highest concentration in human faeces (Austin, 2001, Esrey et al., 1998, Jimenez, 2007).

There were no viable eggs measured in the processed pellets. At a residence time of 4 and 8 min, at a drying temperature of 87 and 136°C, the eggs had an intermediary look between viable and dead, as if they have been recently dead. This result shows that *Ascaris* eggs may not have been immediately destroyed under these conditions, but the process caused fatal damage leading to their eventual deactivation. An increase of pellet diameter from 8 to 14 mm did not influence deactivation of *Ascaris*.

To ensure pasteurisation, the residence time should be higher than 17 min at temperatures above 87°C or 4 min at temperatures above 214°C.

Table 4-3: Viable and dead parasite eggs at different operating conditions

Average MIR Temperature [°C]	Pellet diameter [mm]	Residence Time [min]	<i>Ascaris</i>		<i>Trichuris</i>		<i>Taenia</i>	
			[eggs / g wet solid]		[eggs / g wet solid]		[eggs / g wet solid]	
			Viable	Dead	Viable	Dead	Viable	Dead
87	8	4	13*	6721	0	13	0	0
	8	8	13*	5810	0	0	0	0
	8	17	0	5747	0	3	0	0
	8	25	0	6535	0	4	0	0
136	8	4	18*	6708	0	9	0	0
	8	8	3*	6060	0	10	0	0
	8	17	0	6163	0	3	0	0
	8	25	0	4429	0	0	0	0
214	8	4	0	6410	0	7	0	0
	8	8	0	4606	0	5	0	0
136	14	4	2*	8670	0	15	0	0
	14	8	0	7168	0	10	0	0
	14	17	0	5748	0	1	0	0
	14	25	0	5212	0	9	0	0
Raw sludge			135	4144	0	13	0	0

* eggs that did not look completely dead and may have just been recently deactivated

4.5 Nutrient analysis

Chemical analysis was performed in order to determine the agricultural value of the resultant pellets. The total K, P, Mg and Ca as well as the soluble NH_4^+ , PO_4^{3-} , NO_3^- and NO_2^- were determined. The analysis of these chemicals is important for the evaluation of pellets potential in agriculture as a fertilizer or soil conditioner.

Nutrients required for plant growth include primary and secondary nutrients. Primary nutrients include N, P and K. Nitrogen is mostly utilized by plants in the form of nitrates while phosphorous is absorbed as phosphate ions. Ammonium is usually converted to nitrites and eventually to nitrates in the soil. Secondary nutrients include Mg and Ca.

4.5.1 Elemental Analysis

In this section, the concentration of nutrient elements as a function of the MIR intensity is studied. Processing was done at an emitter height of 115 mm above the belt, a pellet diameter of 8 mm and an airflow of 18.3 m³/s. Primary nutrients, P and K, are firstly presented followed by secondary nutrients, Mg and Ca.

Raw sludge with and without sawdust had an Mg content of 12.36 and 15.35 g / kg dry solid respectively. It also had a Ca content of 28.01 and 38.21 g / kg dry solid with and without sawdust respectively. This shows that addition of sawdust and processing in the LaDePa does not affect either Mg or Ca content.

4.5.1.1 Effect of emitter intensity on P, K, Mg and Ca content on dry basis

The P and K contents on dry basis are shown in **Figure 4-25** as a function of moisture content while the Mg and Ca contents is presented in **Figure 4-26**. Under the explored conditions, the processed pellets had a P content ranging between 60 and 140 g / kg dry solids. These values did not vary significantly under the different conditions investigated. This indicates that processing in the LaDePa machine did not affect the P content of the pellets. These results agree with a study from literature, which concluded that drying only affects the chemical form of phosphorous but not the content in poultry manure (Heidi et al., 2007).

The content of K did not vary in a specific trend and remained constant in the range of 6 and 10 g K / kg dry solid. The Mg and Ca content tended to remain constant and ranged from 10 to 15 g / kg dry solid and 20 to 50 g / kg dry mass respectively.

These results show that K, P, Ca and Mg content was not affected by the emitter intensity.

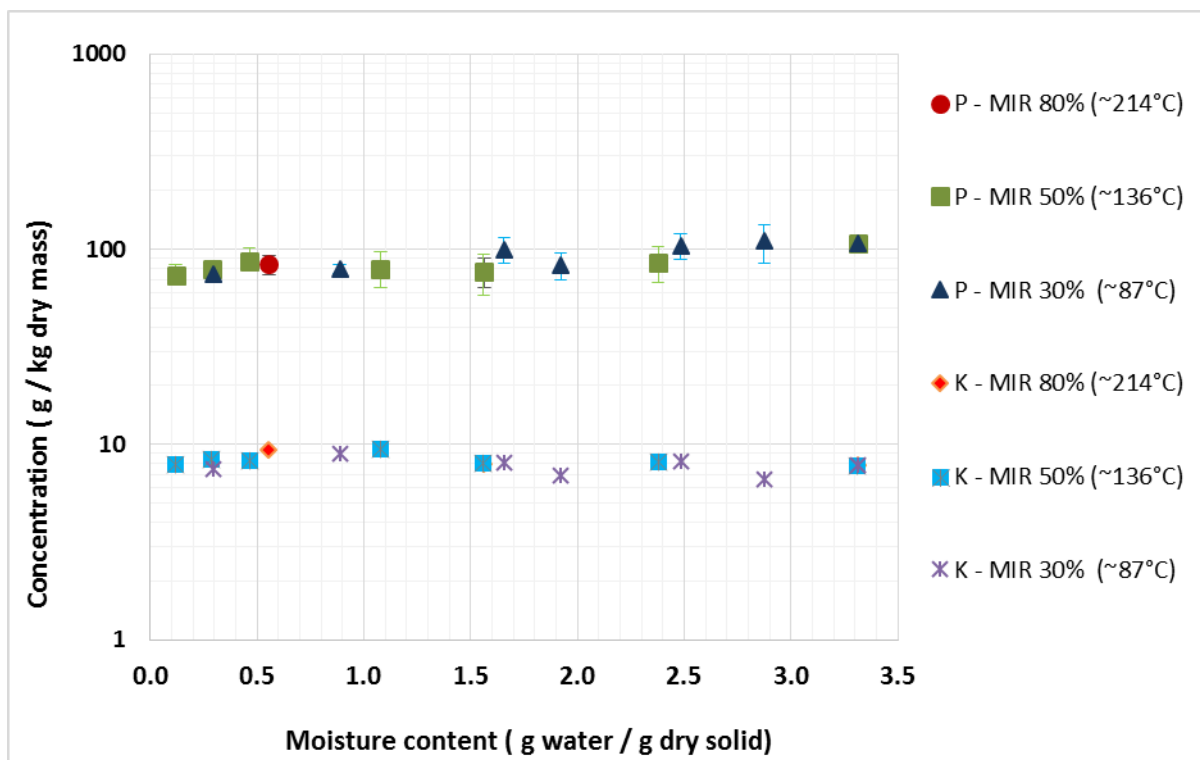


Figure 4-25: P and K content (dry basis) of pellets processed at different MIR intensities

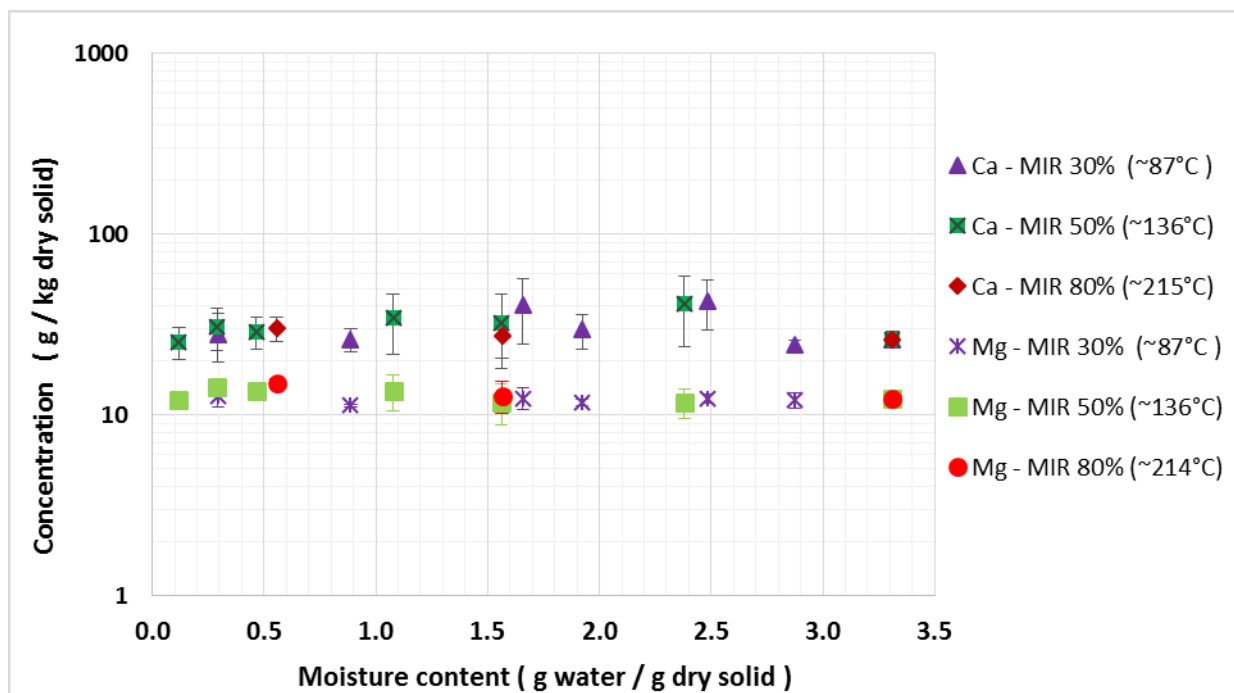


Figure 4-26: Mg and Ca content (dry basis) of pellets processed at different MIR intensities

4.5.1.2 Effect of emitter intensity on P, K, Mg and Ca content on wet basis

The P and K content on wet basis is given in **Figure 4-27** while that of Mg and Ca is given in **Figure 4-28**. The P, K, Mg and Ca content increased with decrease in moisture content. This is because as moisture is removed the constituent elements get more concentrated. However, none of the elements was affected by change in MIR intensity.

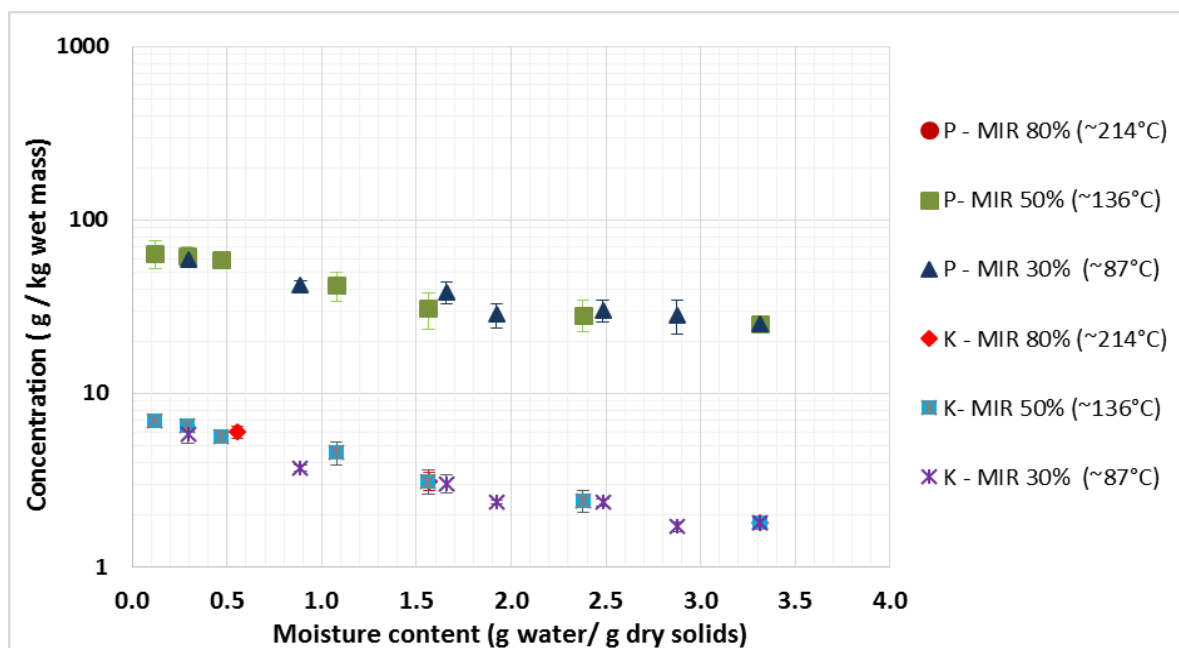


Figure 4-27: P and K content (wet basis) of pellets processed at different MIR intensities

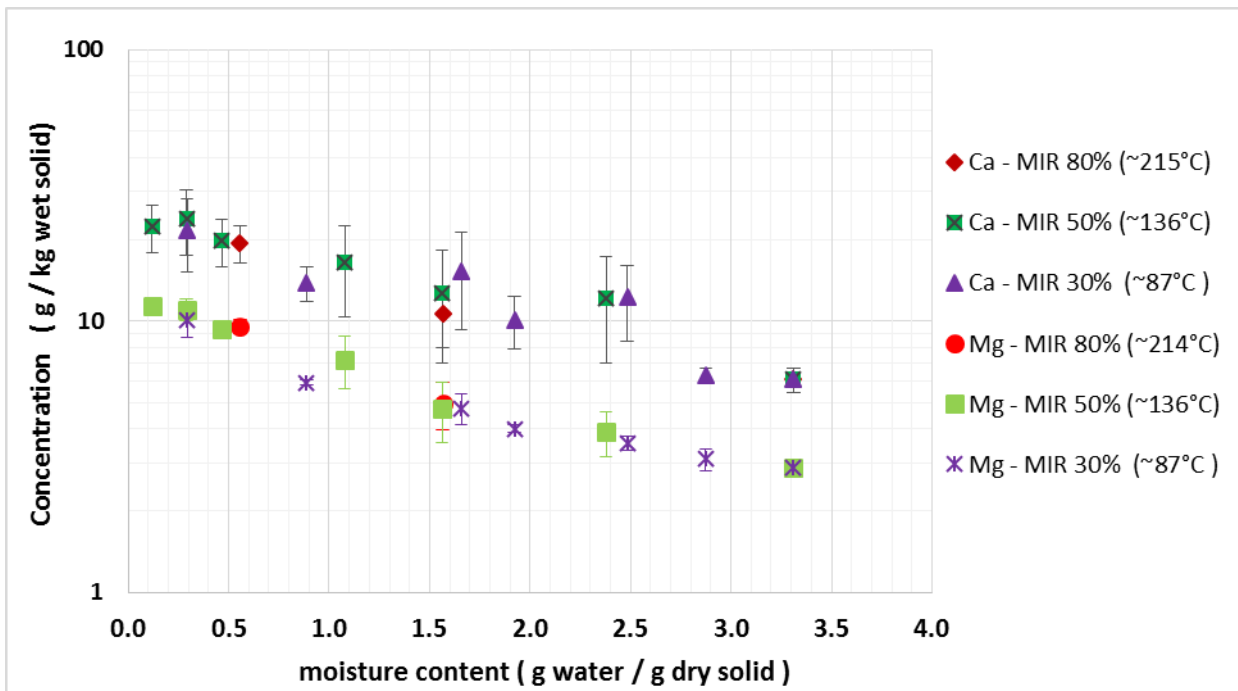


Figure 4-28: Mg and Ca content (wet basis) of pellets processed at different MIR intensities

4.5.2 Soluble Nutrient ions

In this section, the content of soluble ammonium, phosphates, nitrates and nitrates from the pellets processed at different MIR intensities and residence times are shown. The soluble fraction was considered as this is the form in which plants absorb nutrients and thus indicates the useful nutrients in fertilizers. The parameters kept constant were airflow of $18.3 \text{ m}^3 / \text{s}$, emitter height of 115 mm above the belt and a pellet diameter of 8 mm.

4.5.2.1 Ammonium (NH_4^+)

The content of NH_4^+ on dry basis, during the processing of the pellets as a function the MIR intensity and residence time is presented in **Figure 4-29**. The content of NH_4^+ decreased with the increase of residence time and MIR intensity, possibly due to NH_4^+ volatilization caused by heating. Indeed, NH_4^+ is very volatile at ambient conditions and heating should enhance this process. The NH_4^+ content stabilized after reaching a value of $5 \text{ g} / \text{kg}$ wet mass, after moisture content was reduced below $0.2 \text{ g} / \text{g}$ wet mass. The remaining ammonia could probably be strongly bonded to the solid and no further volatilization was possible.

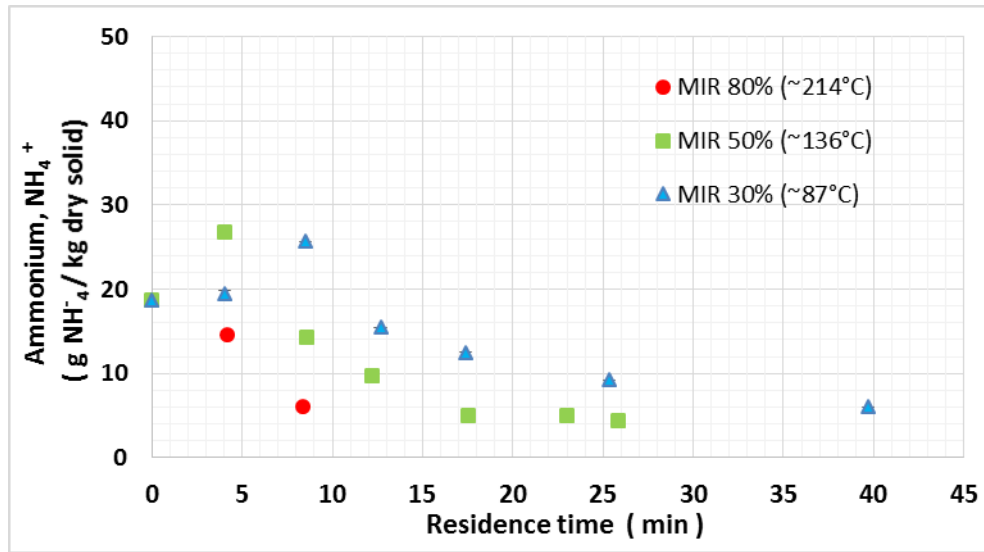


Figure 4-29: NH_4^+ content as a function of residence time for pellets processed at different emitter intensities

4.5.2.2 Nitrates (NO_3^-)

Figure 4-30 displays the NO_3^- content in dry basis as a function of the MIR intensity and residence time. The NO_3^- content decreased with the increase of residence time. On the contrary to NH_4^+ , NO_3^- is not volatile. Nevertheless, it could have been converted into NH_4^+ during processing and then volatilized. The initial NO_3^- content was between 1 and 1.4 g dry solid. It then decreased as drying progressed and reached a value of about 0.3 g /Kg dry solid.

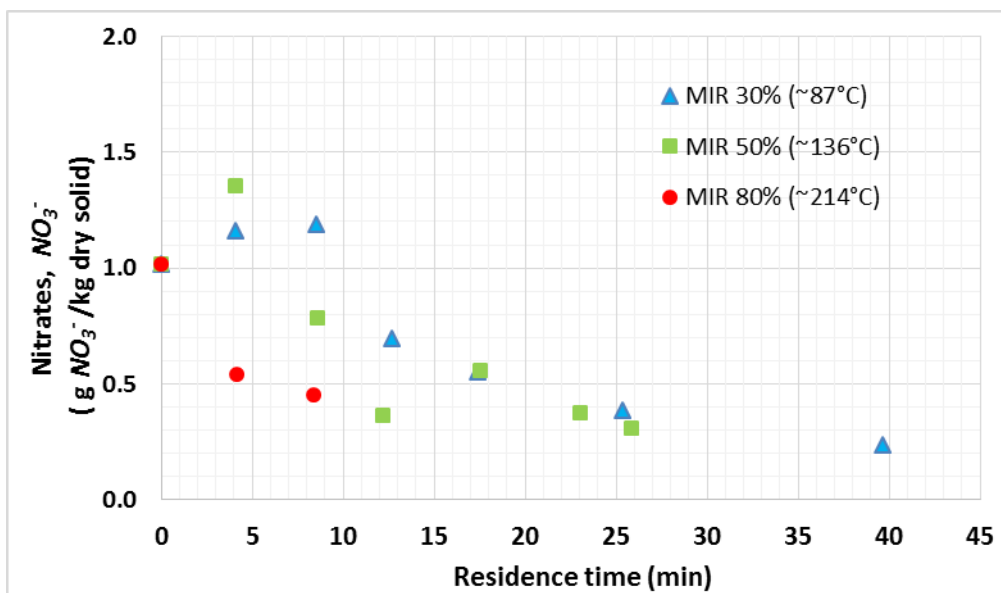


Figure 4-30: NO_3^- content as a function of residence time for pellets processed at varying emitter intensity

4.5.2.3 Nitrites (NO_2^-)

The NO_2^- content, in dry basis, from the processed pellets processed at different MIR intensity as a function of residence time is presented in **Figure 4-31**. The NO_2^- content decreased by increasing the residence time and MIR intensity. This may have been caused by volatilization caused by heating. Unprocessed and pellets with a moisture content above 0.7 g / g dry solid had a content between 3 and 4 g / kg wet solid. The amount of nitrites decreased to an almost null value along drying at a moisture content below 0.2 g / g dry solid.

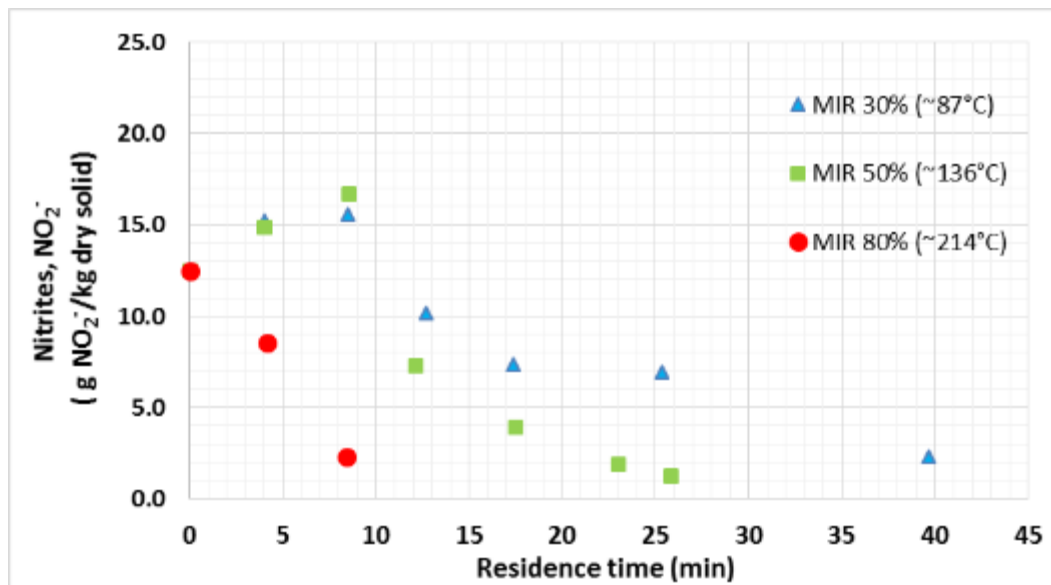


Figure 4-31: NO_2^- content as a function of residence time for pellets processed at varying emitter intensity

4.5.2.4 Phosphates (PO_4^{3-})

Figure 4-32 presents the content of soluble PO_4^{3-} ions at different MIR intensities and residence times. The PO_4^{3-} ions content did not show a particular trend with respect to MIR intensity and residence time and ranged between 5 and 15 g / kg dry mass. The soluble PO_4^{3-} ions was not affected by drying, as it remained constant along the process. This trend is similar to that reported for total P in section 4.4.1.1. It is however in contrast to findings on poultry manure drying (Heidi et al., 2007) where the soluble fraction of P is affected by drying. This could be due to the difference of material type between poultry manure and sludge from VIP latrines.

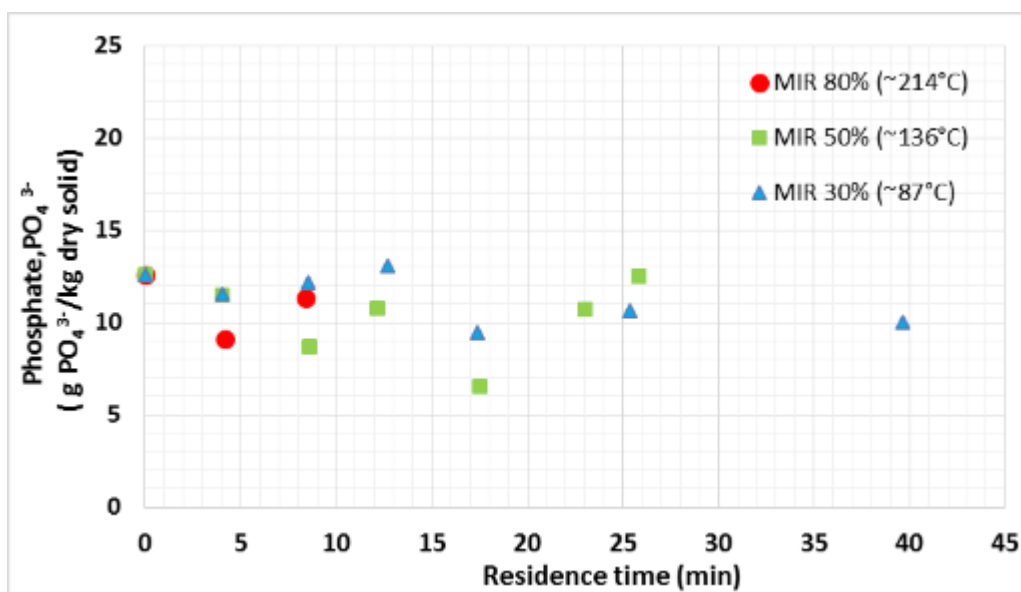


Figure 4-32: PO_4^{3-} content of the pellets processed at different MIR intensities

4.5.3 Comparison with literature

Few studies give detailed information on the characteristics and chemical composition of faecal sludge. Most of the studies focus on faeces from urine diverting toilets (Vinnerås, 2001, Torondel, 2010, Münch and Winker, 2009, Jönsson et al., 2005, Esrey et al., 2001). The reason for this could be the rare recycling of pit latrine sludge.

As seen in the section 4.4.1, the content of P, K, Ca and Mg is not affected by drying. There was only one study found in literature focusing on the effect of heat on nutrient content during mild thermal processes, corresponding to the P distribution in organic manure (Heidi et al., 2007). This is discussed in section 4.4.1.1

The contents of P, K, Ca and Mg were not comparable to the data found in literature, probably due to the different analysis method employed and difference in the source of the faecal material. **Table 4-4** gives the nutrient content of the processed pellets and its comparison with other literature sources. It shows that human manure (UD toilet waste) had a higher K content, and lower P and Ca contents (Mnkeni and Austin, 2009). Only Mg content was within the range of the results obtained in this study. The sum of the composition of urine and faeces gave the opposite trend: the P content is considerably lower (15.7 g / kg dry mass) while the K content is higher (36.8 g / kg dry mass) from values given on elements on human excreta (Esrey et al., 2001). Raw liquid faecal sludge is said to contain 1.1 g / l of P and 2.2 g / l of K (Nikiema et al., 2013, Asare et al., 2003). Results from this study therefore seem to be contradictory where P is 10 times higher than K.

The contents of NH_4^+ , PO_4^{3-} and NO_3^- in pollution load of fresh faeces, reported in literature, are 7.2, 27.9 and 0.14 g / kg dry solids respectively (Lopez et al., 2002, Almeida et al., 1999). These values are close to those found in this study.

The NH_4^+ content of raw sludge was 19 g / kg dry mass (4 g NH_4^+ / kg wet mass). This value is within the range of data obtained by various authors who used similar methods of analysis. Sludge from 10 VIP latrines within the eThekweni municipality had a NH_4^+ content ranging from 0.314 to 5 g / kg wet mass with a moisture content of between 0.66 and 0.81 g / g wet mass (Zuma et al., 2013). (Strande et al., 2014) reported values of 13, 7, 3 and 5 g / kg wet weight for dry VIP, wet VIP, CAB VIP and UD toilets respectively, for faecal sludge from the eThekweni municipality.

Table 4-4: Nutrient content in sludge before and after processing and comparison with literature data (Lopez et al., 2002, Mnkeni and Austin, 2009).

Nutrients	Unprocessed sludge and pellets in initial drying stage (MC > 2.33 g/g dry solid)		Dry pellets (MC < 0.33 g/g dry solid)		Lopez et al. (2002)	Mnkeni and Austin (2009)
	(g/kg dry solid)	(g/kg wet solid)	(g/kg dry solid)	(g/kg wet solid)	Excreta loading rate (g/kg dry solid)	Human manure (g/kg wet solid)
P	98.2 - 115.4	26.3 - 29.1	72.3 - 79.1	58.6 - 64	-	3.0
K	7.4 - 8.4	1.8 - 2.2	7.5 - 8.9	5.8 - 7.0	-	44.0
Ca	21.2 - 30.8	6.2 - 10.2	25.2 - 30.6	21.7 - 23.9	-	4.0
Mg	12.0 - 12.8	3.0 - 3.4	11.9 - 14.1	10.0 - 11.4	-	7.9
NH_4^+	18.7 - 26.7	4.4 - 8.0	3.8 - 3.8	3.5 - 4.7	3.4	-
PO_4^{3-}	11.0 - 12.0	2.9 - 3.5	9.8 - 12.4	8.3 - 10.9	4.5	-
NO_3^-	1.1 - 1.3	0.2 - 0.4	0.2 - 0.4	0.1 - 0.3	0.0	-
NO_2^-	13.1 - 15.9	3.2 - 4.6	1.2 - 2.4	1.1 - 1.9	-	-

4.5.4 Summary of the nutrient analysis

Table 4-5 compares the P, K, Mg and Ca composition of dried pellets, organic fertilizers and manure from different sources. The composition of pellets (wet basis) is the average value of samples with a moisture content below 0.33 g /g dry solid. The content P is lower compared to most inorganic fertilizers. It is however in the range of single super phosphate. P content is about 5 times higher than that in most manure sources. K content is over 30 times lower than that in potassium chloride and potassium sulphate. It is however in the range of most manure sources. Ca and Mg is about 10 times higher than that in manure sources. The content of Ca and Mg is however about 10 times lower than that in inorganic fertilizers (Ghosh et al., 2004, Ecochem., Mnkeni and Austin, 2009, Silva, 2000, Koenig and Rupp, 1999).

In summary, pellets processed in LaDePa have nutrient composition, which is slightly higher than manure and compost sources. They however have a lower nutrient content than most of the inorganic fertilizers. In comparison with inorganic fertilizers, the use of LaDePa pellets for crop production would also provide organic matter. This is due to by the high volatile solid content presented in **section 4.2** (Jönsson et al., 2004).

Table 4-5: Nutrient content in dried pellets and some manure types and inorganic fertilizers

Source	Elemental composition			
	P	K	Ca	Mg
Dried pellets (% total mass)	5.8 – 6.4	0.5 - 0.7	2.2 - 2.4	0.9 - 1.3
Fresh manure composition (% wet mass)				
Farm yard manure ^a	0.2	0.7	-	-
Poultry ^a	1.1	1.2	-	-
Cattle ^b	0.3	0.5	0.3	0.1
Sheep ^b	0.5	0.8	0.2	0.3
Poultry ^b	0.5	0.8	0.4	0.2
Horse ^b	0.3	0.6	0.3	0.1
Swine ^b	0.5	0.4	0.2	0.0
Goat ^c	0.4	4.6	0.7	1.2
Inorganic fertilizer composition (%)				
Rock phosphate ^d	11 - 17	-	25.0	-
Single superphosphate ^d	7 - 10	-	20.0	-
Triple superphosphate ^{d,e}	19 - 23	-	13.0	-
Mono-ammonium phosphate ^{d,e}	21 - 24	-	1.0	-
Di-ammonium phosphate ^d	20 - 24	-	-	-
Potassium chloride ^{d,e}	-	26 – 27		
Potassium sulphate ^d		22 - 23		
Lime ^d			38.00	
Dolomite ^d			22.00	19.0
Magnesium sulphate (Epson salt) ^d				9.8
Magnesium oxide ^d				55.0

data source: ^a (Ghosh et al., 2004), ^b (Ecochem.), ^c (Mnkeni and Austin, 2009), ^d (Silva, 2000), ^e (Koenig and Rupp, 1999)

The content of soluble NH_4^+ in the raw faecal sludge was higher than both NO_3^- and NO_2^- . According to Jonsson et al. (2004), plants can take up N in the form of NH_4^+ although NO_3^- is the most preferential assimilation form. However, there is no problem with the application of higher NH_4^+ in the soil, as it will be converted into NO_3^- . The author reports that in arable soils, NH_4^+ is converted by microbes to NO_3^- within a few days, as given by equation (32). Equations (30) and (31) show the intermediate conversion steps, where NH_4^+ is firstly converted into NO_2^- . The conversion of NH_4^+ into NO_2^- is done by nitrosomonas, while the conversion of NO_2^- to NO_3^- is undertaken by nitrobacters.



The sum of soluble NH_4^+ , NO_3^- and NO_2^- content in the dried pellets is 6.9 g / kg dry solid, which represents 0.7% of the total mass. This fraction is much lower than the total N content of inorganic fertilizers. For example, the N content of inorganic fertilizers such as ammonium sulphate, calcium nitrate and urea are 21, 15 and 46% of total mass respectively (Silva, 2000, Koenig and Rupp, 1999). Nevertheless, the content of NH_4^+ , NO_3^- and NO_2^- in this study represents only the soluble fraction of N. There is however a need to determine the total N for proper comparison, which was not possible in this study due to a technical challenge.

The content of the total soluble N in the dried pellets is however comparable to that found in manure. Values reported in literature are 0.7, 2.1 and 0.8 % of the total mass in farmyard manure, poultry manure and phosphor compost respectively (Ghosh et al., 2004). Other values are 0.5 % total mass in cattle and horse manures, 0.9 % total mass in sheep and poultry manures and 0.6 % total mass in swine manure (Ecochem.). Goat manure, which was compared to human excreta in a study about the effectiveness of human manure to grow vegetables, had a content of 26 g / kg dry solids (Mnkeni and Austin, 2009). The content of NH_4^+ in manure from cattle, pigs and poultry is reported to be in the range of 0.3 to 2.0, 0.5 to 6.0 and 2.4 to 18 g / kg wet mass respectively (Bernal et al., 2009). The content of NH_4^+ in dry pellets, therefore, falls within the range from pig and poultry manures but it is above the range of cattle manure.

4.6 Thermal analysis

Thermal analysis was performed in order to evaluate the use of LaDePa pellets as a biofuel in thermochemical processes such as combustion, pyrolysis and gasification. The analysis include the determination of calorific value, thermal conductivity, heat capacity and thermal diffusivity. The calorific value corresponds to the pellets energy content released during oxidation. Thermal conductivity determines the ability of pellets to conduct heat, while heat capacity determines the heat required to raise the temperature of the material. Thermal diffusivity is the ratio of thermal conductivity to the product of heat capacity and density. It indicates the ability of the material to conduct energy vs its ability to store it. It can be calculated as the thermal conductivity divided by the heat capacity and density of the material.

The parameters kept constant in the experiments conducted were airflow of $18.3 \text{ m}^3/\text{s}$, emitter height of 115 mm above the belt and pellet diameter of 8 mm.

4.6.1 Calorific value

Calorific values of pellets processed at different MIR intensities as a function of moisture content are given in **Figure 4-33**. The calorific value in dry basis show no specific trend at varying intensities and residence times. This results implies that calorific value did not vary along drying and was not affected by the MIR intensity.

Calorific value of raw sludge ranged between 15.5 and 19 MJ / kg dry solids, which is within the range of values reported by different authors. During the analysis of sludge from 10 dry VIP latrines within the eThekweni municipality, most of the samples exhibited a calorific value between 4.9 and 19.3 MJ / kg dry mass. This wide range was due to the heterogeneity of the sludge (Zuma et al., 2013). Untreated sludge from pit latrines and septic tanks in Kumasi, Dakar and Kampala had an average calorific value of 19.1, 16.6 and 16.2 MJ / kg dry solids respectively (Muspratt et al., 2014). Calorific values of the faecal sludge from dry VIP, wet VIP, CAB VIP and UD toilets, analysed within the eThekweni municipality, were found to be 14.1, 13.1, 14.3 and 12.9 MJ / kg dry solids respectively (Strande et al., 2014).

At a moisture content below 0.7 g / g dry solid (0.41 g / g wet solid), the calorific value is above 13.5 MJ / kg wet solid. This is achieved after drying the pellets for 39, 17 and 8 min at temperatures of approximately 87 °C, 136 °C and 214 °C respectively. Complete dry pellets had a calorific value of about 19.9 MJ / kg dry mass.

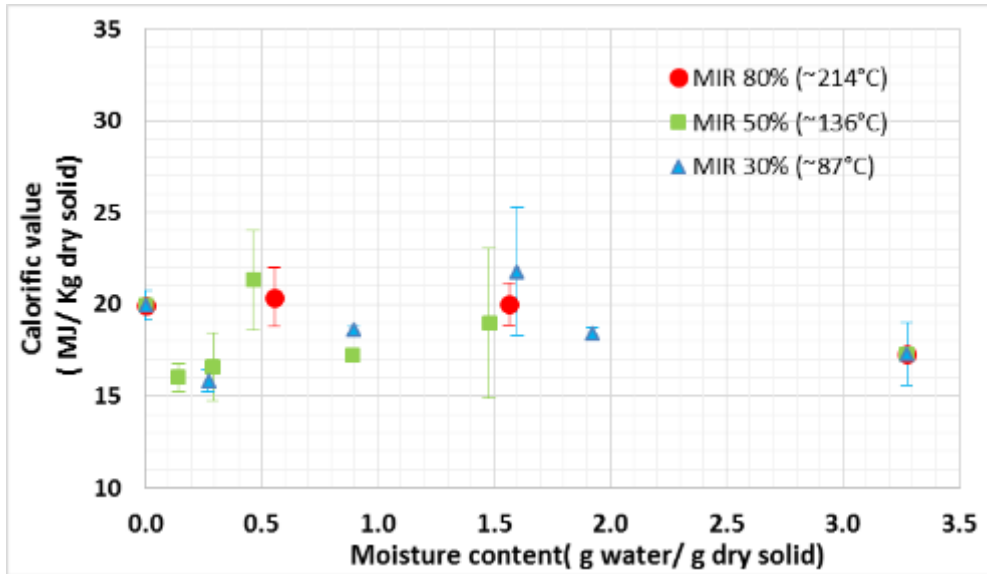


Figure 4-33: Calorific value in dry basis of the pellets processed at different MIR intensities, as a function of moisture content

The calorific value of pellets of different diameters as a function of residence time is presented in **Figure 4-34**. No variation of the calorific value with pellet diameter was observed. Most of the samples had a calorific value between 15 and 25 MJ / g dry solid, which is in the same range as the 8 mm pellets in **Figure 4-33**.

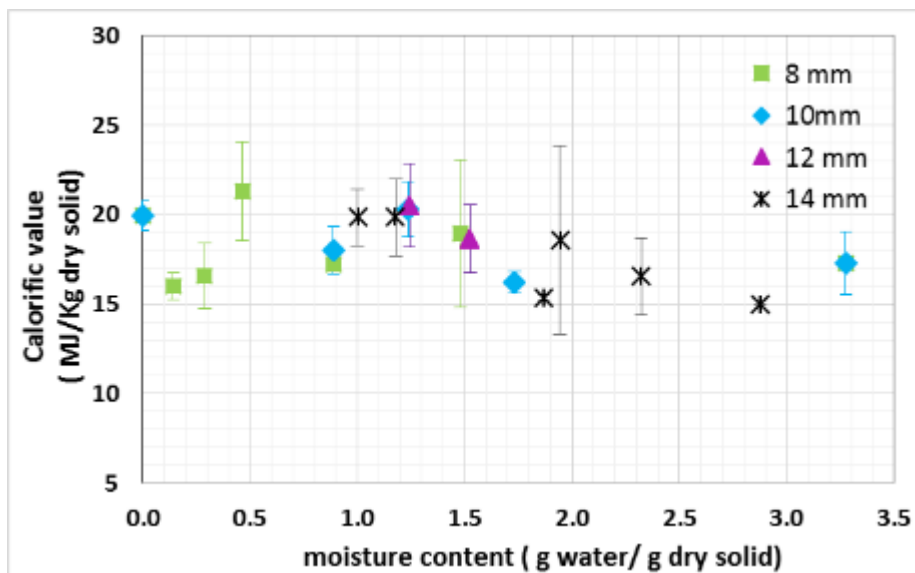


Figure 4-34: Calorific value in dry basis for pellets of different diameters as a function of the moisture content

4.6.2 Thermal conductivity

The thermal conductivity at different MIR intensity is presented in **Figure 4-35** as a function of residence time and in **Figure 4-36** as a function of moisture content. **Figure 4-35** shows a decrease in thermal conductivity with increase in residence time and emitter intensity. This can be related to the reduction in moisture content as shown by **Figure 4-36**. After prolonged drying, thermal conductivity is no longer influenced by moisture content in the solid. A similar trend was observed after drying synthetic sludge from a moisture content of 3.4 to 0.5 g / g dry solid where the thermal conductivity dropped from 0.60 to 0.05 (W/m.K) (Xiangmei et al., 2014).

The thermal conductivity of raw sludge of 0.51 (W/m. K) is close to that of water (0.61 W / m.K). The high thermal conductivity of raw sludge may be due to the high amount of water in the sample (Hanson et al., 2000). It is also within the range of the data reported in literature. The thermal conductivity of VIP sludge was found to be around 0.42 - 0.59 (W/m.K) (Zuma et al., 2013). Samples from dry VIP, wet VIP, CAB VIP and UD toilets exhibited a thermal conductivity of 0.54, 0.55, 0.60 and 0.38 (W/m.K) respectively. The lower value obtained for the UD samples could be related to lower moisture content. Indeed, the UD samples had a moisture content of 1.5 g / g dry solid while VIP samples from wet, dry and CAB latrines had a moisture content of 4.9, 3.8 and 3.3 g/g solid respectively (Strande et al., 2014).

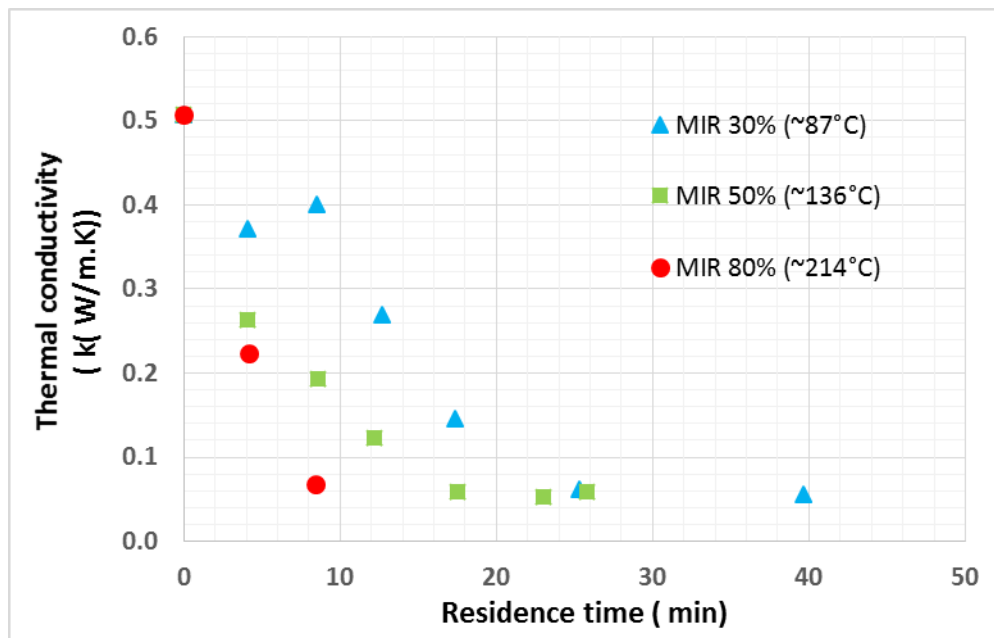


Figure 4-35: Thermal conductivity of pellets processed at different MIR intensities, as a function of residence time

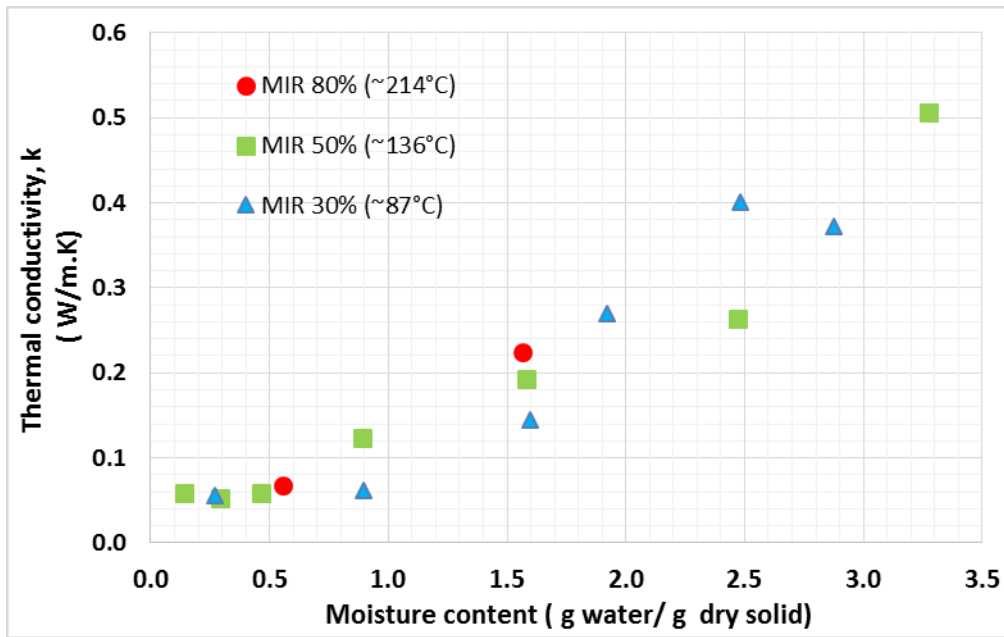


Figure 4-36: Thermal conductivity of pellets processed at different MIR intensities, as a function of moisture content

4.6.3 Heat capacity

The heat capacity of pellets processed at different MIR intensities as a function of residence time and as a function of moisture content are shown in **Figure 4-37** and **Figure 4-38** respectively. Heat capacity decreased with increase in residence time and consequently decreased with reduction in moisture content. It however did not vary with change in emitter intensity. Similar, to thermal conductivity, it decreased from 4.6 kJ/kg.K in raw sludge to 0.4 kJ/kg.K for the processed pellets below a moisture content of 0.3 g / g dry solid.

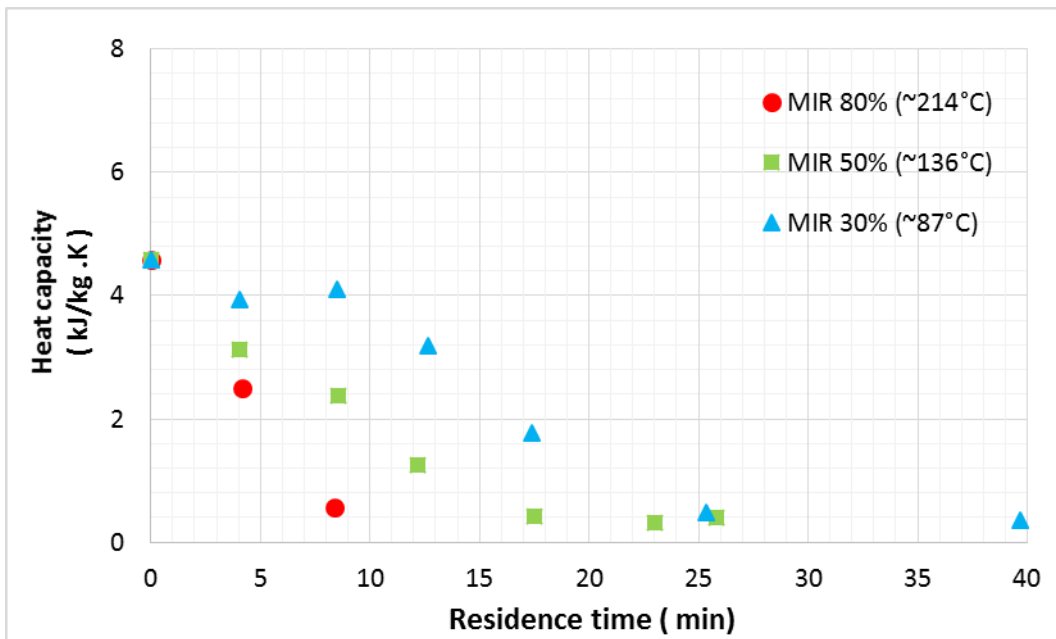


Figure 4-37: Heat capacity of the pellets processed at different MIR intensities, as a function of residence time

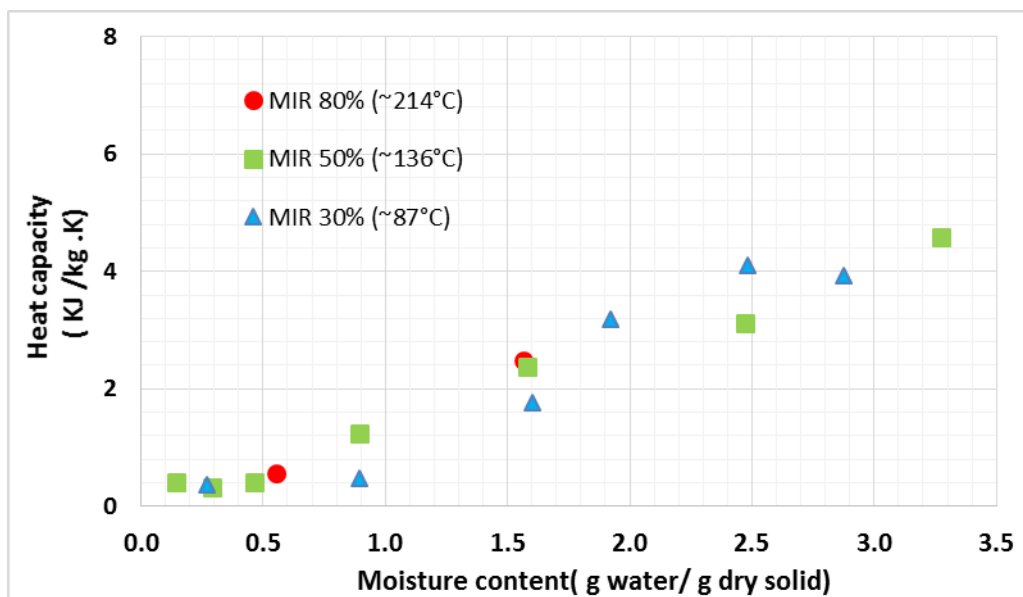


Figure 4-38: Heat capacity of the processed pellets at different MIR intensities, as a function of moisture content

The heat capacity of raw sludge used was 4.6 kJ / kg.K which is within the range of the values from faecal material from 10 VIP latrines, reported to be between 1.87 to 4.73 kJ / kg.K (Zuma et al., 2013). It is also close to the value of water, 4.19 kJ / kg.K.

4.6.4 Thermal diffusivity

The thermal diffusivity of pellets dried at different MIR intensities as a function of residence time and as a function of moisture content is presented in **Figure 4-39** and **Figure 4-40**. It shows that thermal diffusivity increases as drying progresses but does not show a specific trend when emitter intensity was varied. The increase in thermal diffusivity with drying is caused by decrease in moisture content in the sample. This implies that the decrease of heat capacity and density as drying progresses is more predominant compared to the decrease of thermal conductivity. This means that heat is better transferred within dry pellets, leading to lower times for heating.

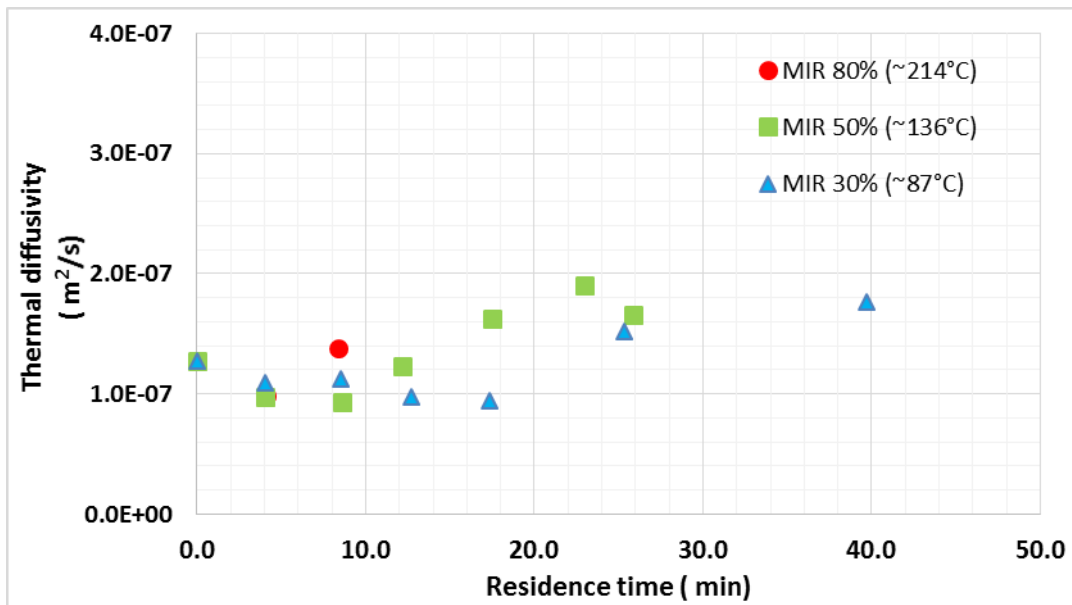


Figure 4-39: Thermal diffusivity of processed pellets at different MIR intensities, as a function of residence time

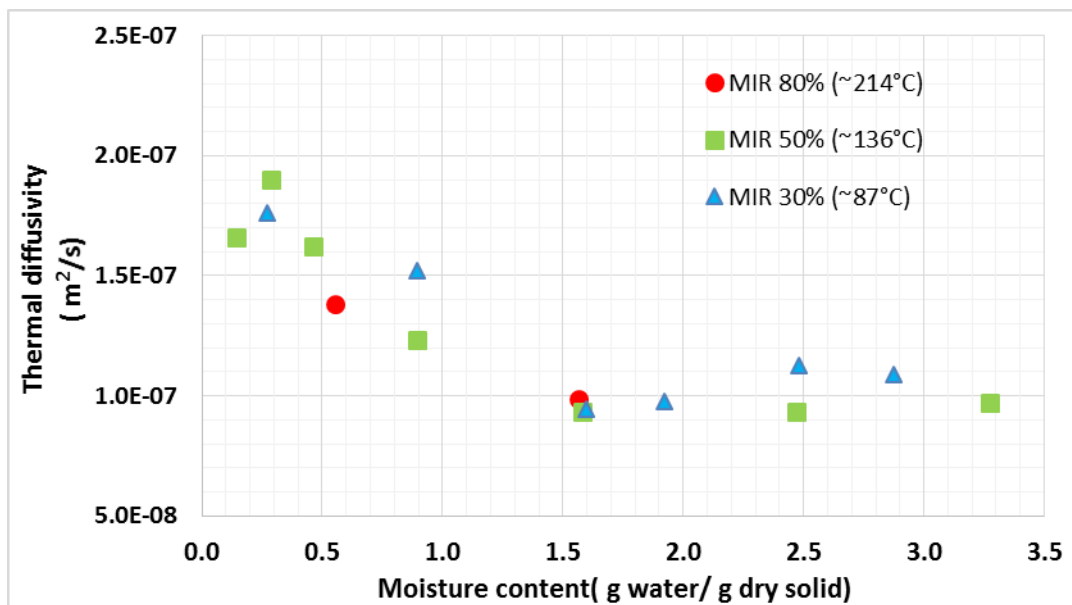


Figure 4-40: Thermal diffusivity of pellets processed at different emitter intensities as a function of moisture content

4.6.5 Summary

The calorific value of pellets with a moisture content below 0.7 g / g dry solid (13.5 g / kg total solid) is slightly lower than that of common biomass fuels. However, common biomass materials have a calorific value close to that of bone-dry pellets (19.9 MJ / kg total solid). The calorific values of pellets from agricultural residues, cotton and cardoon, and forages, *Phragmites australis* and *Typha angustifolia*, were 17.7, 15.0, 16.9 and 17.2 MJ / kg total solid respectively (Gravalos et al., 2010). Wood species analysed had a calorific value between 17.9 and 20.5 MJ / kg total solid (Günther et al., 2012). While comparing different biofuels, the calorific value of some lignocellulosic species laid between 16.8 and 19.1 MJ /kg total solid (González et al., 2012). These results show that pellets from LaDePa process are equivalent to fuel from other biomass sources in terms of calorific value.

In contrast, dry pellets have a lower calorific value compared to most common fossil fuels. Example of this is diesel, bituminous coal, mineral coal and propane have a calorific value of 44.2, 31.8, 37.7 and 43.9 MJ / kg total solid respectively. In contrast, peat has a calorific value similar to LaDePa pellets, i.e. 19 MJ /kg. In spite of lower calorific values compared to fossil fuel, LaDePa pellets have the advantage of being a renewable energy source, with lower environmental footprint.

Thermal conductivity of the dry pellets (0.05 ± 0.01 W / m.K) is close to that of air (0.03 W / m.K). It is also in the range of most thermal insulating materials that ranges between 0.02 and 0.06 W / m.K. Examples of these are cotton, paper, plastic, fibre grass, which have a thermal conductivity of 0.04, 0.05, 0.03, and 0.04 W / m.K respectively. The low thermal conductivity is negative for use as biofuel as it indicates that the dry faecal material has high resistance for heating.

The heat capacity of the dry pellets (0.25 g / g wet solid) is lower than that of wood with a moisture content of 0.2 g / g wet solid and completely dried wood which were 1.90 and 1.30 kJ / kg.K respectively (Simpson and TenWolde, 1999). It is also lower than the values reported in an overview of biomass fast pyrolysis oils, which were found to be between 2.50 and 3.50 kJ / kg.K (Lu et al., 2009). The lower heat capacity implies that the processed pellets were a better material than wood. This is because their temperature increases with less heat input compared to wood.

Thermal diffusivity of dried pellets is close to that of other materials, for example fibrous and sedimentary peat, 1.8 and $1.5 \times 10^{-7} m^2/s$ respectively (Hanson et al., 2000), and wood, $1.6 \times 10^{-7} m^2/s$ (Simpson and TenWolde, 1999).

In general, thermal analysis show that dry pellets have similar properties as most organic materials. Therefore, dried pellets have potential to be used as a biofuel and as a substitute for wood, which is one of the primary sources of energy in the world.

5 Conclusion

The focus of this study was to investigate drying and pasteurisation in the LaDePa process and to evaluate the value of the resultant pellets in agriculture and as a biofuel.

The results obtained reveal that the pellets are isothermal in the initial stage of drying. In the later stage, a considerable temperature difference appears between the core and surface: the surface temperature increases after drying, while the core remains wet and thus has a relatively constant temperature, which is below 100°C.

The increase of the MIR intensity leads to the increase of the drying temperature, resulting in higher drying rates. Processing at the highest emitter intensity, corresponding to approximately 214°C, leads to the fastest drying rates and highest energetic efficiency to achieve a given moisture content. An example of this is that a residence time of 6, 9 and 27 min is required to reduce the moisture content of pellets to 0.8 g water /g dry solid at approximate temperatures of 214, 136 and 87°C respectively. The energy utilized to achieve this was 0.7, 1.1 and 1.3 kWh at corresponding temperatures of 214, 136 and 87°C. However, at the highest temperature, the pellets were subjected to undesirable thermal degradations after 8 min of residence time. Therefore, for an optimal operation, the MIR intensity should be high enough to enhance drying but should not exceed a value from which thermal degradation can occur. Drying at high MIR intensity shows that most of the moisture is reduced in the falling rate period implying that drying rate is controlled by internal mass transfer. Therefore, morphological characteristic of the material, such as porosity influence the process under these conditions. At lower intensity, drying mostly occurs in the constant rate period and thus external mass transfer becomes more relevant. Under these conditions, influencing factors are the airflow rate, humidity, pellets size and geometry.

Reducing the height of the emitters above the belt increases the drying temperature at a constant MIR intensity. This increases the rate of drying, due to a higher irradiation received by the pellets. The emitter, therefore, should then be placed at the lowest distance possible with respect to the belt. This would enhance the drying process and lead to lower operating costs due to energy savings.

The increase of airflow increases the drying rate due to faster removal of evaporated moisture from the pellets surface to the surroundings. This is despite the air getting into the drying chamber cooling the surface of the pellets. However this air was heated, this would enable reduction in energy required by the emitters to attain a given moisture removal. Heating of this air should be from an inexpensive source such that it does not add to the cost of operation. This could be from solar heating or recovery of thermal energy from the waste stream of the process.

Pellets of lower diameters have higher drying rates and require less energy for drying. To achieve a moisture content of 1.5 g water/g dry solid the residence time and energy consumption is 20 min and 2.0 kWh for 14 mm diameter pellets, 9 min and 0.8 kWh for 8 mm diameter pellet. Therefore, for an optimal drying process, the size of pellets should be the reduced as low as possible. This will depend on the ability of the extruder to produce pellets from faecal sludge.

Addition of sawdust did not have significant influence on drying. Sawdust could be then added to the faecal sludge to improve extrusion, without altering the drying behaviour of the material.

The LaDePa process gave positive results relative to faecal sludge pasteurization. During processing in the LaDePa, *Ascaris* eggs are considerably damaged and no viable eggs are observed in the processed pellets. To ensure pasteurisation, pellets should be processed for a minimum residence time of 4 min at temperatures between 87 and 214°C.

Chemical analysis shows that the processed pellets have an agricultural value. The nutrient composition of the dry bone material is not affected by drying, except for the soluble ammonium, nitrates and nitrites. The content of these compounds decrease along the process, leading to the decrease of soluble nitrogen from the resultant pellets. The content of P, K, Ca, and Mg in the pellets are concentrated as drying progresses, due to the reduction of moisture content. This is illustrated by an increase of P, K, Ca and Mg content from 24, 2, 3 and 6/g dry solid at a moisture content of 3.3 g/g dry solid to 63, 7, 11 and 22g/g wet solid respectively at moisture content of 0.1g/g dry solid. The K, Ca and Mg contents from the pellets dried at moisture contents below 25 % (wet basis) are lower than most that from inorganic fertilizers. The P content is in the same range as some inorganic fertilizers. The P, K, Ca and Mg are generally higher than manures and composts. The P content in the sludge shows it is not affected by the drying process. It is also able to compete with inorganic sources most of which are non-renewable. (Syers et al., 2011). This therefore, implies that sludge recycling and indeed the LaDePa process can be one of the system of sludge recycling that may help complement and perhaps substitute the unsustainable rock sources

According to the thermal analysis, the processed pellets have suitable characteristics to be used as a biofuel. The calorific value of dry pellets was 20 MJ/kg dry mass, a value in the range of common biofuels, such as wood. Heat capacity and thermal conductivity decreased with the reduction of moisture content, while thermal diffusivity increased. Overall, heat is then better transferred in dried pellets compared to the raw material.

The experiments in the laboratory scale LaDePa demonstrated that this process is an interesting alternative for the treatment of faecal sludge from VIP latrines. The final product are pellets that demonstrates to be suitable for use in agriculture or as a biofuel.

6 Perspectives

The following actions could be performed in the future in order to improve the existing equipment and to provide more data that would enable to have a better understanding of the process and lead to further optimization.

- **Modification of the laboratory scale LaDePa**

A technical difficulty during this study was to set precise values for the power to the emitters, the speed of the belt and the airflow rate. This difficulty can be overcome by adding a digital display in the control panel to set the power to the emitters and the motor used to drive the belt. For better control of the airflow rate, a pressure gauge should be placed at the air pipe connected to the blower and the damper valve should be modified such that it can be easily adjusted for various pressure gauge readings.

- **Further pellet characterisation**

In this study, the carbon, nitrogen and sulphur contents could not be determined due to technical problems with the analyser. These analyses should be done in the future, as they provide relevant data on the agricultural and fuel value of the processed pellets.

- **Construction of a MIR drying thermobalance rig**

A MIR drying thermobalance could be designed and constructed in order to study the process in more controlled conditions and then to obtain more precise data. This is important for the development of a model of the LaDePa process.

- **Modelling of the process**

Modelling could enable to the optimization of LaDePa process. This will help in ensuring that the process operates at the highest efficiency where minimal energy will be used to produce high value pellets.

- **Improvement of the extruder**

The screw extruder intended for this study was not able to operate in continuous mode due to clogging. Studies should be carried out to understand this issue and to propose modification of a new design of the extruder to avoid clogging.

- **Investigation on the use of LaDePa for different types of sludge**

A study about the treatment of different types of material in LaDePa could be undertaken. This could include sludge from wastewater treatment works and septic tanks, manure from animals, human excreta from UD toilets and blending of organic municipal wastes.

- **Ascaris egg inactivation**

In the study, conducted analysis done on ascaris eggs was not carried out immediately after processing. Therefore, a method should be devised such that this analysis is carried just before and after processing. Other methods such as spiking the samples with individual pathogens and helminth eggs and studying the survival during pasteurisation process should also be investigated.

- Determination of level of thermal degradation during processing
The level of thermal degradation at varying conditions should be investigated. This would help determine the setting that minimises it from occurring.
- Temperature profiles
More temperature profiles should be obtained at various processing conditions. Temperature measurement at the bottom of the pellets should also be investigated.
- Study on the various physical changes occurring to pellets during drying
To better understand the drying process physical changes such as density, porosity, shrinkage and colour change should be investigated.
- Study on recycle of the heat from the exhaust air from the drying chamber
The exhaust air from the drying chamber contains some heat which could be utilized in heating up the incoming air to the drying chamber or which could be recycled. This would minimise cooling of pellets by the air introduced to the drying chamber.
- Study on possible ways of reducing or eliminating loss in N content
A study should be carried out on possibilities of capturing or fixing Nitrogen in the sludge before or during the drying process.

References

- ALMEIDA M., BUTLER D. & FRIEDLER E. 1999. At-source domestic wastewater quality. *Urban water*, 1, 49-55.
- ASARE I., KRANJAC-BERISAVLJEVIC G. & COFIE O. 2003. Faecal sludge application for agriculture in Tamale, Ghana. *Urban Agriculture Magazine*, 10, 31-33.
- ATKINSON B. & MAVITUNA F. 1983. *Biotechnology and Biochemical Engineering Handbook*, London, UK, Macmillan Publishers Ltd.
- AUSTIN A. 2001. Health aspects of ecological sanitation. *Abstract Volume, First International Conference on Ecological Sanitation*, 5, 104-111.
- BAKARE B., FOXON K., BROUCKAERT C. & BUCKLEY C. 2012. Variation in VIP latrine sludge contents. *Water SA*, 38, 479-486.
- BERNAL M. P., ALBURQUERQUE J. & MORAL R. 2009. Composting of animal manures and chemical criteria for compost maturity assessment. A review. *Bioresource technology*, 100, 5444-5453.
- BOUCHER R. M. (ed.) 1980. *Process for ultrasonic pasteurization*, New York, United States: Bio-physics Research & consulting Corporation.
- BROUCKAERT C., FOXON K. & WOOD K. 2013. Modelling the filling rate of pit latrines. *Water SA*. Durban, South Africa: Pollution Research Group, university of Kwa-Zulu Natal.
- BUCKLEY C. A., BROUCKAERT C. J., RODDA N., NWANERI C., BALBONI E., COUDERC A. & MAGAGNA D. 2008. Scientific Support for the Design and Operation of Ventilated Improved Pit Latrines (VIPs) and the Efficacy of Pit Latrine Additives. *WRC REPORT NO TT 357/08*.
- BUTZ P. & TAUSCHER B. 2002. Emerging technologies: chemical aspects. *Food research international*, 35, 279-284.
- CAVUSOGLU C. 2008. *Investigations into the high-temperature air drying of tomato pieces*. PhD in Engineering, Universitäts-und Landesbibliothek Bonn.
- COFIE O., KRANJAC-BERISAVLJEVIC G. & DRECHSEL P. 2005. The use of human waste for peri-urban agriculture in Northern Ghana. *Renewable Agriculture and Food Systems*, 20, 73-80.
- COULSON J. M., RICHARDSON J. F., BACKHURST J. R., HARKER J. H. & 2005. Chemical engineering. Fourth ed. Oxford, United Kingdom: Butterworth-Heinemann.
- CSERTA E. 2012. *Drying process of wood using infrared radiation*. Doctor of Philosophy, University of West Hungary.
- DUPONT C., BOISSONNET G., SEILER J.-M., GAUTHIER P. & SCHWEICH D. 2007. Study about the kinetic processes of biomass steam gasification. *Fuel*, 86, 32-40.
- DWAF 2003. Strategic Framework for Water Services. Pretoria, South Africa: ministry of water affairs and forestry.
- DWAF , DPME & DHS 2012. Report on the status of sanitation services in South Africa. Pretoria, South Africa.
- ECOHEM. MANURE IS AN EXCELLENT FERTILIZER. http://www.ecochem.com/t_manure_fert.html [Accessed 25/5/2015].
- ESREY S. A., ANDERSSON I., HILLERS A. & SAWYER R. 2001. Closing the loop. *Ecological sanitation for food security*. SIDA, Stockholm (Sweden).
- ESREY S. A., GOUGH J., RAPAPORT D., SAWYER R., SIMPSON-HÉBERT M., VARGAS J. & WINBLAD U. (eds.) 1998. *Ecological sanitation*, stockholm, Sweden: Department for Natural Resources and the Environment, .
- FEACHEM R., MARA D. D. & BRADLEY D. J. 1983. Sanitation and disease. *Health Aspects of Excreta and Wastewater Management*. N.W., Washington, D.C. 20433, U.S.A.: John Wiley & Sons.

- FLAGA A. 2005. Sludge drying. *Integration and optimisation of urban sanitation systems. Proceedings of Polish-Swedish seminars, Cracow March*, 17-18.
- FRANCEYS R., PICKFORD J. & REED B. 1992. *A guide to the development of on-site sanitation*, Geneva, World Health Organization
- GHOSH P., RAMESH P., BANDYOPADHYAY K., TRIPATHI A., HATI K., MISRA A. & ACHARYA C. 2004. Comparative effectiveness of cattle manure, poultry manure, phosphocompost and fertilizer-NPK on three cropping systems in vertisols of semi-arid tropics. I. Crop yields and system performance. *Bioresource technology*, 95, 77-83.
- GIDNER A. V., STENMARK L. B. & CARLSSON K. M. 2001. TREATMENT OF DIFFERENT WASTES BY SUPERCRITICAL WATER OXIDATION. *IT3 Conference Philadelphia, USA*.
- GONZÁLEZ Z., FERIA M. J., VARGAS F. & RODRÍGUEZ A. 2012. Comparison of the Heating Values of Various Types of Fuel from Non-Wood Raw Materials. *American Journal of Environmental Engineering*, 2, 91-96.
- GRAVALOS I., KATERIS D., XYRADAKIS P., GIALAMAS T., LOUTRIDIS S., AUGOUSTI A., . . .TSIROPOULOS Z. 2010. A study on calorific energy values of biomass residue pellets for heating purposes. *Proceedings on Forest Engineering: Meeting the Needs of the Society and the Environment, Padova, Italy*, 11-14.
- GÜNTHER B., GEBAUER K., BARKOWSKI R., ROSENTHAL M. & BUES C.-T. 2012. Calorific value of selected wood species and wood products. *European Journal of Wood and Wood Products*, 70, 755-757.
- HABIB K., NESE YILMAZ, BARIS TUNCEL, SARP SUMER & BUYUKCAN B. 2014. The effects of middle infrared radiation intensity on the quality of dried tomato products. *International Journal of Food Science & Technology*, 49, 703-710.
- HANSON J. L., EDIL T. B. & YESILLER N. 2000. Thermal properties of high water content materials. http://digitalcommons.calpoly.edu/cgi/viewcontent.cgi?article=1261&context=cenv_fac [Accessed 17/06/2016].
- HARRISON J. & WILSON D. 2012. Towards sustainable pit latrine management through LaDePa. http://www.susana.org/docs_ccbk/susan_download/2-1624-harrison.pdf [Accessed 13/02/2014].
- HEBBAR H. U., VISHWANATHAN K. H. & RAMESH M. N. 2004. Development of combined infrared and hot air dryer for vegetables. *Journal of Food Engineering*, 65, 557-563.
- HEIDI D., HE Z., SUSAN ERICH M. & WAYNE HONEYCUTT C. 2007. Effect of drying on phosphorus distribution in poultry manure. *Communications in soil science and plant analysis*, 38, 1879-1895.
- HEWITT G. F., SHIRES G. L. & BOTT T. R. 1994. *Process heat transfer*, Boca Raton, Florida 33431, U.S.A, CRC press.
- JIMENEZ B. 2007. Helminthes (Worms) eggs control in wastewater and sludge. *International symposium on new directions in urban water management*. 12-14.
- JÖNSSON H., BAKY A., JEPPSSON U., HELLSTRÖM D. & KÄRRMAN E. 2005. Composition of urine, faeces, greywater and biowaste for utilisation in the URWARE model. *Urban water report*.
- JÖNSSON H., STINTZING A. R., VINNERÅS B. & SALOMON E. 2004. *Guidelines on the use of urine and faeces in crop production*, Stockholm Environment Institute, Stockholm, Sweden, EcoSanRes Programmethe and the Stockholm Environment Institute.
- JUFFS H. & DEETH H. 2007. Scientific evaluation of pasteurisation for pathogen reduction in milk and milk products. Available: <https://www.foodstandards.gov.au/code/proposals/documents/Scientific%20Evaluation.pdf> [Accessed 22nd April 2014]
- KOENIG R. & RUPP L. 1999. Selection and Using Inorganic Fertilizers. https://extension.usu.edu/files/publications/publication/HG_509.pdf [Accessed 25/05/2015].

- KRISHNAMURTHY K., KHURANA H. K., SOOJIN J., IRUDAYARAJ J. & DEMIRCI A. 2008. Infrared heating in food processing: an overview. *Comprehensive Reviews in Food Science and Food Safety*, 7, 2-13.
- LEWIS W. 1921. The Rate of Drying of Solid Materials. *The Journal of Industrial chemistry and Engineering*, 13, 427-432.
- LIU Y., ZHU W., LUO L., LI X. & YU H. 2014. A Mathematical Model for Vacuum Far-Infrared Drying of Potato Slices. *Drying Technology*, 32, 180-189.
- LOPEZ Z., MIGUE L. A., FUNAMIZU N. & TAKAKUWA T. 2002. Characterization of Feces for Describing the Aerobic Biodegradation of Feces. *Environmental system and Engineering*, 99-105.
- LU Q., LI W.-Z. & ZHU X.-F. 2009. Overview of fuel properties of biomass fast pyrolysis oils. *Energy Conversion and Management*, 50, 1376-1383.
- LUKER M. A., MENIFEE & CALIF. 2000. Continuous flow pasteurization of sewage sludge. 09/206,879 [Online], <https://docs.google.com/viewer?url=patentimages.storage.googleapis.com/pdfs/US6103191.pdf> [Accessed 04/04/2014].
- MARA D. D. 1984. *The design of ventilated improved pit latrines*, Washington, DC, USA, International Bank for Reconstruction and Development/The World Bank.
- MAYA C., TORNER-MORALES F. J., LUCARIO E. S., HERNÁNDEZ E. & JIMÉNEZ B. 2012. Viability of six species of larval and non-larval helminth eggs for different conditions of temperature, pH and dryness. *Water Research*, 46, 4770-4782.
- MCCORMICK P. Y. 2000. Drying, Kirk-Othmer Encyclopedia of Chemical Technology. <http://onlinelibrary.wiley.com/login-options> [Accessed 18/02/2014].
- MNKENI P. & AUSTIN L. 2009. Fertiliser value of human manure from pilot urine-diversion toilets. *Water SA*, 35, 133-138.
- MONGPRANEET S., ABE T. & TSURUSAKI T. 2004. Kinematic Model for a far infrared vacuum dryer. *Drying technology*, 22, 1675-1693.
- MOYERS C. G. & BALDWIN G. 1997. Psychrometry, evaporative cooling, and solids drying. *Perry's Chemical Engineers' Handbook*, 1-90.
- MUJUMDAR A. S. 2006. *Handbook of industrial drying*, New York, U.S.A, Marcel Dekker.
- MUJUMDAR A. S. & DEVAHASTIN S. 2000. Fundamental principles of drying. <http://staff.sut.ac.ir/haghighi/download/documents/drying.pdf> [Accessed 31/03/2014].
- MÜNCH E. V. & WINKER M. 2009. Technology Review| Urine diversion components. *Overview of urine diversion components such as waterless urinals, urine diversion toilets, urine storage and reuse systems. Sustainable sanitation–ecosan program. Eschborn.*
- MUSPRATT A. M., NAKATO T., NIWAGABA C., DIONE H., KANG J., STUPIN L., . .STRANDE L. 2014. Fuel potential of faecal sludge: calorific value results from Uganda, Ghana and Senegal. *Journal of Water, Sanitation and Hygiene for Development*, 4, 223-230.
- NAJAFPOUR G. D. 2007. *Biochemical engineering And biotechnology*. 1 ed. Boulevard, Langford Lane, Kidlington, Oxford OX5 1GB, UK: Elsevier
- NEWTON L., SHEPPARD C., WATSON D., BURTLE G. & DOVE R. 2005. Using the black soldier fly, *Hermetia illucens*, as a value-added tool for the management of swine manure. *Animal and Poultry Waste Management Center, North Carolina State University, Raleigh, NC*, 17.
- NIKIEMA J., COFIE O., IMPRAIM R. & ADAMTEY N. 2013. Processing of fecal sludge to fertilizer pellets using a low-cost technology in Ghana. *Environment and Pollution*, 2, p70.

- NIKIEMA J., COFIE O., IMPRAIM R. & DRECHSEL P. 2012. Fortified excreta pellets for agriculture. *Second international fecal sludge management conference* Durban, South Africa. International water Management Institute.
- NOWAK D. & LEWICKI P. P. 2004. Infrared drying of apple slices. *Innovative Food Science & Emerging Technologies*, 5, 353-360.
- PENG X., YE L., WANG C., ZHOU H. & SUN B. 2011. Temperature-and duration-dependent rice straw-derived biochar: Characteristics and its effects on soil properties of an Ultisol in southern China. *Soil and Tillage Research*, 112, 159-166.
- PHASHA M. C. 2006. *Health and Safety Aspects of the Use of Products from Urine-diversion Toilets*. M.Sc. Microbiology, University of Pretoria.
- POMPEI F. 1998. Infrared thermocouple improvements. Google Patents.
- PRAVEEN K., DG, UMESH HEBBAR H., SUKUMAR D. & RAMESH M. 2005. Infrared and hot-air drying of onions. *Journal of food processing and preservation*, 29, 132-150.
- RATTI C. & MUJUMDAR A. 1995. Infrared drying. *Handbook of industrial drying*. Boca Raton, Florida, U.S.A: CRC press, Taylor & Francis Group.
- ROBERT T. 1981. Mass-Transfer Operations. New York City, U.S: McGraw-Hill Book Company.
- ROMDHANA M. H., LECOMTE D., LADEVIE B. & SABLAYROLLES C. 2009. Monitoring of pathogenic microorganisms contamination during heat drying process of sewage sludge. *Process Safety and Environmental Protection*, 87, 377-386.
- RUIZ CELMA A., ROJAS S. & LOPEZ-RODRÍGUEZ F. 2008. Mathematical modelling of thin-layer infrared drying of wet olive husk. *Chemical Engineering and Processing: Process Intensification*, 47, 1810-1818.
- SAKAIN. & HANZAWA T. 1994. Applications and advances in far-infrared heating in Japan. *Trends in Food Science & Technology*, 5, 357-362.
- SCHRAMM G. 2000. A practical approach to rheology and rheometry Germany Gebrueder Haake.
- SCHROEDER E. 2011. Marketing Human Excreta. *A study of possible ways to dispose of urine and faeces from slum settlements*. Kampala, Uganda: Deutsche Gesellschaft für Technische Zusammenarbeit.
- SEPTIEN S. S. 2011. *High temperature gasification of millimetric wood particles between 800°C and 1400°C*. Process Engineering and Environment PhD, University of Toulouse.
- SEVILLA M. & FUERTES A. B. 2009. The production of carbon materials by hydrothermal carbonization of cellulose. *Carbon*, 47, 2281-2289.
- SHARMA G. P., VERMA R. C. & PATHARE P. B. 2005. Thin-layer infrared radiation drying of onion slices. *Journal of Food Engineering*, 67, 361-366.
- SILVA J. 2000. Inorganic Fertilizer Materials. *Plant Nutrient Management in Hawaii's Soils, Approaches for Tropical and Subtropical Agriculture*, 117-120.
- SIMPSON W. & TENWOLDE A. 1999. Physical properties and moisture relations of wood. Available: <http://www.slideshare.net/MidoOoz/physical-properties-and-moisture-relations-of-wood> [Accessed 02/04/2014]
- SOBSEY M. D. & MESCHKE J. S. 2003. Virus survival in the environment with special attention to survival in sewage droplets and other environmental media of fecal or respiratory origin. *Report for the World Health Organization, Geneva, Switzerland*, 70.
- STILL D. & FOXON K. 2012a. Tackling the challenges of full pit latrines. *WRC Project No. K5/1745*, 2.
- STILL D. & FOXON K. 2012b. Tackling the challenges of full pit latrines. *WRC Project No. K5/1745*, 1.
- STILL D., WALKER N. & HAZELTON D. 2009. Basic Sanitation services in South Africa, learning from the past, Planning for the future. *Project K5/1632*.

- STRANDE L., RONTELTAP M. & BRDJANOVIC D. 2014. *Faecal sludge management: Systems approach for implementation and operation*, IWA Publishing.
- SWASDISEVI T., DEVAHASTIN S., NGAMCHUM R. & SOPONRONNARIT S. 2007. Optimization of a drying process using infrared-vacuum drying of Cavendish banana slices. *Optimization*, 29, 810.
- SWASDISEVI T., DEVAHASTIN S., SA-ADCHOM P. & SOPONRONNARIT S. 2009. Mathematical modeling of combined far-infrared and vacuum drying banana slice. *Journal of Food Engineering*, 92, 100-106.
- SYERS K., BEKUNDA M., CORDELL D., CORMAN J., JOHNSTON J., ROSEMARIN A. & SALCEDO I. 2011. Phosphorus and food production. *UNEP Year Book*, 34-45.
- TEUNIS P. F. & HAVELAAR A. H. 2002. Risk assessment for protozoan parasites. *International biodeterioration & biodegradation*, 50, 185-193.
- TILLEY E., SUPPLY W. & COUNCIL S. C. 2008. Compendium of sanitation systems and technologies.
- TOĞRUL H. 2006. Suitable drying model for infrared drying of carrot. *Journal of Food Engineering*, 77, 610-619.
- TORONDEL B. 2010. Sanitation Ventures Literature Review: on-site sanitation waste characteristics. *Scientific report. London School of Hygiene & Tropical Medicine. London. England.*
- VERIANSYAH B. & JAE-DUCK K. 2007. Supercritical water oxidation for the destruction of toxic organic wastewaters: A review. *Journal of Environmental Sciences*, 19, 513-522.
- VINNERÅS B. 2001. Faecal separation and urine diversion for nutrient management of household biodegradable waste and wastewater.
- WELTY J., WICKS C. E., RORRER G. L. & WILSON R. E. 2007. *Fundamentals of Momentum, Heat and Mass Transfer*, River street, Hoboken, U.S.A, John Wiley & sons Inc.
- WILLIAMS P. T. 2013. *Waste treatment and disposal*, John Wiley & Sons.
- WOLGAST M. 1993. Recycling system. *Brochure produced by WM-Ekologen, AB, Stockholm, Sweden.*
- WOOLLEY S. M., COTTINGHAM R. S., POCOCK J. & BUCKLEY C. A. 2013. Some rheological properties of fresh human faeces with a variation in moisture content.
- XIANGMEI M., MARTIJN S., MIRARA S. & WIEBREN D., JONG. 2014. Experimental Study Of Drying Different Sludges Using A Belt-Mir Ladepa Dryer. *European Biomass Conference and Exhibition Delft, Netherlands.*
- ZUMA L., VELKUSHANOVA K. & BUCKLEY C. 2013. Chemical and thermal properties of dry VIP latrine sludge. (unpublished work)

7 Appendix

7.1 Appendix A: Calibration tests

Various parameters were calibrated in the laboratory scale LaDePa, including; the drying temperature, the power consumed by the MIR emitters and the speed of the porous steel belt.

7.1.1 Drying temperature

Calibration of drying temperature was done to determine the temperature that would be obtained at different MIR intensities and emitter height. For the calibration of temperature, two thermocouples were placed below the centre of each MIR emitter, 20 mm from the edge and 10 mm above the porous steel belt. The emitters were placed at a height of 115 mm above the belt surface. Belt speed was set at maximum speed and the damper valve was fully opened. The dial reading was set at 20 % for each of the emitters and the corresponding temperature was recorded by the use of data loggers. The dial reading was then increased in increments of 10 % up to 80% for each of the emitters. This procedure was repeated at an emitter height of 80 and 50 mm. Results obtained are presented in **Figure 7-1 A** and **Figure 7-2 A**.

Temperature could not be measured above 300°C and so the MIR intensity could not go beyond 80%. This was because the insulation on the thermocouples could not withstand this high temperature.

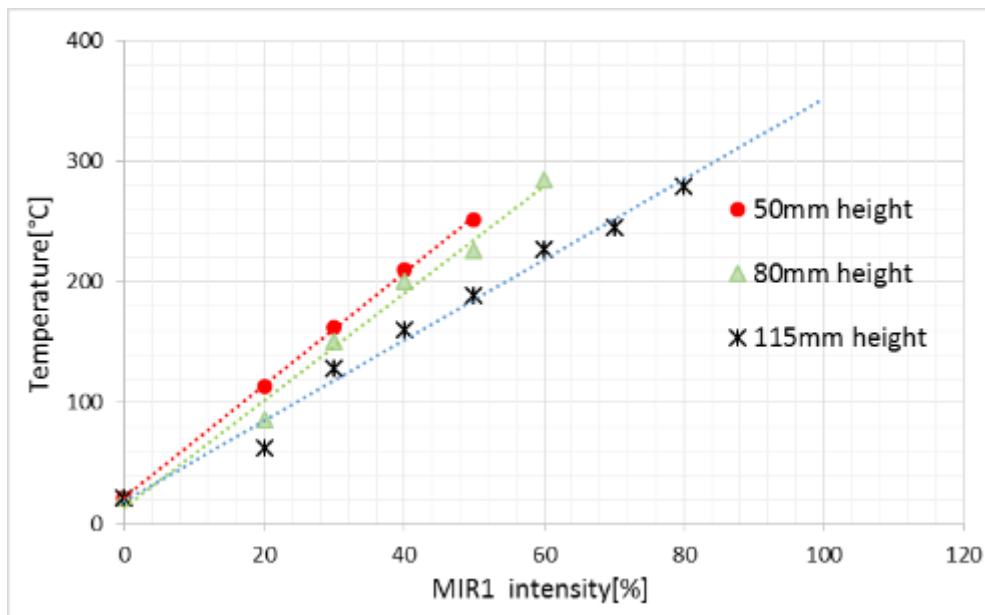


Figure 7-1 A: Temperature of the MIR emitter 1 at different intensities and height above the belt

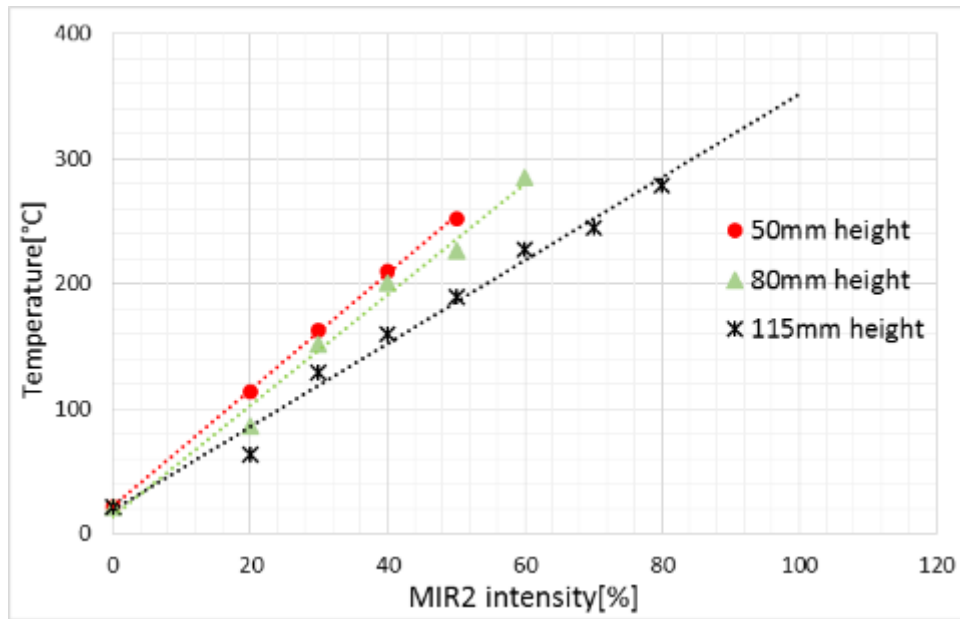


Figure 7-2 A: Temperature of the MIR emitter 2 at different intensities and height above the belt

For both emitters, the temperature increases linearly with the increase of the MIR intensity. It also increases by reducing the distance between the MIR emitter and the belt surface. The increase of the drying temperature with the increase of the MIR intensity is due to a higher power supply, which leads to higher heating intensity. The increase of the drying temperature with the decrease of the emitter height is because of a higher MIR radiation flux concentration on the belt surface and lower radiation loss from the sides of the belt. The same temperature could be obtained by different MIR intensity and emitters height combinations. As an example of this, a drying temperature of 200°C can be obtained at intensity of 38, 42, and 56% at a height of 50, 80 and 115 mm respectively (for emitter 2).

The temperature data given indicate the chamber temperature as measured using the K-type thermocouples. A limitation to this is that the thermocouples used are considered as contact type. Moreover, the emissivity of thermocouples increases with wavelength thus increasing measurement inaccuracies (Pompei, 1998). At the time of measurement, they were however considered the best alternative to monitor the drying process. The inaccuracy in measurement however may not be considered so high based on the results obtained. It was noted that as the drying chamber temperature exceeded 200°C charring occurred. Biomass is said to start charring at around this temperature (Peng et al., 2011). This therefore indicates that the actual temperature is in the range of that measured.

7.1.2 Power input into emitters

To determine the power input for each of the emitters, the belt and the blower were turned off and a clamp type ammeter was used to determine the current flowing into each of the emitters at different dial readings. The results were then converted into corresponding power by multiplying by the supply voltage, 240 V. The calibration results for the two emitters are presented in **Figure 7-3 A**.

The power input increases with the increase of the MIR intensity as expected. The first emitter (MIR 1) has a slightly higher power consumption as compared to the second emitter (MIR 2). This explains the different temperatures obtained at the same dial reading for both emitters. As the MIR intensity approaches 100%, the two emitters have almost the same power input.

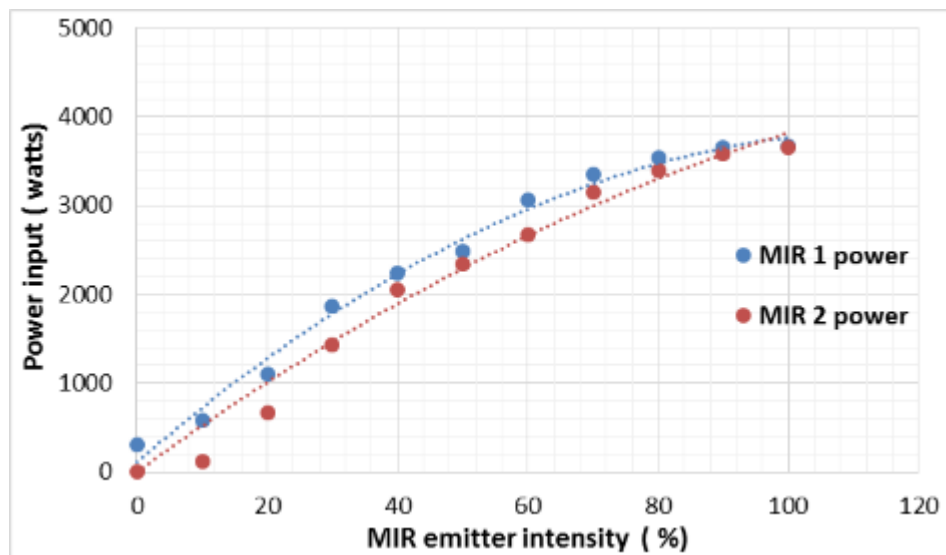


Figure 7-3 A: Corresponding power input for different MIR intensities

7.1.3 Belt speed calibration

The speed of the porous steel belt was calibrated by setting the dial reading for the belt at 100%, with the emitter and blowers turned off. To deduce the belt speed, the time taken to a portion of the belt to travel towards a given distance was recorded. This operation was repeated by reducing the dial reading by steps of 10%.

The residence time achieved at different dial settings for the porous steel belt is presented in **Figure 7-4 A**. This figure shows that as the dial reading is reduced the residence time increases. At lower dial settings, a slight change causes an important variation of the residence time as displayed by the exponential nature of the data obtained.

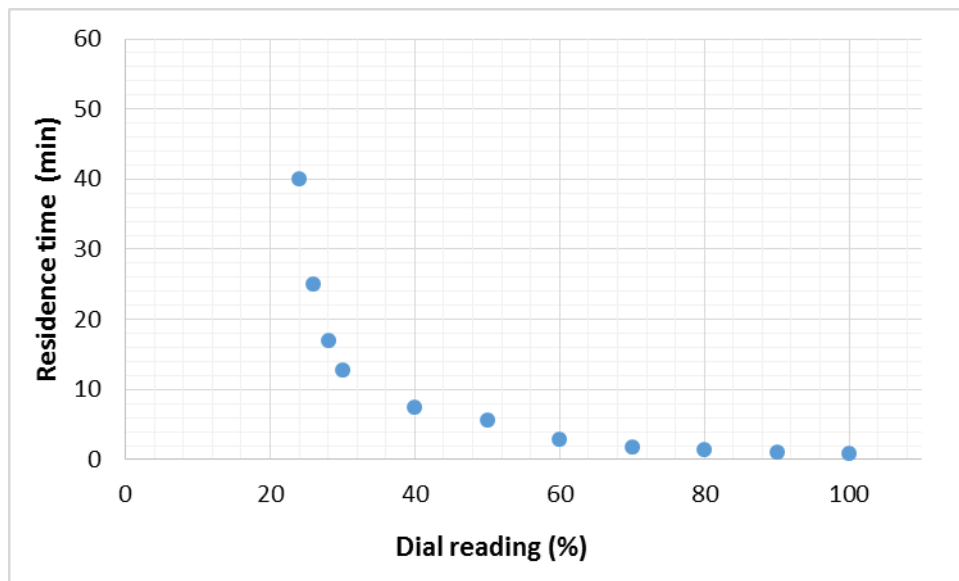


Figure 7-4 A: Residence time as a function of dial readings of the porous steel belt

7.2 Appendix B: Rheological analysis of raw sludge

Rheology is the study of flow and deformation behaviour of materials when subjected to stresses. In this study, the rheological characteristics of faecal sludge were determined by a rheometer model MCR51 Anton Paar. The standard operating procedures (SOP) from the Pollution Research Group were followed for these analyses.

The rheological analysis was done on the raw sludge for sludge with and without sawdust. Two runs were performed with the first batch, corresponding to sample without sawdust. The amount of sawdust added was 4% of total weight. The analysis included the determination of viscosity, storage modulus, loss modulus and complex viscosity. Viscosity is the measure of fluids resistance to deformation. Storage modulus (G') is the measure of the materials ability to store elastic energy after deformation. Loss modulus (G'') shows the viscous behaviour of a material during a deformation, with the energy dissipated as heat. Complex viscosity (η^*) indicates the material ability to resist deformation and is the sum of the storage and loss modulus (Schramm, 2000).

7.2.1 Viscosity of sludge as function of the shear rate

Figure 7-5 B presents the viscosity obtained at different shear rates for the faecal sludge with and without sawdust. The viscosity of the samples decreased with the increase of the shear rate, implying that VIP sludge is a shear thinning material. These results are similar to the rheological properties observed for fresh faeces (Woolley et al., 2013). Viscosity of sludge with sawdust is slightly higher than that without sawdust. This implies that more pressure may be required to form pellets when sawdust is added.

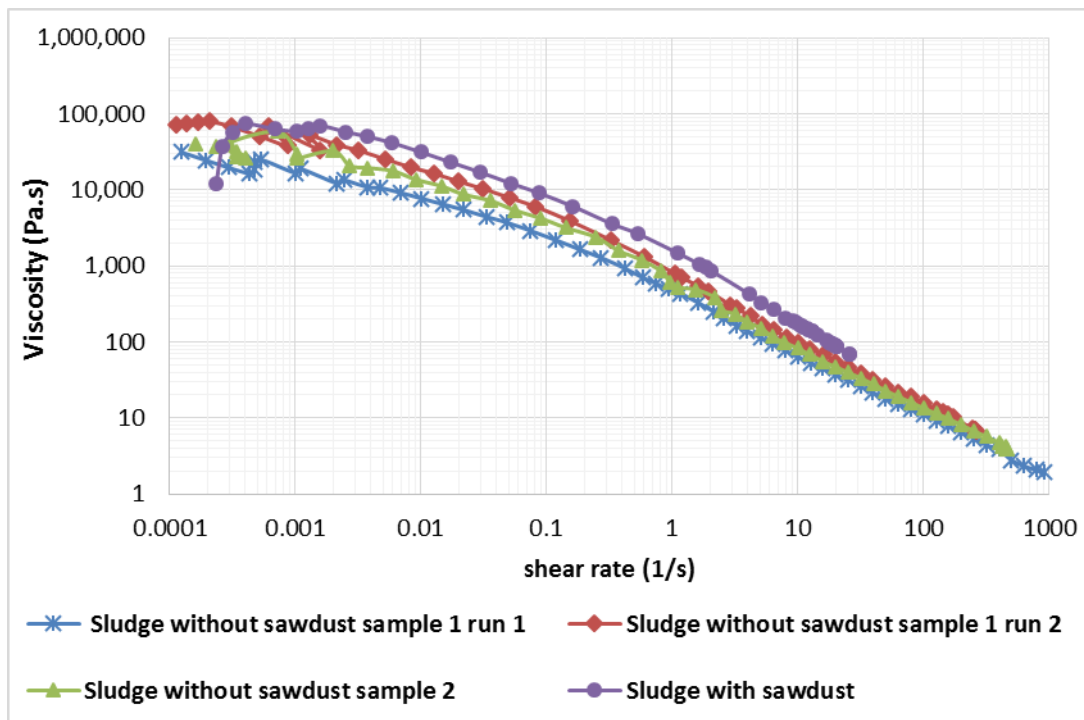


Figure 7-5 B: Viscosity of faecal sludge with and without sawdust as a function of shear rate

7.2.2 Storage modulus as a function of the angular frequency

The storage modulus of sludge before and after the addition of sawdust, as a function of the angular frequency, is presented in **Figure 7-6 B**. It shows that storage modulus increased with the increase of angular frequency. It also increased after the addition of sawdust. This implies that the elastic ability of pellets was increased after sawdust addition.

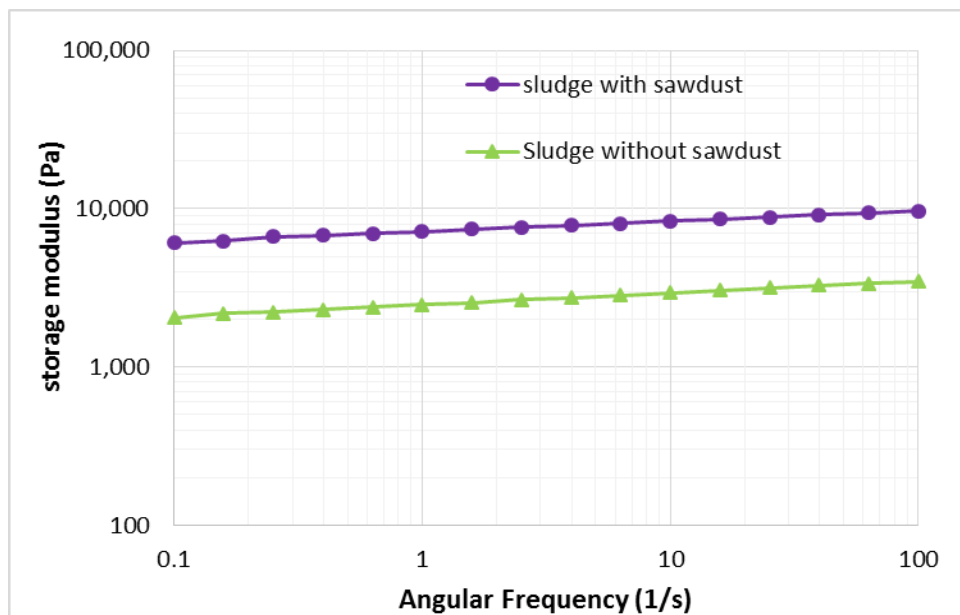


Figure 7-6 B: Storage modulus of faecal sludge with and without sawdust, as a function of the angular frequency

7.2.3 Loss modulus as a function of the angular frequency

The loss modulus of sludge with and without sawdust, as a function of angular frequency, is given in **Figure 7-7 B**. The loss modulus was relatively constant with respect to the angular frequency. The addition of sawdust led to the increase of the loss modulus thus increasing the viscous behaviour of sludge.

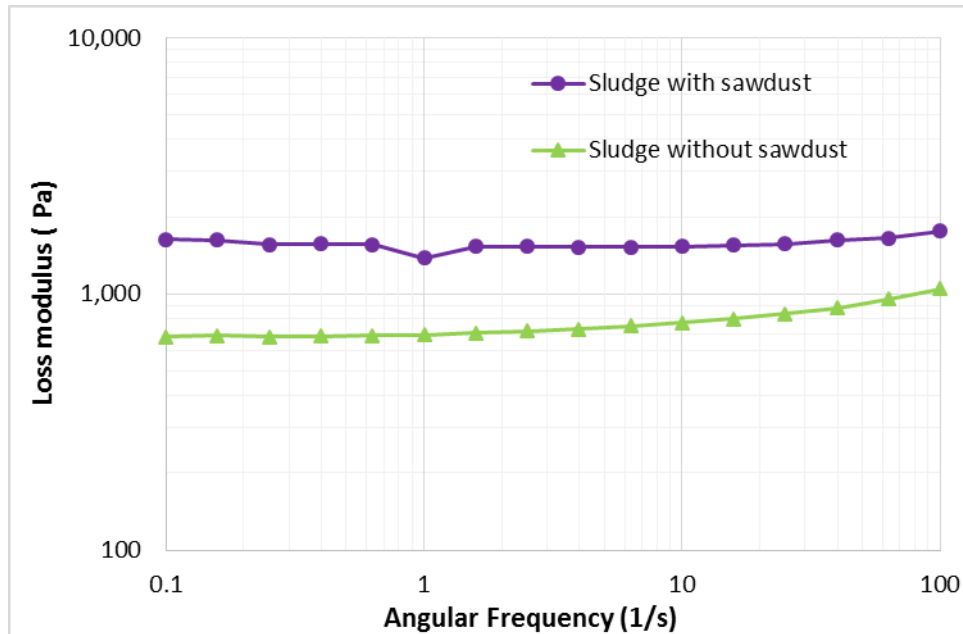


Figure 7-7 B: Loss modulus of faecal sludge with and without sawdust, as a function of the angular frequency

7.2.4 Storage and complex modulus comparison

The combined plot of complex and storage modulus as a function of angular frequency is shown in **Figure 7-8 B**. It shows that the storage modulus was higher than loss modulus before and after addition of sawdust, at any angular frequency. Therefore, faecal sludge from this study behaves more as an elastic material than a viscous material at low shear strains. Increase of storage modulus is much higher than that of loss modulus after addition of sawdust. This means that the elastic behaviour of the sludge with respect to its viscous behaviour is higher after adding sawdust.

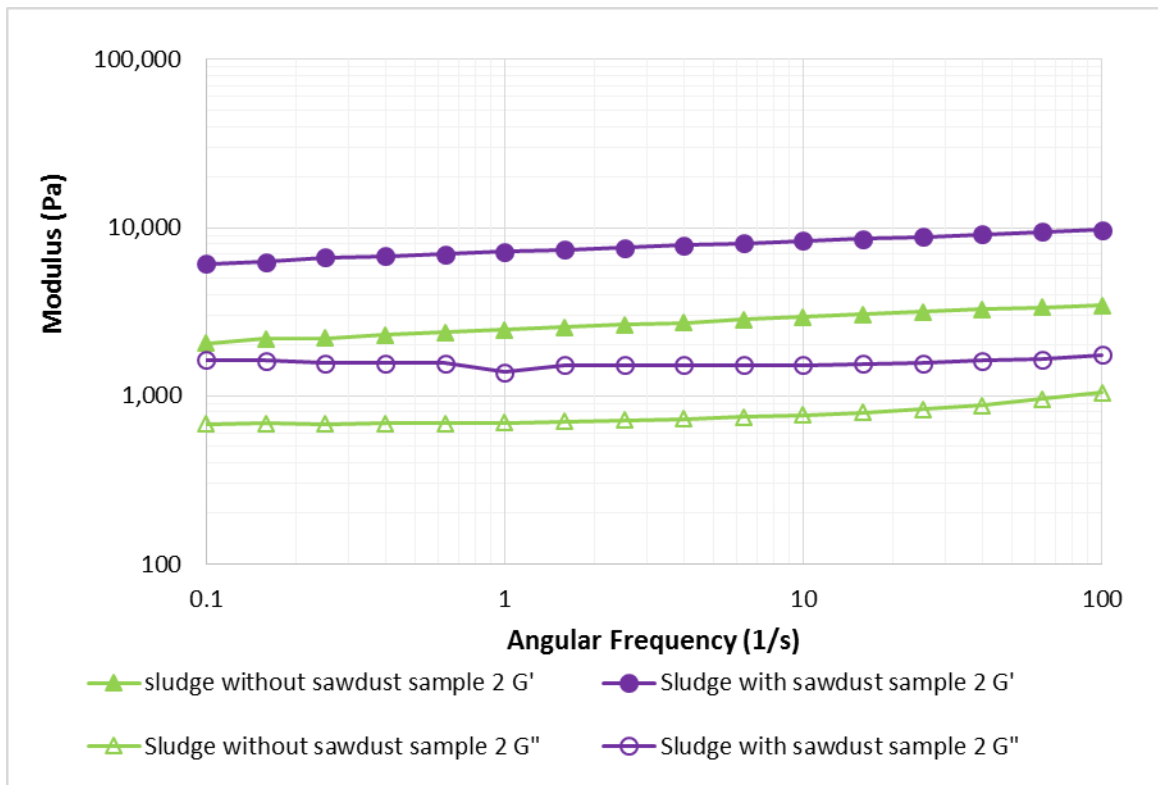


Figure 7-8 B: Storage and complex modulus as a function of angular frequency

7.3 Appendix C: Temperature profiles

Temperatures measured at the core and the surface of the 8 mm pellets are presented in **Figure 7-9 C**. Repeatability of the temperature measurements at the surface and core of the pellets can be observed.

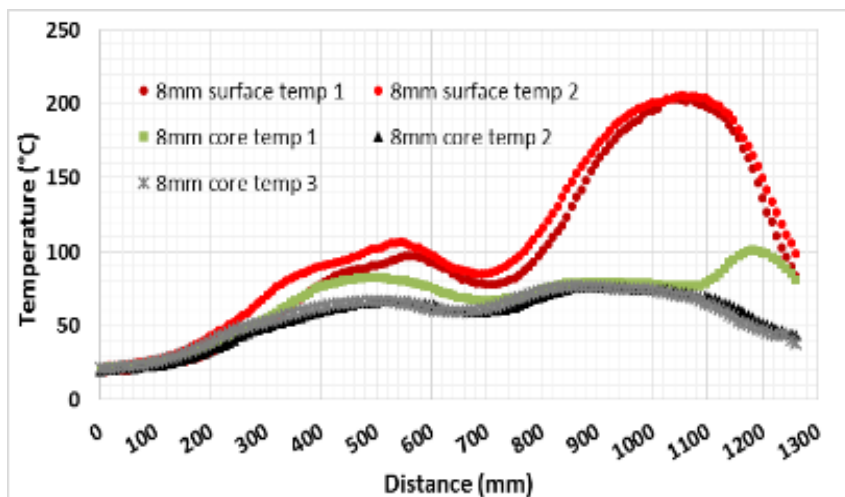


Figure 7-9 C: Temperature of the 8 mm diameter pellets at the surface and at the core

7.4 Appendix D: Psychrometric charts for low, high and medium temperatures

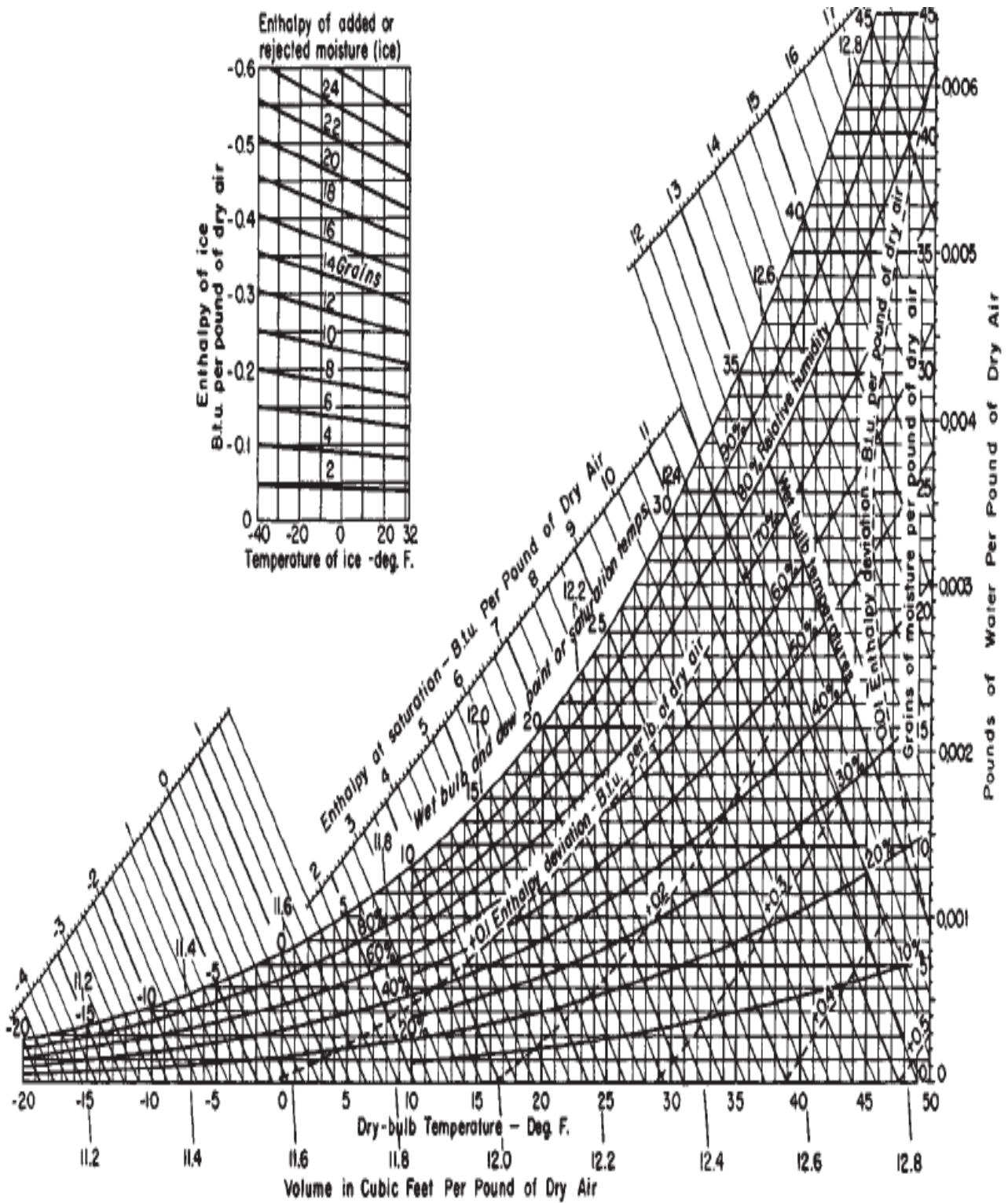


Figure 7-10 E: Psychrometric chart for low temperatures

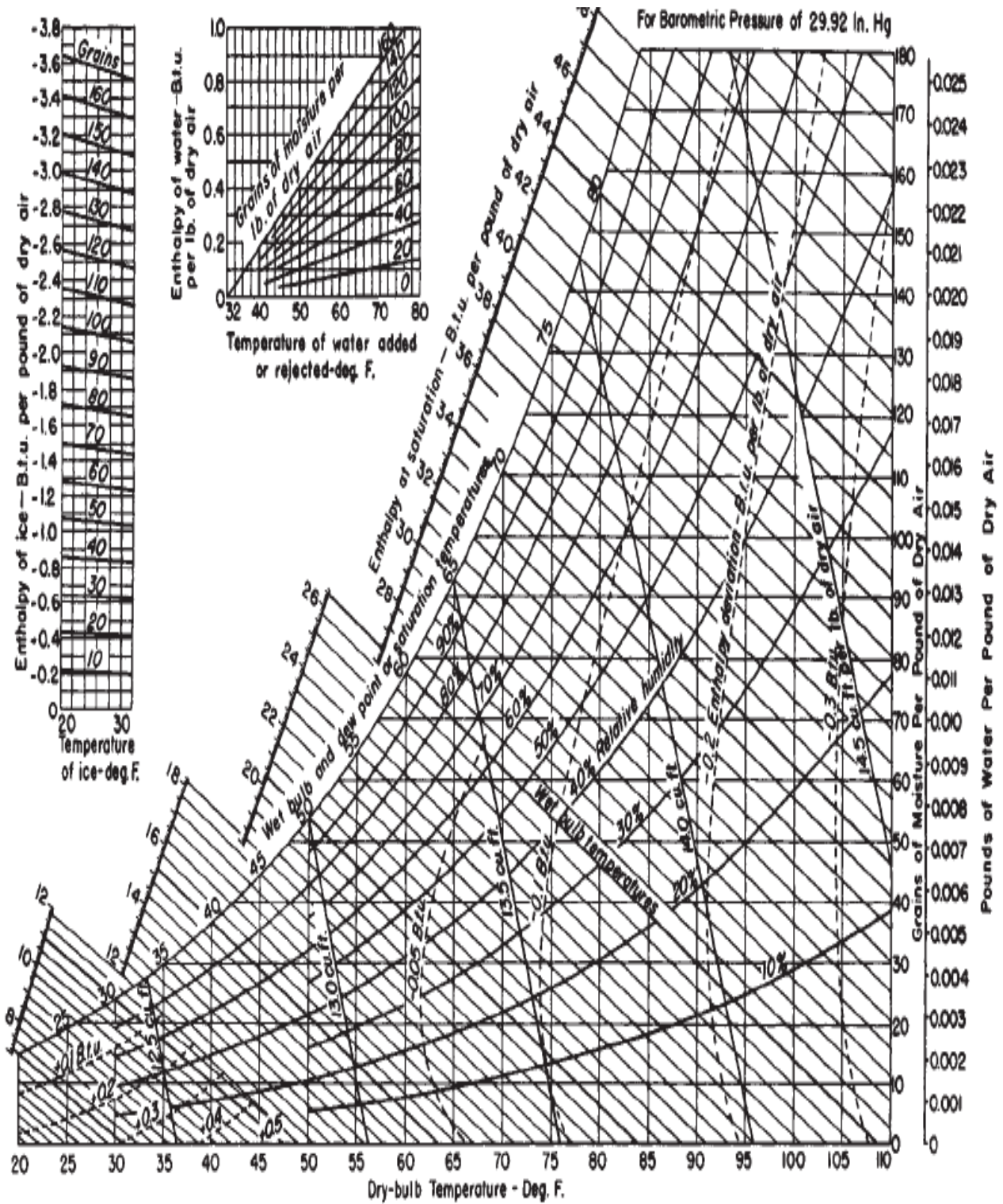


Figure 7-11 E: Psychrometric chart for medium temperatures

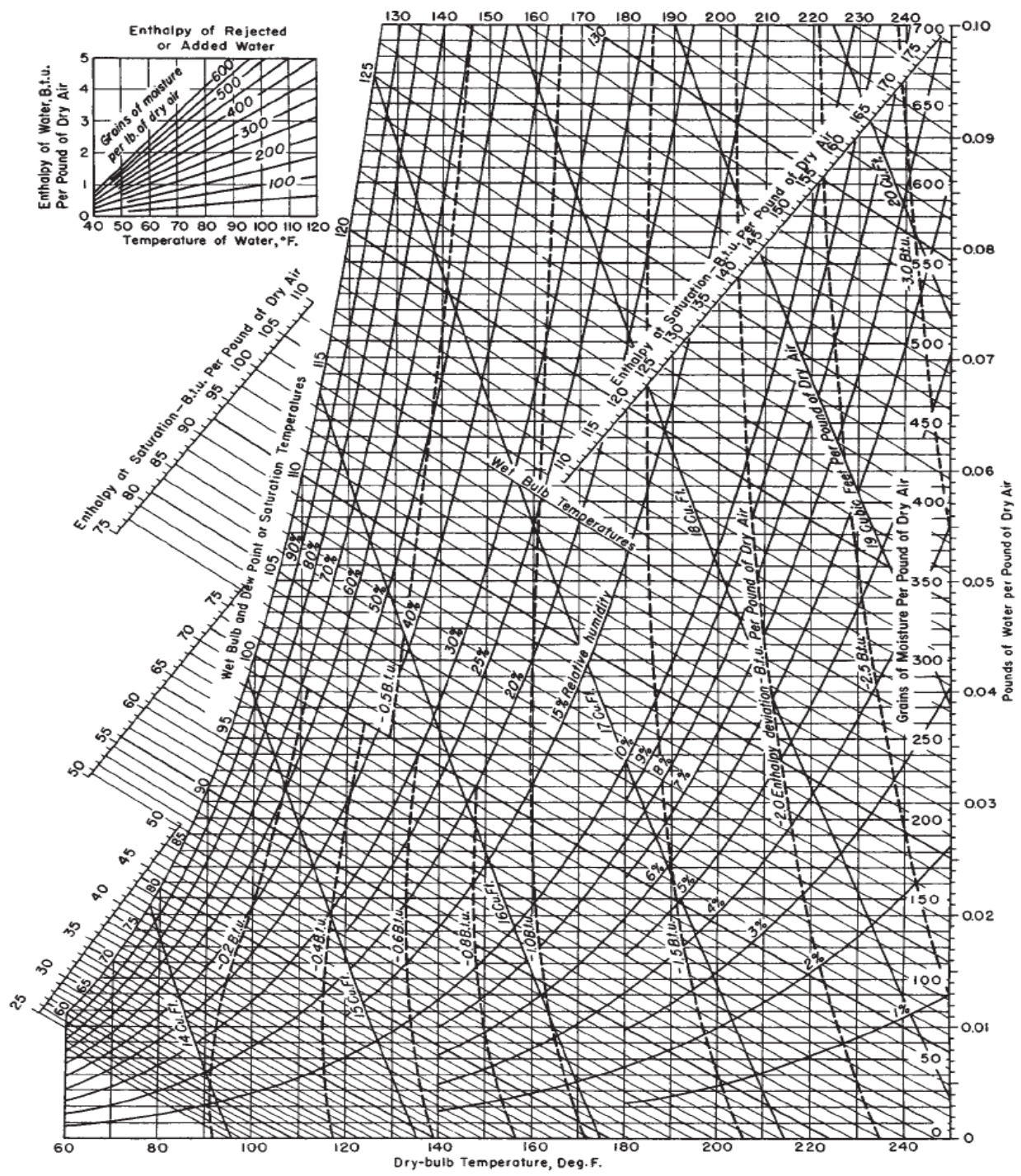


Figure 7-12 D: Psychrometric chart for high temperatures

7.5 Appendix E: Deliverables submitted to Water Research Commission

This research project was funded by the Water Research Commission (project K5/2137). The fund also included a project on the characterization of waste from pour-flush toilets. Various deliverables were submitted during the course of the project. The deliverables related to the LaDePa study are shown in **Table 7-1 E**. The missing deliverables are those directly related to pour-flush toilets.

Table 7-1 E: Deliverables submitted as part of WRC project K5/2137

No	Deliverable	Description	Date of submission
1	Protocol for laboratory drying testing	Report on the protocol for the laboratory-based drying and pasteurisation tests for VIP latrine sludge	28 th February 2013
2	Protocol for LaDePa sludge characterisation	Report on the protocol and methods for the VIP latrine sludge characterisation	28 th February 2013
3	Preliminary report on drying	Progress report on the drying and pasteurisation of VIP latrine sludge	10 th February 2014
4	Assessment of LaDePa machine	Report on the instrumentation and the online energy monitoring requirements and specifications	17 th March 2014
5	Preliminary report on LaDePa	Progress report on the laboratory trials and analysis of the feedstock and the processed pellets	17 th March 2014
6	Protocol for LaDePa pellet characterisation	Report on the protocol and methods for pellet characterisation	30 th June 2014
9	Final report on the LaDePa process	Final report on the LaDePa process	28 th October 2014
11	Draft final report	Draft final report incorporating pour-flush toilets study	4 th March 2015
12	Final report	Final report of the LaDePa and pour-flush study	30 th April 2015

7.6 Appendix F: Poster presented at MILE symposium 2014



PASTEURISATION AND DRYING OF FAECAL SLUDGE BY USE OF MEDIUM WAVE INFRARED (MIR) RADIATION

S.W. Mirara, S. Santiago*, A. Singh, K. Vekushanova & C.A. Buckley**

Pollution Research Group, University of KwaZulu-Natal
sepliens@ukzn.ac.za *, buckley@ukzn.ac.za **

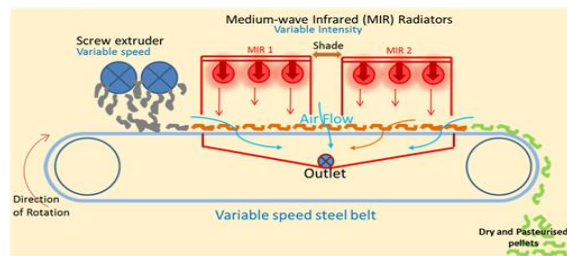


INTRODUCTION

- eThekweni Water and Sanitation (EWS) commitment to provide adequate sanitation in urban, peri-urban and rural areas of the municipality
- Sanitation facilities that require emptying
 - > 160,000 VIP latrines within municipality
 - > Emptying of pits in a 5 years cycle
- Need to dispose of sludge in an environmentally safe way
 - > Disposal of sludge in wastewater treatment works (WWTW) not viable due to overloading
 - > Deep row entrenchment cause ground water pollution and a waste of nutrients
- Latrine Dehydration and Pasteurisation (LaDePa) field-scale pelletiser developed by EWS and Particle Separation Systems (PSS)
- Laboratory-scale LaDePa developed to study operation
 - > Phenomenological process
 - > Nutrient content and thermal properties important for agriculture and fuel application



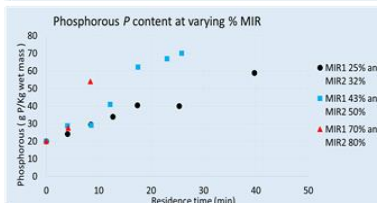
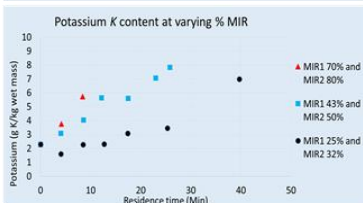
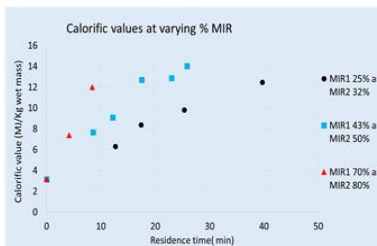
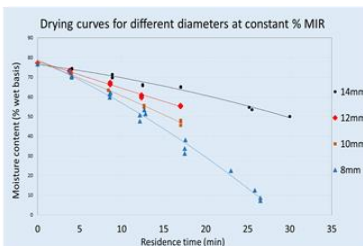
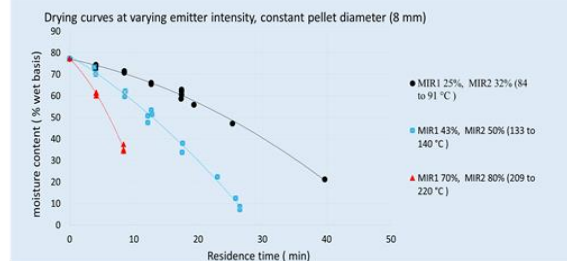
EXPERIMENTAL FACILITY



EXPERIMENTAL METHODOLOGY

- 1) Study on the phenomenological process
 - > The effect of MIR intensity from emitters on drying (changing dial reading between 0 to 100%)
 - > The effect of pellet diameter (8mm, 10mm, 12mm and 14mm)
- 2) Characteristics of resultant pellets
 - > Potassium K, phosphorous, P determined in the MP-AES (Microwave Plasma – Atomic Emission Spectroscopy)
 - > Calorific value determined in a bomb calorimeter
 - > Moisture content (m.c.) determined by oven drying at 105°C for 24hrs

RESULTS



DISCUSSION

- Increase in emitter intensity increases drying temperature and reduces the drying time
 - > At the lowest intensity, drying is relatively slow
 - > At the highest intensity, drying is the fastest, but the chance of charring and burning is considerably increased
 - > Best drying occurs at medium intensity, in an acceptable time to achieve very low m.c. without charring
- Drying time increases with pellet diameter
 - > 30 min to reduce m.c. by 27% for 14 mm pellets
 - > 13 min to reduce m.c. by 27% for 8mm pellets
- Calorific value of pellets increases with decrease in m.c.
 - > Similar to calorific value of wood (16MJ/Kg) at 16% m.c.
 - > About a third of the calorific value of coal (40MJ/Kg) and diesel (46MJ/kg)
- K and P content increases with reduction in moisture content
- Amount of P in pellets (70g/Kg maximum) is very low compared to inorganic fertilizer such as DAP (460g/Kg)

CONCLUSION

- Drying at higher MIR intensities reduces drying time but can cause charring of pellets when temperature exceed 209°C
- The use of pellets would be beneficial as a soil conditioner rather than a fertilizer due to the lower levels of nutrients
- Dried pellets could be used for energy generation as a fuel source for energy generation

ACKNOWLEDGEMENT

- eThekweni water and sanitation for facilitating this work
- Particle Separation Systems (PSS) for material support
- Water Research Commission for funding
- PRG technical staff for facilitating and assisting with experiments